AD-A121 500 ZENER OSCILLATIONS(U) WASHINGTON UNIV ST LOUIS MO DEPT 1/1
OF ELECTRICAL ENGINEERING P ROBIN ET AL. SEP 82
TR-ONR-82-6 N00014-79-C-0840

UNCLASSIFIED F/G 9/1 NL

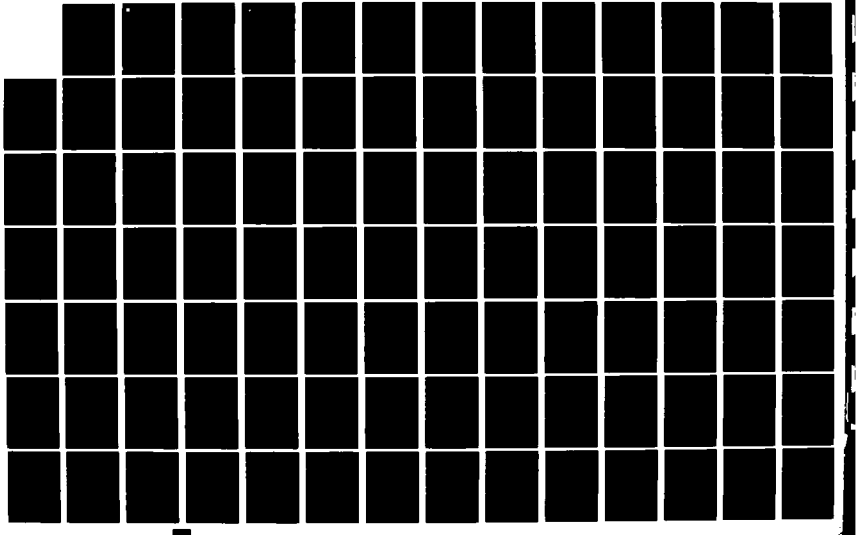

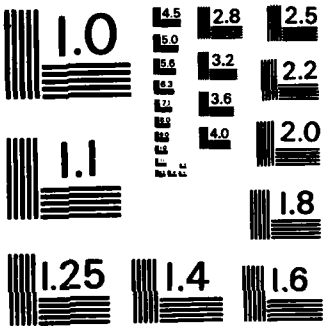

MICROCOPY RESOLUTION TEST CHART
NATIONAL BUREAU OF STANDARDS - 1963 - A

WASHINGTON UNIVERSITY IN ST. LOUIS

ZENER OSCILLATIONS

P. ROBLIN
M.W. MULLER

Department of Electrical Engineering
Washington University
St. Louis, MO 63130

SEPTEMBER 1982

TECHNICAL REPORT ONR-82-8
Office of Naval Research
Arlington, VA 22217

Contract: N00014-79-C-840
Contract Authority: NR SRO-004

SECURITY CLASSIFICATION OF THIS PAGE (When Data Entered)

REPORT DOCUMENTATION PAGE		READ INSTRUCTIONS BEFORE COMPLETING FORM
1. REPORT NUMBER	2. GOVT ACCESSION NO. AD-A121 500	3. RECIPIENT'S CATALOG NUMBER
4. TITLE (and Subtitle) Zener Oscillations		5. TYPE OF REPORT & PERIOD COVERED Special Report
		6. PERFORMING ORG. REPORT NUMBER
7. AUTHOR(s) P. Roblin, M.W. Muller		8. CONTRACT OR GRANT NUMBER(s) N00014-79-C-0840
9. PERFORMING ORGANIZATION NAME AND ADDRESS Department of Electrical Engineering Washington University St. Louis, MO 63130		10. PROGRAM ELEMENT, PROJECT, TASK AREA & WORK UNIT NUMBERS PE61153N, RR021-02-03 SRO-004
11. CONTROLLING OFFICE NAME AND ADDRESS Office of Naval Research - Code 414 800 North Quincy Street Arlington, VA 22217		12. REPORT DATE September 1982
		13. NUMBER OF PAGES 106
14. MONITORING AGENCY NAME & ADDRESS(if different from Controlling Office)		15. SECURITY CLASS. (of this report) UNCLASSIFIED
		15a. DECLASSIFICATION/DOWNGRADING SCHEDULE

16. DISTRIBUTION STATEMENT (of this Report)

Approved for public release; distribution unlimited

17. DISTRIBUTION STATEMENT (of the abstract entered in Block 20, if different from Report)

18. SUPPLEMENTARY NOTES

ONR - Scientific Officer (M.N. Yoder) Tel: (202) 696-4218

19. KEY WORDS (Continue on reverse side if necessary and identify by block number)

High-field effects, Zener oscillations, inertial transport, coherent states, band structure

20. ABSTRACT (Continue on reverse side if necessary and identify by block number)

This work discusses the periodic motion, called Zener oscillation, of a crystal in a uniform steady applied field.

We ~~construct~~ semiclassical electron wave packets ARE CONSTRUCTED in the Stark and Houston one-band representations and show that they are periodic with the Zener period. ~~We determine~~ Quasicoherent states localized in both position and momentum with minimized fluctuations ARE DETERMINED.

We ~~compute~~ the Zener oscillation spectrum of a GaAs conduction electron, the spectrum's stability under directional deviations, and the electron's electromagnetic coupling ARE COMPUTED.

DD FORM 1 JAN 73 1473 EDITION OF 1 NOV 65 IS OBSOLETE S/N 0102-014-6601

SECURITY CLASSIFICATION OF THIS PAGE (When Data Entered)

WASHINGTON UNIVERSITY IN ST. LOUIS

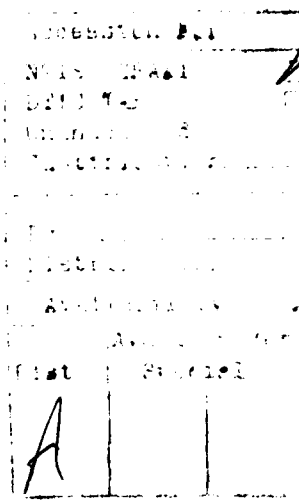

ZENER OSCILLATIONS

P. ROBLIN
M.W. MULLER

Department of Electrical Engineering
Washington University
St. Louis, MO 63130

SEPTEMBER 1982

TECHNICAL REPORT ONR-82-6

Office of Naval Research
Arlington, VA 22217

Contract: N00014-79-C-840
Contract Authority: NR SRO-004

TABLE OF CONTENTS

TABLE OF CONTENTS
(continued)

LIST OF FIGURES

ZENER OSCILLATIONS

1. INTRODUCTION

The question of the existence of Zener oscillations has remained controversial for more than forty years. Experimental observations indirectly supporting their existence have been reported by Koss and Lambert (1)*, but so far this widely quoted work is the only credible experimental evidence.

In the present report we continue the Zener oscillation studies begun in the 1980 progress report on Semiconductor Millimeter Wavelength Electronics (2). In that report an extensive critical review of band structure dominated carrier dynamics was presented. It was concluded that the phenomena limiting the realization of Zener oscillations are scattering and interband tunneling. A discussion and numerical estimate of the tunneling probability indicated that this is not a serious limiting factor, and it was concluded that Zener oscillations would require an adequate lengthening of the scattering lifetime.

The motivation for studying Zener oscillations is their potential of realizing a device for generating tunable submillimeter radiation. Like any other effective electronic generator of radiation, a practical

*The numbers in parentheses in the text indicate references in the Bibliography.

Zener oscillator will have to rely on phase coherence of the electrons coupled to the radiation. A possible scheme for obtaining the required phase initialization and phase focusing has been suggested by D. L. Rode (private communication) and will be reported on elsewhere. In the present work we discuss the theoretical aspects of such a device from the viewpoint of quantum theory. Specifically we examine an electronic state analogous to the coherent states of a harmonic oscillator ("Glauber states"(3)) with a wave function whose mean square position and momentum uncertainty product approaches the minimum uncertainty level. Such a state can be described by a wave packet of states of the conventional representation. The dynamics of such a wave packet must be determined.

In view of our goals we have inquired into the physical meaning of several existing solutions of the problem of an electron in a crystal in the presence of an applied electric field. We begin by quoting the standard theoretical methods and their results. No derivations are given, since they can be found in the 1980 report and in references (4), (5), (6) and (7).

Based on the interpretation of these results, we propose two kinds of wave packets to represent coherent band-electron states. Furthermore we calculate absorption and emission probabilities of Zener oscillations in a one-band scheme. These probabilities are directly related to the spectral analysis of the Zener oscillations in a given band structure. We report on a computation of these spectral components for a variety of applied field directions for the conduction band of GaAs.

2. THEORETICAL BACKGROUND

The standard technique for studying the electronic properties of crystals is the one-electron model. In such a model the electron is viewed as moving in an average periodic potential. It is assumed that in an applied electric field this average potential is unaffected. This approximation is based on the relative weakness of the applied field when compared with the effective fields of the lattice bonds.

There are several different approaches to the solution of the one electron model equations in the presence of an applied electric field. In all cases the Schroedinger equation to be solved is

$$\left(\frac{\bar{p}^2}{2m} + V(\bar{r}) - e\bar{\varepsilon}\cdot\bar{r}\right)\psi(\bar{r},t) = i\hbar\frac{d}{dt}\psi(\bar{r},t) \qquad (1)$$

(choosing the sign convention $e = -|e|$).

For our purpose it is useful to show the solution in each of three different representations: The Bloch, or crystal momentum, Wannier or lattice site; and the $\bar{k}\bar{q}$ representation.

2.1 FORMULATION OF THE SCHROEDINGER EQUATION IN THREE REPRESENTATIONS

2.1.1 Bloch Functions

A natural basis for crystal electron wave functions is the set of Bloch functions $\psi_n(\bar{k},\bar{r})$. The Bloch functions are eigenfunctions of the periodic Hamiltonian $H_0 = \frac{\bar{p}^2}{2m} + V(\bar{r})$, and they are labeled by the two indices $\bar{k}$,n. The index n is the band index defined by the Hamiltonian

$$H_0\psi_n(\bar{k},\bar{r}) = E_n(\bar{k})\psi_n(\bar{k},\bar{r}).$$

The index $\bar{k}$ is defined by the lattice translation operator $T(\bar{a}_m) = \exp(i\bar{p}\cdot\bar{a}_m)$ through

$$T(\bar{a}_m)\psi_n(\bar{k},\bar{r}) = e^{i(\bar{k}\cdot\bar{a}_m)}\psi_n(\bar{k},\bar{r}).$$

The indices n, $\bar{k}$ are good quantum numbers since they are generated by commuting operators

$$[T(\bar{a}_m),\ H_0] = 0.$$

The presence of the field term $e\bar{\varepsilon}\cdot\bar{r}$ in Equation (1) breaks the periodicity of the Hamiltonian and $\bar{k}$ is no longer a good quantum number. Therefore we write the solution to Equation (1) in the Bloch function representation as

$$\psi(\bar{r},t) = \sum_n \int d\bar{k}\phi_n(\bar{k},t)\psi_n(\bar{k},\bar{r}).$$

If we choose the x axis to lie along the field $\bar{\varepsilon}$, substitute in the Schroedinger Equation (1), and evaluate the matrix element of the position x that appears in the field term (Appendix 6.3)

$$\langle n,\bar{k}|x|n',\bar{k}'\rangle = i\delta_{nn'}\frac{\partial}{\partial k_x}\delta(\bar{k}-\bar{k}') + X_{nn'}\delta(\bar{k}-\bar{k}') \qquad (2)$$

we obtain the equation of motion of the envelope ϕ_n

$$[E_n(\bar{k}) - ie\varepsilon\frac{\partial}{\partial k_x} - i\hbar\frac{\partial}{\partial t}]\phi_n(\bar{k},t) = e\varepsilon\sum_e X_{ne}\phi_e(\bar{k},t) \qquad (3)$$

where $X_{ne} = \frac{(2\pi)^3 i}{\Omega}\int u_n^*(\bar{k},\bar{r})\frac{\partial}{\partial k_x}u_e(\bar{k},\bar{r})d\bar{r}$

is the polarization matrix. The integral is taken over a unit cell, with Ω the volume of the cell.

2.1.2 Wannier Functions

Another useful representation is formed from the set of Wannier functions, defined in terms of the Bloch functions by

$$W_n(\bar{r}-\bar{R}_n) = \sqrt{\frac{\Omega}{(2\pi)^3}} \int_{B.Z.} e^{-i\bar{k}\cdot\bar{R}_n}\psi_n(\bar{k},\bar{r})d\bar{k}$$

where $\bar{R}_n$ is a lattice site vector.

In the Wannier representation the solution of Equation (1) is

$$\psi(\bar{r},t) = \sum_n \sum_m b_n(\bar{R}_m,t)W_n(\bar{r}-\bar{R}_m)$$

where $b_n(\bar{R}_m,t)$ is a solution of

$$[E_n(-i\bar{\nabla})-i\hbar\frac{\partial}{\partial t}]_{\bar{r}=\bar{R}_m} b_n(\bar{r},t) = \sum_{n'} \sum_{\bar{R}_{m'}} U_{nn'}(\bar{R}_{m'},\bar{R}_m)b_{n'}(\bar{R}_{m'},t) = 0 \quad (4)$$

where $U_{nn'}(\bar{R}_{m'},\bar{R}_m) = \int W_{n'}(\bar{r}-\bar{R}_{m'})e^{\bar{\varepsilon}\cdot\bar{r}}W_n(\bar{r}-\bar{R}_m)d\bar{r}$

2.1.3 The $\bar{k}\bar{q}$ Representation

A representation specifically designed for a periodic medium which suppresses the band index (its basis functions, in terms of the Bloch or Wannier representations, are sums over all the bands) is generated by the translation operators in the direct and reciprocal lattice. These operators $T(\bar{a}_n) = \exp(i\bar{p}\cdot\bar{a}_n)$ and $T(\bar{b}_m) = \exp(i\bar{q}\cdot\bar{b}_m)$ are a complete set of observables $[\bar{a}_n,\bar{b}_m] = 2T\delta_{nm}$ and they define wave functions

$$T(\bar{a}_n)\psi_{\bar{k}\bar{q}} = \exp\left(\frac{i}{\hbar}\bar{k}\cdot\bar{a}_n\right)\psi_{\bar{k}\bar{q}}$$

$$T(\bar{b}_n)\psi_{\bar{k}\bar{q}} = \exp\left(\frac{i}{\hbar}\bar{q}\cdot\bar{b}_n\right)\psi_{\bar{k}\bar{q}}$$

with

$$\psi_{\bar{k}\bar{q}} = \sqrt{\frac{\Omega}{(2\pi)^3}} \sum_{\bar{R}_n} \exp(i\bar{k}\cdot\bar{R}_n)\delta(\bar{r}-\bar{q}-\bar{R}_n)$$

where $\bar{a}$ is a lattice vector.

In the $\bar{k}\bar{q}$ representation the solution of Equation (1) is

$$\psi(\bar{r},t) = \int d\bar{k} \int d\bar{q} C(\bar{k},\bar{q},t) \psi_{\bar{k}\bar{q}}(\bar{r})$$

where $C(\bar{k},\bar{q},t)$ is a solution of

$$\left[-\frac{\hbar^2}{2m} \frac{\partial^2}{\partial q^2} + V(\bar{q}) - e\bar{\varepsilon}\cdot\left(i \frac{\partial}{\partial \bar{k}} + \bar{q}\right) \right] C(\bar{k},\bar{q},t) = i\hbar \frac{\partial}{\partial t} C(\bar{k},\bar{q},t) \quad (5).$$

2.2 THE ACCELERATION THEOREM IN THREE REPRESENTATIONS

The solution of the Schroedinger equation can be carried out in each of these representations. The full solutions must, of course, be identical, but each affords a different view of the problem. This will enable us to gain physical insight, to choose superpositions of states to correspond to various initial and boundary conditions, and to make appropriate approximations.

The solution of Equation (1) and of its equivalent forms Equations (3), (4) and (5) is the motion of an electron in an electric field, thus an acceleration theorem. We shall take up the solution in the three representations in the reverse order to their introduction, because in that way we can proceed from the most general and abstract to the most intuitive form of the acceleration theorem.

2.2.1 The $\bar{k}\bar{q}$ Representation

In this representation, generated by the translation operators in direct and reciprocal space, the coordinate and momentum operators are

$$\bar{p} = i \frac{\partial}{\partial \bar{q}}, \quad \bar{r} = i \frac{\partial}{\partial \bar{k}} + \bar{q} \quad .$$

These operators are defined within the unit cell of their respective spaces, but because the translation operators contain an arbitrary phase factor $2n\pi$, they are not localized in a particular cell and act

equally in all the cells of their space. Another way of stating this property is to say that $\psi_{\bar{k}\bar{q}}$ places the electron on an infinite point lattice in both direct and reciprocal space, with the lattice point exactly localized both in the unit cell and in the Brillouin zone. $\psi_{\bar{k}\bar{q}}$ does not belong to a band; indeed the exact localization within the cell is possible, in the language of the more familiar Bloch or Wannier representations, because $\psi_{\bar{k}\bar{q}}$ contains a superposition of all the bands.

For this same reason, the acceleration theorem, deduced by Zak in the form of a Heisenberg operator equation of motion

$$\frac{d\hat{k}}{dt} = \frac{i}{\hbar}[\hat{H},\hat{k}] = \frac{i}{\hbar} e\bar{\mathcal{E}}$$

is exact and not a one-band approximation. It is, of course, this property that prompted Zak to invent this representation.

The Heisenberg operator $\hat{k}(t)$ is

$$\hat{k} = e^{\frac{i}{\hbar}H(t-t_0)}\bar{k}_e - \frac{i}{\hbar}H(t-t_0) \quad ;$$

The physically meaningful crystal momentum is the expectation value

$$\langle\psi(\bar{r},t_0)|\hat{k}(t)|\psi(r,t_0)\rangle = \langle\psi(\bar{r},t)|\bar{k}|\psi(\bar{r},t)\rangle \ .$$

2.2.2 Wannier Representation

The Wannier representation leads very directly to a very useful correspondence between classical and quantum dynamics of the crystal electron quasiparticle. In this representation $\bar{k}$ is an operator ($i \text{ grad}_{\bar{r}}$). If the interband and nonlocal terms $n \neq n'$, $m \neq m'$ are dropped in Equation (3), the one-band Schroedinger equation for "weak" fields is reduced to

$$[E_n(-i\bar{\nabla}) - i\hbar \frac{\partial}{\partial t} + e\bar{\varepsilon}\cdot\bar{r}]b_n(\bar{r},t) = 0 \quad .$$

Here $E_n(-i\bar{\nabla})$ is the modified kinetic energy operator that includes the effect of the periodic crystal potential, and the envelope function $b_n(\bar{r},t)$ can be viewed as describing a wave packet of Wannier functions. Its trajectory is given by the equivalent classical Hamiltonian

$$E_n(-i\bar{\nabla}) + e\bar{\varepsilon}\cdot\bar{r} \rightarrow E_n(\bar{k}) + e\bar{\varepsilon}\cdot\bar{r}$$

This correspondence recognizes $\hbar\,\bar{k}$ as a crystal momentum, and leads to the classical Hamilton equations of motion

$$\dot{\bar{r}} = \frac{\partial H}{\partial \bar{p}} = \frac{1}{\hbar}\frac{\partial E_n(\bar{k})}{\partial \bar{k}}$$

$$\dot{\bar{p}} = \hbar\,\dot{\bar{k}} = -\frac{\partial H}{\partial \bar{r}} = e\bar{\varepsilon}$$

which can be integrated to give the classical position of the electron

$$\bar{r}(t) - \bar{r}(t_0) = \frac{1}{e\varepsilon}[E_n(\bar{k}(t)) - E_n(\bar{k}(t_0))] \qquad (6)$$

with $\bar{k}(t) - \bar{k}(t_0) = \frac{e\bar{\varepsilon}}{\hbar}(t-t_0)$.

It should be remembered that this elegant deduction of the Zener oscillation dynamics is based on a wavepacket formalism in a one band scheme.

2.2.3 The Bloch Representation

The Bloch, or momentum representation leads very directly to a group of intuitively appealing results on Zener oscillations. Starting with Equation (3) we can obtain an exact equation of motion for the probability density of the momentum distribution

$$(e\varepsilon \frac{\partial}{\partial k_x} + \hbar \frac{\partial}{\partial t}) \sum_n \phi_n^*(\bar{k})\phi_n(\bar{k}) = 0$$

which is satisfied by any arbitrary initial distribution $G(\bar{k})$ that changes with time according to

$$\sum_n |\phi_n(\bar{k})|^2 = G(k_x - e\varepsilon \frac{t}{\hbar}, k_y, k_z).$$

Hence for any initial superposition of momentum eigenstates, the expectation value of the momentum, defined as

$$\langle \bar{k} \rangle = \sum_n \int |\phi_n(\bar{k})|^2 \bar{k}\, d\bar{k}$$

behaves as

$$\langle k_x(t) \rangle = \langle k_x(t_0) \rangle + \frac{e\varepsilon}{\hbar} (t - t_0) \quad .$$

Note again, as in the $\bar{k}\bar{q}$ representation, that this acceleration theorem is obtained without neglecting interband terms; unlike the classical trajectory of Equation (6), the time dependence of the crystal momentum is unaffected by interband mixing.

In a one-band model Equation (3) becomes

$$[E_n(\bar{k}) - e\varepsilon X_{nn} - ie\varepsilon \frac{\partial}{\partial k_x}]\phi_n = i\hbar \frac{\partial \phi_n}{\partial t} \quad .$$

We can write, for the polarized band structure

$$E_n^{(1)}(\bar{k}) = E(\bar{k}) - e\varepsilon X_{nn};$$

Then the solution can be written

$$\phi_n(\bar{k}, t) = \phi_\nu(\bar{k}) e^{-\frac{1}{\hbar} E_\nu(t)}$$

with

$$\phi_\nu(\bar{k}) = \frac{1}{\sqrt{\kappa}} \delta(k_y - k_{y0}) \delta(k_z - k_{z0}) \exp\left[\frac{i}{e\mathcal{E}} \int_0^{k_x} (E_\nu - E^{(1)}(\bar{k})) dk_x\right] \quad (7)$$

where κ is the length of the reciprocal lattice vector lying along the field direction (chosen as the x axis). (If the field direction is a principal lattice direction, κ is the "diameter" of the Brillouin zone along the x-axis).

The wave function ϕ_ν is periodic in the extended Brillouin zone, traversing a phase shift of $2\pi\nu$ radians as k_x traverses κ wave numbers. Thus the energy eigenvalues are

$$E_\nu = 2\pi\nu \frac{e\mathcal{E}}{\kappa} + \frac{1}{\kappa} \int_0^{\kappa} E^{(1)}(\bar{k}) dk_x .$$

These energies have been called Wannier levels or Stark levels, and they form the "Stark ladder" which has been the subject of so much controversy. We use the terminology Stark levels for E_ν and Stark functions for ϕ_ν, to avoid confusion with the Wannier functions $W(\bar{r}-\bar{R}_n)$.

It is possible to form a superposition of all the Stark states of a crystal with equal weight for each state in such a way that the resulting superposition has a definite-albeit time-dependent-value of k_x. We only indicate the result without giving any of the intermediate manipulations:

$$\psi(\bar{r},t) = \sum_\nu \int \phi_\nu(\bar{k}) e^{-\frac{i}{\hbar} E_\nu t} \psi(\bar{k},\bar{r}) d\bar{k}$$

$$= \sqrt{\kappa}\, \psi\left(\frac{e}{\hbar}\mathcal{E}t, k_{yo}, k_{z0}\right) \exp\left[\frac{-i}{e\mathcal{E}} \int_0^{\frac{e\mathcal{E}t}{\hbar}} dk_x E^{(1)}(\bar{k})\right] \quad (8)$$

where

$$\psi\left(\frac{e}{\hbar}\mathcal{E}t, k_{y0}, k_{z0}\right) = u_n(\bar{k}(t), \bar{r})e^{i\,\bar{k}(t)\cdot\bar{r}}$$

is a "time dependent Bloch function". The designation "Houston function" is used for both $\psi(\bar{r},t)$ and $\psi(\bar{k}(t),\bar{r})$.

2.2.4 Summary

By reviewing these three approaches to the acceleration theorem we have attempted to emphasize the relation of the dynamical and geometrical aspects of the electron motion in a crystal. The time dependence of the crystal momentum is an exact result, independent of the one-band approximation. The Stark ladder and the localization of the electron in a correspondence principle sense does require this approximation. This must be distinguished from the localization in the $\bar{k}\bar{q}$ representation which has no classical analogy. We will study questions of charge localization below, after a brief mention of the current literature.

2.3 RECENT LITERATURE

The quasiclassical electron dynamics, Zener oscillations, and their quantization in a Stark ladder of energy levels are seen to follow in straightforward fashion from a one-band scheme. The controversy about the observability of Zener oscillations or the Stark ladder revolves about the justifiability of neglecting the interband terms $X_{m,\, n\neq m}$. The Stark ladder could be destroyed by the broadening of the Stark levels due to the finite lifetime of the states.

This question has been debated in the literature for more than forty years. The only credible observation that has been reported (1) is the existence of a "staircase" modulation of the Franz-Keldysh effect as a function of the field. This modulation effect of the field on the interband absorption was predicted by Callaway (8), and while

its verification of the Stark ladder is indirect, it appears difficult to account for on any other basis.

Most of the calculations in the current literature appear to be in agreement that in crystals with moderate or wide bandgaps the contribution to the Stark level lifetime due to the applied electric field-that is to say, the tunneling probability-is small. In one of the most recent such calculations (7) interband tunneling was studied using a time evolution operator. The wave function used in the calculation includes the tunneling process and therefore the broadening of the Stark levels is directly computed. Results were obtained for nearly-free-electron approximation in a two-band scheme representative of GaAs. The broadening, calculated to second order in the field, is found to be neglibible for fields up to 10^6V cm^{-1}.

The theoretical evidence thus supports the reality of the Stark ladder. It suggests that the limitation of the observability of Zener oscillations is set not by the intrinsic lifetimes of the energy levels but is to be ascribed to scattering. The one-band approximation may be accepted as well supported by the current best estimates, and our further discussion will be based on it.

3. PHYSICAL INTERPRETATION: LOCALIZATION AND CORRESPONDENCE PRINCIPLE

3.1 THE HARMONIC OSCILLATOR ANALOGY

In the "moderate" fields under discussion ($\varepsilon < 10^6$ V cm^{-1}), the classical excursion Δx of the electron oscillation orbit for Zener oscillations is $\Delta E_n/\varepsilon$, where ΔE_n is the width in energy of the nth band. Since ΔE is a few eV, $\Delta x \geq 10^{-6}$ cm, that is to say, many times the lattice parameter a. Inspection of the form of the Stark function ϕ_ν of Equation (8) shows that the total phase shift experienced by ϕ_ν as k_x traverses the Brillouin Zone is of order $\Delta x/a$, so ϕ_ν is many electron wavelengths long.

Thus a Stark level in a moderate field is similar, in this respect, to a coulombic or harmonic oscillator energy eigenstate with a large quantum number. A particle in such a high energy eigenstate is localized to the extent of having an appreciable probability of being found only where its kinetic energy is positive (near the nucleus or near the potential minimum respectively). Within this range, its probability density is time-independent.

However, a particle with this much average energy can be localized more closely by forming a coherent superposition of several adjacent energy states in such a way that at some particular time their wave functions all add in phase at some particular point along the orbits, and cancel elsewhere. Such a localization would not in general be expected to persist, but in some form it underlies the correspondence principle for the formulation of classical orbits from quantum theory.

For the example of a harmonic oscillator the theory of such coherent superpositions of energy eigenstates is highly developed, since it can serve as the basis of the quantum coherence theory of light. Harmonic oscillator eigenstates $|a\rangle$ of the destruction operator $\hat{a}$ have wave functions of Gaussian shape with a localization as narrow as that of the oscillator ground state, and they oscillate in the quadratic potential with the oscillator frequency, and without spreading. Any narrower localization requires a wider range of energy eigenstates $|n\rangle$ and will cause the coherent state to spread with time. The states $|a\rangle$ have minimum uncertainty products for simultaneous measurement of position and momentum.

Our purpose here is to initiate a similar study of coherent states of a crystal electron in an applied field, to serve as models for the quasi-classical electron executing Zener oscillations. Relying on the conclusions outlined in Section II above, we will confine our attention to one-band states. We have available two types of one-band wave functions: Houston functions and Stark functions, eigenfunctions respectively of momentum and of energy. We work out the relations between the two types of wave function, and the localization of electrons in each. We then discuss the localization of electrons in wave packets formed from superpositions of eigenstates, and an approach to the construction of minimum uncertainty wave packets. We also compute transition probabilities between Stark states, since they are related to the emission and absorption of Zener radiation.

3.2 HOUSTON FUNCTIONS

A crystal electron generated by thermal excitation across a bandgap (e.g. phonon absorption) is unlocalized, and so it is not

unreasonable, in the presence of a field, to represent it by a Houston function (see II 2c above)

$$\psi(\bar{r},t) = \psi(\bar{k}(0) + \frac{e\bar{\varepsilon}t}{\hbar}, \bar{r})e^{-\frac{i}{\hbar}\int_0^t E^{(1)}(k(0) + \frac{e\bar{\varepsilon}t'}{\hbar})dt'}$$

$$= \psi(\bar{k}(0) + \frac{e\bar{\varepsilon}t}{\hbar}, \bar{r})e^{-\frac{i}{e\varepsilon}\int_{k_x(0)}^{k_x(0)+\frac{e\varepsilon t}{\hbar}} E^{(1)}(k')dk'_x}$$

where we have used the acceleration theorem $\hbar\dot{\bar{k}} = e\bar{\varepsilon}$; this explicitly represents the Houston function as a Bloch function with time-dependent label $\bar{k}$ and phase, and shows that it can be labeled by the initial crystal momentum $k_x(0)$.

Although the electron is unlocalized, in some sense it must be, in the presence of the field, in accelerated motion, and the Houston function should be capable of describing this motion. The most direct approach to a description of the motion, the computation of the expectation value $\langle x \rangle$ of the position, fails because its matrix elements are singular, as seen from Equation (2). The divergence arises from the δ- function normalization of the Houston functions which we can write in the form

$$\langle k'_x(0), \bar{r} | k_x(0), \bar{r} \rangle = \delta(k_x(0) - k'_x(0));$$

to obtain physically meaningful results, it is useful to avoid such singularities except as limits of finite procedures.

δ- function normalization is commonly used for wave functions of unlimited extent such as the plane waves representing free particles, or Bloch functions, or Houston functions.

For all these functions one could argue that a normalization in a finite volume V permits easy physical interpretation, through the quantization of the label k introduced by periodic boundary conditions. This leads to a normalization

$$\langle k'|k\rangle = \delta_{kk'},$$

and expectation values such as $\langle k'|x^n|k\rangle$ are easily computed. However, such "box normalization" hampers the description of the time-dependence of $\bar{k}$ for accelerated particles, and indeed the postulation of periodic boundary conditions is questionable at best in the presence of a field which destroys the postulated equivalence of the boundary points. Therefore it is necessary that we deal with the finitely non-normalizable infinite-crystal Houston functions.

The method for avoiding divergent expectation values can be developed by analogy with free-particle plane waves. Here we have

$$\langle k'|x^n|k\rangle = \int_{-\infty}^{\infty} dx e^{-ik'x}\left(-i\frac{\partial}{\partial k}\right)^n e^{ikx} = i^n \frac{\partial^n}{\partial k^n}\delta(k-k')$$

which is meaningless for $k = k'$. A meaningful expression can be obtained, however, by using the states $|k\rangle$ as a basis for the construction of normalizable wave packets.

A wave packet

$$\psi(x,t) = \int f(k)\psi(k)dk$$

has the norm

$$\langle\psi(x,t)|\psi(x,t)\rangle = \int dx \int dk' f^*(k')\psi^*(k') \int dk f(k)\psi(k)$$

$$= \int dk' \int dk f^*(k') f(k) \delta(k-k')$$

$$= \int dk f^*(k) f(k)$$

and so can be normalized by normalizing f(k); evidently the same procedure will yield convergent expectation values $\langle\psi(x,t)|x^n|\psi(x,t)\rangle$.

We shall make use of the Gaussian distribution

$$f_\sigma(k-k_0) = \sigma^{-1/2}(2\pi)^{-1/4} e^{-\frac{(k-k_0)^2}{4\sigma^2}}$$

normalized to

$$\int_{-\infty}^{\infty} dk f_\sigma^2(k-k_0) \equiv \int dk N(k_0,\sigma) = 1.$$

The notation $N(k_0,\sigma)$ stands for a Gaussian with mean at k_0 and variance σ.

The Gaussian free particle wave packet is

$$\psi_\sigma(x,t) = \int_{-\infty}^{\infty} dk f_\sigma(k-k_0) e^{-ikx} e^{-i\frac{\hbar k^2}{2m}t}$$

The behavior of such a wavepacket is well known; at t=0 it has the form

$$\psi_\sigma(x,0) = (8\pi\sigma^2)^{1/4} e^{-ik_0x} e^{-\sigma^2x^2}$$

and the time-development of the wave packet is well described by the expectation values

$$\langle k \rangle = k_0$$

$$\langle k^2 \rangle = k_0^2 + \sigma^2$$

$$\langle x \rangle = \frac{\hbar k_0}{m} t$$

$$\langle x^2 \rangle = \frac{\hbar^2 k_0^2}{m^2} t^2 + \frac{1}{4\sigma^2}$$

From these expressions one concludes that the centroid of a gaussian wavepacket moves according to Newton's law and is unaffected by the momentum uncertainty, and that the uncertainty of its position is inversely proportional to the momentum uncertainty. Moreover, since this observation holds no matter how narrow the packet, it is not implausible to pass to the limit of an infinitely narrow packet, that is to say, to a momentum eigenstate $|k_0\rangle$, and to attribute to a particle in such a state a quasi-newtonian motion, albeit with an infinite position uncertainty.

This argument can be made more formally, and we will now show that it is possible to construct physically meaningful wavepackets which are equivalent to plane waves, Bloch states, or Houston functions, and which form sets of orthogonal basis states. The procedure is to generate these states from gaussian wavepackets whose variance approaches zero so that

$$\lim_{\sigma \to 0} |f_\sigma(k-k_0)|^2 = \delta(k-k_0).$$

To begin with, we demonstrate the orthogonality of the states. For any wave packets

$$\psi(k_0,x,t) = \int_{-\infty}^{\infty} dk f(k-k_0)\,|k\rangle$$

of δ-function normalized states satisfying $\langle k'|k\rangle = \delta(k'-k)$ we have

$$\int_{-\infty}^{\infty} dx \psi^*(k_0',x,t)\psi(k_0,x,t) =$$

$$= \int_{-\infty}^{\infty} dk' \int_{-\infty}^{\infty} dk f^*(k'-k_0')\langle k'|k\rangle f(k-k_0)$$

$$= \int_{-\infty}^{\infty} dk f^*(k-k_0')f(k-k_0)$$

and if we use gaussian wave packets

$$f_\sigma(k-k_0) = (2\pi)^{-1/4}\sigma^{-1/2}\, e^{-\frac{(k-k_0)^2}{4\sigma^2}}$$

to form packets $\psi_\sigma(k_0,x,t)$, then

$$\langle k_0',x,t|k_0,x,t\rangle = \int \psi_\sigma^*\psi_\sigma dx = (2\pi)^{-1/2}\sigma^{-1} \int e^{-\frac{(k-k_0')^2+(k-k_0)^2}{4\sigma^2}} dk$$

$$= (2\pi)^{-1/2}\sigma^{-1}\, e^{-\frac{(k_0'-k_0)^2}{8\sigma^2}} \int e^{-\frac{\left[k-\frac{(k_0+k_0')}{2}\right]^2}{2\sigma^2}} dk = e^{-\frac{(k_0'-k_0)^2}{8\sigma^2}}$$

so that

$$\lim_{\sigma\to 0} \int \psi_\sigma^*\psi_\sigma dx = \delta_{k_0k_0'} .$$

This demonstrates the orthogonality of the states. It also provides a basis for the evaluation of matrix elements in which singularities can be avoided until a final limiting procedure.

Thus we confirm the validity of the informal interpretation advanced above of the free particle motion represented by a momentum eigenstate. We can provide a basis for a similar treatment of the motion of an unlocalized crystal electron by a similar development in Bloch functions for the field-free crystal, and Houston functions in the presence of a field.

The results for Bloch functions $\psi(\bar{k},\bar{r}) = e^{i\bar{k}\cdot\bar{r}}\, u_{\bar{k}}(\bar{r})$ can be worked out using the results of Appendix 6.3. We find

$$\langle\psi_{\sigma\to 0}(k_0)|\psi_{\sigma\to 0}(k_0)\rangle = 1$$

$$\langle\psi_{\sigma\to 0}(k_0)|k|\psi_{\sigma\to 0}(k_0)\rangle = k_0$$

$$\langle\psi_{\sigma\to 0}(k_0)|k^2|\psi_{\sigma\to 0}(k_0)\rangle = \lim_{\sigma\to 0}\,(\sigma^2+k_0^2) = k_0^2$$

$$\langle\psi_{\sigma\to 0}(k_0)|x|\psi_{\sigma\to 0}(k_0)\rangle = X_{nn}(k_0) + \frac{t}{\hbar}\frac{\partial E}{\partial k_x}\,(k_0)$$

$$\langle\psi_{\sigma\to 0}(k_0)|x^2|\psi_{\sigma\to 0}(k_0)\rangle - |\langle\psi_{\sigma\to 0}(k_0)|x|\psi_{\sigma\to 0}(k_0)\rangle|^2$$

$$= \lim_{\sigma\to 0}\left[\frac{1}{4\sigma^2} + \Xi(k_0) - |X_{nn}(k_0)|^2\right] \to \infty$$

where $\Xi(k_0) = \dfrac{(2\pi)^3}{\Omega}\displaystyle\int \frac{\partial u^*(k_0)}{\partial k_x}\,\frac{\partial u(k_0)}{\partial k_x}\,d\bar{r}$

and Ω is the volume of a unit cell.

The calculation for Houston functions wave packets differs from that for Bloch functions only in that the time dependence of the Bloch function

$$\exp\left[-\frac{i}{\hbar}E(k)t\right]$$

is replaced by

$$\exp\left[-\frac{i}{e\varepsilon}\int_{k_x}^{k_x+\frac{e\varepsilon t}{\hbar}}E^{(1)}(\bar{k}')dk'_x\right]$$

so that the differentiation with respect to k_x yields

$$\frac{\partial}{\partial k_x}\exp\left[-\frac{i}{e\varepsilon}\int_{k_x}^{k_x+\frac{e\varepsilon t}{\hbar}}E^{(1)}(\bar{k}')dk'_x\right]=$$

$$=-\frac{i}{e\varepsilon}\left[E^{(1)}\left(k_x+\frac{e\varepsilon t}{\hbar}\right)-E^{(1)}(k_x)\right]\exp\left[-\frac{i}{e\varepsilon}\int_{k_x}^{k_x+\frac{e\varepsilon t}{\hbar}}E^{(1)}(\bar{k}')dk'_x\right]$$

and we find, for infinitely narrow gaussian wave packets starting from rest

$$\langle x\rangle_{\sigma\to 0}=\frac{1}{e\varepsilon}\left[E\left(\frac{e\varepsilon t}{\hbar}\right)-E(0)\right]-X_{nn}(0)$$

$$\langle x^2\rangle_{\sigma\to 0}\to\infty$$

Thus we finally verify that in the absence of collisions or tunneling a Houston function does indeed describe Zener oscillations with a precisely defined phase and completely undeterminate position.

We originally constructed the Houston representation as an equal-weight superposition of all the Stark states. It is of interest to invert this procedure and determine the superposition of Houston functions that is needed to form a Stark state.

The Houston function

$$\psi(\bar{r},t) = \sqrt{\kappa}\,\psi\left(\frac{e\varepsilon t}{\hbar}\right)e^{-\frac{i}{e\varepsilon}\int_{k_x(0)}^{k_x(0)+\frac{e\varepsilon T}{\hbar}} E^{(1)}(\bar{k}')dk'_x}$$

can be written in the form

$$\psi(\bar{r},t) = \sqrt{\kappa}\int dk_x \delta\left(k_x - k_x(0) - \frac{e\varepsilon t}{\hbar}\right)\psi(\bar{k},\bar{r})e^{-\frac{i}{e\varepsilon}\int_{k_x(0)}^{k_x} E^{(1)}(\bar{k}')dk'_x}$$

and with the Fourier series representation for the δ-function

$$\delta\left(k_x - k_x(0) - \frac{e\varepsilon t}{\hbar}\right) = \frac{1}{\kappa}\sum_{\nu} \exp i\left[\frac{2\pi\nu}{\kappa}\left(k_x - k_x(0) - \frac{e\varepsilon t}{\hbar}\right)\right]$$

a wave packet of Houston functions with weight $f(k_x(0))$ becomes

$$\frac{1}{\sqrt{\kappa}}\int dk_x \psi(\bar{k},\bar{r})\int dk_x(0) f(k_x(0))\sum_{\nu} \exp\frac{i2\pi\nu}{\kappa}\left(k_x - k_x(0) - \frac{e\varepsilon t}{\hbar}\right).$$

$$\cdot e^{-\frac{i}{e\varepsilon}\int_{k_x(0)}^{0} E^{(1)}(\bar{k}')dk'_x} e^{-\frac{i}{e\varepsilon}\int_{0}^{k_x} E^{(1)}(\bar{k}')dk'_x}$$

$$= \int dk_x \psi(\bar{k},\bar{r}) \sum_{\nu} \phi_{\nu}(\bar{k},t)\int dk_x(0) f(k_x(0)) e^{-\frac{i2\pi\nu}{\kappa}k_x(0)}$$

$$e^{+\frac{i}{e\varepsilon}\int_{0}^{k_x(0)} E^{(1)}(\bar{k}')dk'_x}$$

where we have recognized the functional form of the Stark wave functions as in Equation (8).

We see that a wave packet of Houston states $\psi(k_{x0},\bar{r},t)$ of the form

$$\int dk_x(0) f(k_x(0))\psi(k_{x0},\bar{r},t)$$

is equivalent to a wave packet of Stark states $\int dk\phi_\nu(\bar{k},t)\psi(\bar{k},\bar{r})$ of the form

$$\sum g(\nu)\int d\bar{k}\phi_\nu(\bar{k},t)\psi(\bar{k},\bar{r})$$

$$\text{if } g(\nu) = \int dk_x(0)f(k_x(0))e^{\frac{i}{e\varepsilon}\int_0^{k_x(0)} E^{(1)}(\bar{k}')dk'_x} e^{-\frac{i2\pi\nu}{\kappa}k_x(0)},$$

the coefficient in the Fourier expansion of

$$f(k_x(0))\exp\left[\frac{i}{e\varepsilon}\int_0^{k_x(0)} E^{(1)}(\bar{k}')dk'_x\right].$$

Therefore to construct a single Stark state, say with index ν_0, energy E_{ν_0}, we must have $g(\nu) = \delta_{\nu\nu_0}$ which will result if

$$f(k_x(0)) = \exp\left[\frac{-i}{e\varepsilon}\int_0^{k_x(0)} E^{(1)}(\bar{k}')dk'_x\right]\exp\left[-\frac{i2\pi\nu}{\kappa}k_x(0)\right].$$

3.3 STARK STATES

We have introduced the Stark states in Chapter 2, 2.1.3 above, and related them to the Houston states in that section, and in Chapter 3, 3.2. The wave function of a Stark state is localized by the requirement that the kinetic energy of a carrier in such a state be non-negative. In the present section we shall study the details of this localization.

Apart from tunneling, the Stark states are stationary states of crystal electrons in an applied field. The question whether a crystal has exactly stationary states in a field (the existence of "closed bands") has been discussed by Wannier and Fredkin (9), but this question has little bearing on the problem we are addressing. We can view tunneling as a perturbation that produces an energy uncertainty in the Stark levels. The magnitude of this uncertainty affects the

observability of the Stark ladder, and it has been argued (4) we believe incorrectly, that it is large enough to destroy the ladder. Independently of this argument, however, we shall show that in the moderate fields of interest to us, the carrier localization is negligibly affected by the energy uncertainty.

The wave function of a Stark state can be expressed as a superposition of Bloch functions

$$\psi_\nu(\bar{r},t) = e^{-\frac{i}{\hbar} E_\nu t} \psi_\nu(\bar{r})$$

where $\psi_\nu(\bar{r}) = \int_{-\kappa/2}^{\kappa/2} dk_x \phi_\nu(\bar{k}) \psi(\bar{k},\bar{r})$

and $\phi_\nu(\bar{k}) = \kappa^{-1/2} \exp\left[\frac{i}{e\varepsilon}\left(E_\nu k_x - \int_0^{k_x} E^{(1)}(\bar{k}')dk'_x\right)\right]$.

As in Equation (7), we assume definite values of k_y, k_z. Such a choice is in no way restrictive, since $\bar{k}_\perp = (0,k_y,k_z)$ is conserved throughout all computation.

The Stark state $\psi_{\nu n}(\bar{r})$ is an eigenstate of the one-band Hamiltonian of the nth band

$$H_n \psi_{\nu n}(\bar{r}) = E_{\nu n} \psi_n(\bar{r}).$$

More precisely, this expression means that the E_ν are eigenvalues of the Schroedinger equation if the interband terms are neglected. The statement can be interpreted to mean that ψ_ν, E_ν are the eigenfunctions and eigenvalues of a truncated Hamiltonian H_n whose (field-free Bloch) eigenfunctions have $X_{mn}=0$, $m\neq n$. In keeping with this interpretation, it can be shown that the ψ_ν are orthogonal and form a basis (Appendix

6.1). We also show in Appendix 6.2 that the Stark levels E_ν give the expectation values of the complete Hamiltonian

$$\langle\psi_\nu(\bar{r},t)|H_{total}|\psi_\nu(\bar{r},t)\rangle = E_\nu$$

where H_{total} includes the untruncated crystal Hamiltonian and the electric field

$$H_{total} = \frac{p^2}{2m} + V(\bar{r}) - e\mathcal{E}x.$$

The energy eigenvalue E_ν of the Stark state ψ_ν is given by

$$E_\nu = \frac{2\pi\nu e\mathcal{E}}{\kappa} + \frac{1}{\kappa}\int_{-\kappa/2}^{\kappa/2} E^{(1)}(\bar{k})dk_x$$

$$= \frac{2\pi\nu e\mathcal{E}}{\kappa} + \langle E^{(1)}\rangle_\kappa$$

where we have defined the notation

$$\langle f\rangle_\kappa = \frac{1}{\kappa}\int_{-\kappa/2}^{\kappa/2} f dk_x \ .$$

The localization of the state is described by the expectation value of the position $\langle\nu|x|\nu\rangle$ and by its root mean square deviation

$$\Delta x = \left[\langle\nu|x^2|\nu\rangle - |\langle\nu|x|\nu\rangle|^2\right]^{1/2}$$

We show this calculation in detail, since it is useful in the study of Stark state wave packets.

$$\langle\nu|x|\nu\rangle = \int\int dk_x' dk_x \phi_\nu^*(\bar{k}')\ \phi_\nu(\bar{k}) \int d\bar{r}\psi^*(\bar{k}',\bar{r}) x \psi(\bar{k},\bar{r})$$

$$= \int_{-\kappa/2}^{\kappa/2} dk_x' \phi_\nu^*(\bar{k}') \int_{-\kappa/2}^{\kappa/2} dk_x \delta(\bar{k}-\bar{k}') \left(i \frac{\partial}{\partial k_x} + X_{nn}(\bar{k}) \right) \phi_\nu(\bar{k})$$

$$= \int_{-\kappa/2}^{\kappa/2} dk_x \phi_\nu^*(\bar{k}) \left[\frac{(i)^2}{e\varepsilon} (E_\nu - E^{(1)}(\bar{k})) + X_{nn}(\bar{k}) \right] \phi_\nu(\bar{k})$$

$$= \frac{1}{\kappa} \int_{-\kappa/2}^{\kappa/2} \left[\frac{(i)^2}{e\varepsilon} (E_\nu - E^{(1)}(\bar{k}) + X_{nn}(\bar{k}) \right] dk_x$$

$$= - \frac{2\pi\nu}{\kappa} + \langle X_{nn} \rangle_\kappa \tag{9}$$

where we have used $\phi_\nu^* \phi_\nu = \kappa^{-1}$.

Similarily

$$\langle\nu|x^2|\nu\rangle = \int_{-\kappa/2}^{\kappa/2} \int dk_x' dk_x \phi_\nu^*(\bar{k}') \phi_\nu(\bar{k}) \int d\bar{r}\psi(\bar{k}',\bar{r}) x^2 \psi(\bar{k},\bar{r})$$

$$= \int_{-\kappa/2}^{\kappa/2} dk_x \phi_\nu^*(\bar{k}) \left(- \frac{\partial^2}{\partial k_x^2} + 2i X_{nn}(\bar{k}) \frac{\partial}{\partial k_x} + i \frac{\partial X_{nn}}{\partial k_x} + \Xi_{nn} \right) \phi_\nu(\bar{k}).$$

Now

$$\frac{\partial}{\partial k_x} \phi_\nu(\bar{k}) = \left[\frac{i}{e\varepsilon} (E_\nu - E^{(1)}(\bar{k}) \right] \phi_\nu(\bar{k}) \tag{10}$$

$$\frac{\partial^2}{\partial k_x^2} \phi_\nu(\bar{k}) = \left[\frac{i}{e\varepsilon} (E_\nu - E^{(1)}(\bar{k})) \right]^2 \phi_\nu(\bar{k}) - \frac{i}{e\varepsilon} \frac{\partial E^{(1)}(\bar{k})}{\partial k_x} \phi_\nu(\bar{k})$$

$$= \left[- \frac{1}{e^2\varepsilon^2} (E_\nu^2 + E^{(1)}(\bar{k})^2 - 2E^{(1)}(\bar{k}) E_\nu) - \frac{i}{e\varepsilon} \frac{\partial E^{(1)}(\bar{k})}{\partial k_x} \right] \phi_\nu(k) \tag{11}$$

so

$$\langle\nu|x^2|\nu\rangle = \frac{1}{\kappa}\int_{-\kappa/2}^{\kappa/2} dk_x \left[\frac{1}{e^2q^2}(E_\nu^2+E^{(1)}(\bar{k})^2-2E^{(1)}(\bar{k})E_\nu) - \frac{i}{e\varepsilon}\frac{\partial E^{(1)}}{\partial k_x}\right.$$

$$\left. + 2iX_{nn}\frac{i}{e\varepsilon}(E_\nu - E^{(1)}(\bar{k})) + i\frac{\partial X_{nn}}{\partial k_x} + \Xi_{nn}(\bar{k})\right]$$

Since κ is a reciprocal lattice vector, the imaginary terms properly vanish. The expression can be simplified somewhat by using $E^{(1)}(\bar{k}) = E(\bar{k}) - e\varepsilon X_{nn}$, yielding

$$\langle\nu|x^2|\nu\rangle = \left\langle\frac{1}{e^2\varepsilon^2}(E_\nu - E(\bar{k}))^2 - X_{nn}^2(\bar{k}) + \Xi_{nn}(\bar{k})\right\rangle_\kappa \tag{12}$$

To compute Δx, we write

$$\langle\nu|x|\nu\rangle = -\frac{2\pi\nu}{\kappa} + \langle X_{nn}\rangle_\kappa = -\frac{E_\nu}{e\varepsilon} + \frac{1}{e\varepsilon}\langle E^{(1)}(\bar{k})\rangle_\kappa + \langle X_{nn}\rangle_\kappa$$

$$= \frac{1}{e\varepsilon}(-E_\nu + \langle E(\bar{k})\rangle_\kappa)$$

so

$$|\langle\nu|x|\nu\rangle|^2 = \frac{1}{e^2\varepsilon^2}(E_\nu^2 + |\langle E(\bar{k})\rangle_\kappa|^2 - 2E_\nu\langle E(\bar{k})\rangle_\kappa)$$

and

$$(\Delta x)^2 = \frac{1}{e^2E^2}\left[\langle E^2(\bar{k})\rangle_\kappa - |\langle E(\bar{k})\rangle_\kappa|^2\right] + \langle -X_{nn}^2 + \Xi_{nn}\rangle_\kappa$$

This result is easily interpreted. If we consider the "classical" Zener trajectory, described by

$$x(t) - x(0) = \frac{1}{e\varepsilon}\left[E(\bar{k}(t)) - E(\bar{k}(0))\right]$$

where $\bar{k}(t) = \bar{k}(0) + \frac{1}{\hbar}e\bar{\varepsilon}t$, we can compute the mean square displacement along this trajectory as a time average. We find

$$\langle x(t)\rangle_t = \frac{1}{e\varepsilon}\left[\frac{1}{T}\int_0^T E(\bar{k}(t))dt - E(\bar{k}(0))\right]$$

$$= \frac{1}{e\varepsilon}\left[\frac{e\varepsilon}{\hbar\kappa}\int_0^{\kappa} E(\bar{k}(t))\,\frac{dk_x}{dk_x/dt} - E(\bar{k}(0))\right]$$

$$= \frac{1}{e\varepsilon}\left[\frac{\hbar}{\hbar\kappa}\int_0^{\kappa} E(\bar{k}(t))dk_x - E(\bar{k}(0))\right]$$

$$= \frac{1}{e\varepsilon}\left[\langle E(\bar{k})\rangle_{\kappa} - E(k(\bar{0}))\right]$$

where we have used $T = \frac{\hbar\kappa}{e\varepsilon}$, the Zener oscillation period. Similarly

$$\langle x^2(t)\rangle_t = \frac{1}{e^2\varepsilon^2}\,\frac{1}{T}\int dt\left[E^2(\bar{k}) - 2E(\bar{k})E(0) - E^2(0)\right]$$

$$= \frac{1}{e^2\varepsilon^2}\,\frac{e\varepsilon}{\hbar\kappa}\left[\int_0^{\kappa}\frac{E^2(\bar{k})dk_x}{dk_x/dt} - 2E(0)\int_0^{\kappa}\frac{E(\bar{k})dk_x}{dk_x/dt} + E^2(0)\right]$$

$$= \frac{1}{e^2\varepsilon^2}\left[\frac{1}{\kappa}\int_0^{\kappa}E^2(\bar{k})dk_x - 2E(0)\,\frac{1}{\kappa}\int_0^{\kappa}E(\bar{k})dk_x + E^2(0)\right]$$

$$= \frac{1}{e^2\varepsilon^2}\left[\langle E^2(\bar{k})\rangle_{\kappa} - 2E(0)\langle E(\bar{k})\rangle_{\kappa} + E^2(0)\right]$$

and

$$\langle x^2(t)\rangle - |\langle x(t)\rangle|^2 = \left[\langle E^2(\bar{k})\rangle_{\kappa} - 2E(0)\langle E(\bar{k})\rangle_{\kappa} + E^2(0)\right.$$

$$\left. - |\langle E(\bar{k})\rangle_{\kappa}|^2 - E^2(0) + 2E(0)\langle E(\bar{k})\rangle_{\kappa}\right]$$

$$= \frac{1}{e^2\varepsilon^2}\left[\langle E^2(\bar{k})\rangle_{\kappa} - |\langle E(\bar{k})\rangle_{\kappa}|^2\right]$$

which is seen to be identical with the squared uncertainty of position of a Stark state, except for a small term associated with the polarization of the band.

The crystal momentum expectation and uncertainty in a Stark state is

$$\langle \nu | k_x | \nu \rangle = 0$$

$$(\Delta k_x)^2 = \langle \nu | k_x^2 | \nu \rangle = \frac{\kappa^2}{12} .$$

This indicates that the crystal momentum is entirely indeterminate along the electron's trajectory in the Brillouin zone.

We can now see that both one-band Houston and Stark wave functions describe the Zener oscillations of a crystal electron, but in rather different ways. In Houston states the crystal momentum, which represents the phase of the Zener oscillation, is sharply defined, at the cost of complete delocalization of the electron. In a Stark state, the energy is sharply defined, and the electron is localized to the extent determined by the requirement of a positive kinetic energy, but the phase of the oscillation is random. According to Equation (11), the electron oscillation is centered about a lattice site, with a small shift due to the band's polarization. The amplitude of the oscillation, for the conduction band of GaAs, is of the order of 200 lattice parameters in a field of 200 kv/cm.

3.4 WAVE PACKETS OF STARK STATES

The most appropriate representation of a quantum mechanical system is normally determined by the experiment that is to be described. We have already suggested earlier that an electron thermally excited across the bandgap is unlocalized and might be represented by a Houston function. The excitation will usually be to the edge of a band, $\bar{k} = 0$ in a direct band gap semiconductor. This fixes the phase, but it

ignores the randomness of the excitation. One way to prepare a Stark state might be by Auger tunneling from a bound impurity level, giving a precisely defined total energy, again with a random phase.

Although both of these states represent electrons executing Zener oscillations, evidently neither is suited for the generation of coherent radiation.* As we pointed out in Chapter 3, 3.1, we can hope to find a coherent superposition of states in which both the position and the crystal momentum of the electrons are specified within the limits permitted by the uncertainty principle. Leaving aside for the time being the engineering problem of how such a state is to be prepared experimentally, we now discuss a possible way of constructing it from Stark states.

3.4.1 Minimum Uncertainty Product

For a pair of operators A, B, with commutator

$$[A,B] = iK$$

the uncertainty relation is

$$\Delta A \Delta B \geq \frac{1}{2} K \ .$$

We wish to construct a minimum uncertainty wave function, for which

$$\Delta A \Delta B = \frac{1}{2} K \ .$$

*An extreme (and rather ludicrous) example of this unsuitability of Houston states with a range of phases is offered by the filled valence band of an insulator. In an applied field, the motion of every electron in this band is governed by the equation $\hbar\dot{k} = q\mathcal{E}$, and it executes Zener oscillations. Furthermore, none of the electrons can be scattered, since there are no empty final states available. But, of course, the oscillations are unobservable, because there is perfect phase cancellation.

A gaussian wave packet of plane waves can describe the motion of an unaccelerated particle in vacuum. Such a wave packet can be constructed to have a minimum uncertainty product of position and momentum at a given time, but because the Schroedinger equation in vacuum is dispersive, the wave packet spreads and the minimum uncertainty product grows with time.

In the presence of a potential, there can exist minimum uncertainty wave packets that do not spread with time. An example is furnished by the Glauber states in the quadratic potential of a harmonic oscillator. As we mentioned in Chapter 3, 3.1, these eigenstates of the destruction operator do not spread, and they have a minimum uncertainty product of position and momentum, as well as of occupation number and phase. When the harmonic oscillator is a mode of the electromagnetic field, a Glauber state corresponds to maximally coherent radiation, as exemplified by laser light.

The minimum uncertainty product of the position x and crystal momentum k_x can be obtained from the commutator; for example, in a momentum representation

$$x = i \frac{\partial}{\partial k_x} + X_{nn}(\bar{k})$$

so

$$[x, k_x]\phi(\bar{k}) = xk_x\phi - k_x x\phi$$

$$= i\phi + ik_x \frac{\partial\phi}{\partial k_x} + X_{nn}k_x\phi - ik_x \frac{\partial\phi}{\partial k_x} - k_x X_{nn}\phi$$

$$= i\phi$$

and therefore

$$\Delta x \Delta k_x \geq \frac{1}{2} \quad .$$

3.4.2 Periodicity of Expectation Values

We propose to construct a normalized wave packet of Stark states

$$\psi(\bar{r},t) = \sum_{\nu=-\infty}^{\infty} f(\nu_0-\nu)\psi_\nu(\bar{r})e^{-\frac{1}{\hbar}E_\nu t}$$

with $\sum_{-\infty}^{\infty} |f(\nu_0-\nu)|^2 = 1$

and with the additional constraint, imposed in order to simplify the calculation of certain averages, that the weighting function be symmetric about ν_0,

$$f(\nu_0-\nu)=f(\nu_0+\nu)$$

We can generalize the calculation of Chapter 3, 3.3 of the expectation values and uncertainties of position and crystal momentum.

Let A be an operator having the property

$$\langle \bar{k}',\bar{r}|A|\bar{k},\bar{r}\rangle \phi_\nu(\bar{k}) = \delta(k_x'-k_x)\left[G_\nu(\bar{k}_x)\phi_\nu(\bar{k})+C_\nu\phi_\nu(\bar{k})\right]$$

with $|\bar{k},\bar{r}\rangle$ Bloch functions and ϕ_ν the Stark state envelopes as defined above. The operators x,x^2, k_x, k_x^2 are all of this type. We can now establish that the expectation value of such an operator for a Stark state wave packet $\psi(\bar{r},t)$ is periodic with the period of the Zener oscillation:

$$\langle\psi(\bar{r},t)|A|\psi(\bar{r},t)\rangle \equiv \langle A\rangle_{f_\nu} =$$

$$= \int d\bar{r} \sum_\mu f^*(\nu_0-\mu) \int_{-\kappa/2}^{\kappa/2} dk'_x \phi^*_\mu(\bar{k}')\psi(\bar{k}'\bar{r})A\, e^{\frac{i}{\hbar}(E_\mu-E_\nu)t}$$

$$\sum_\nu f(\nu_0-\nu) \int_{-\kappa/2}^{\kappa/2} dk_x \phi_\nu(\bar{k})\psi(\bar{k},\bar{r})$$

$$= \sum_\mu \sum_\nu f^*(\nu_0-\mu) f(\nu_0-\nu) e^{\frac{i}{\hbar}(E_\mu-E_\nu)t} \int_{-\kappa/2}^{\kappa/2} \int dk'_x dk_x \phi^*_\mu(k') \delta(k'_x-k_x) \cdot$$

$$\left[G(k_x)\phi_\nu(\bar{k}) + C_\nu\phi_\nu(\bar{k})\right]$$

$$= \sum_\mu \sum_\nu f^*(\nu_0-\mu) f(\nu_0-\nu) e^{\frac{i}{\hbar}(E_\mu-E_\nu)t} \cdot \frac{1}{\kappa} \int_{-\kappa/2}^{\kappa/2} e^{\frac{i}{e\varepsilon} k_x (E_\nu-E_\mu)}$$

$$\left[G_\nu(k_x)+C_\nu\right]dk_x$$

since $\phi_\mu^*\phi_\nu = \frac{1}{\kappa} e^{\frac{i}{e\varepsilon} k_x (E_\nu-E_\mu)}$.

But $E_\nu - E_\mu = (\nu-\mu)\frac{2\pi e\varepsilon}{\kappa}$.

and hence the last term vanishes except when $\mu=\nu$, and

$$\langle A\rangle_{f_\nu} = \sum_\mu \sum_\nu f^*(\nu_0-\mu) f(\nu_0-\nu) e^{\frac{i}{\hbar}(E_\nu-E_\mu)t} \cdot \frac{1}{\kappa} \int dk_x G_\nu(k_x) e^{i2\pi(\nu-\mu)\frac{k_x}{\kappa}}$$

$$+ \sum_\nu |f(\nu_0-\nu)|^2 C_\nu$$

With $\alpha=\nu-\mu$ we can rewrite this

$$\langle A\rangle_{f_\nu} = \sum_\alpha e^{i\alpha\left(\frac{2\pi e\varepsilon}{\hbar\kappa}\right)t} \sum_\nu f^*(\nu_0-\nu+\alpha) f(\nu_0-\nu) \frac{1}{\kappa} \int_{-\kappa/2}^{\kappa/2} dk_x G_\nu(k_x) e^{\frac{i2\pi\alpha k_x}{\kappa}}$$

$$+ \sum_\nu |f(\nu_0-\nu)|^2 C_\nu\}$$

which can be recognized as a Fourier series representing a periodic function of period $\hbar\kappa/e\varepsilon$ (the Zener oscillation period), with coefficients

$$\sum_{\nu} f^*(\nu_0-\nu+\alpha) f(\nu_0-\nu) \left[F_\alpha(G_\nu) + C_\nu \delta_{\alpha 0} \right]$$

where

$$F_\alpha(F(k_x)) \equiv \frac{1}{\kappa} \int_{-\kappa/2}^{\kappa/2} dk_x F(k_x) e^{i2\pi\alpha \frac{k_x}{\kappa}}$$

This means that for such a wave packet of Stark states not only the expectation values $\langle x \rangle$ and $\langle k_x \rangle$ recur periodically, as might indeed have been anticipated, but also all their moments. The wave packet reforms to its original shape after a period of oscillation. It may deform as it oscillates, but there is no long-term spreading. In this respect the Zener oscillation is similar to the motion of a harmonic oscillator, and unlike that of a free particle.

The reason for the periodicity in time of the packet wave function is the uniform energy spacing of the Stark levels. Since the time dependence of each of the wave functions in the superposition is of the form $\exp\left[(i/\hbar)E_\nu t\right]$ with each energy an integral multiple of $\hbar\,\omega_{zener}$, the periodicity follows immediately.

3.4.3 Position and Momentum Uncertainties

The time-dependent crystal momentum expectation value of k_x is

$$\langle k_x \rangle_{f_\nu} = \sum e^{i\alpha\left(\frac{2\pi e\varepsilon}{\hbar\kappa}\right) t} g(\alpha) F_\alpha(k_x) \qquad (13)$$

where $g(\alpha) \equiv \sum_{\nu=-\infty}^{\infty} f^*(\nu_0-\nu+\alpha) f(\nu_0-\nu)$

and (see Appendix 6.4)

$$F_\alpha(k_x) = \begin{cases} (-1)^\alpha \frac{\kappa}{i2\pi\alpha} & \alpha \neq 0 \\ 0 & \alpha = 0 \end{cases}$$

Similarly (Appendix 6.4)

$$\langle k_x^2 \rangle_{f_\nu} = \frac{\kappa^2}{12} + \sum_{\alpha \neq 0} (-1)^\alpha \frac{\kappa^2}{2\pi^2\alpha^2} e^{i\alpha \left(\frac{2\pi e\epsilon}{\hbar\kappa}\right) t} g(\alpha) \tag{14}$$

The spread in k_x of the wave packet, given by

$$(\Delta k_x(t))^2 = \langle k_x^2(t) \rangle_{f_\nu} - |\langle k_x(t) \rangle|^2_{f_\nu}$$

varies in a complicated fashion in the course of an oscillation period, but because of the periodicity of the wave packet, it is easy to obtain a time average. We have

$$\frac{1}{T}\int_0^T |\langle k_x \rangle_{f_\nu}|^2 dt = \frac{1}{T}\int_0^T dt \sum_\beta \sum_\alpha e^{i(\alpha-\beta)\left(\frac{2\pi e\epsilon}{\hbar\kappa}\right) t} g^*(\beta) g(\alpha) F_\beta^*(k_x) F_\alpha(k_x)$$

$$= \sum_\alpha |g(\alpha)|^2 |F_\alpha(k_x)|2 = \sum_{\alpha \neq 0} \left(\frac{\kappa}{2\pi}\right)^2 \frac{|g(\alpha)|^2}{\alpha^2}$$

and

$$\frac{1}{T}\int_0^T \langle k_x^2 \rangle_{f_\nu} dt = \frac{\kappa^2}{12}$$

so that

$$\frac{1}{T}\int_0^T (\Delta k_x(t))^2 dt = \frac{\kappa^2}{12} - \sum_{\alpha \neq 0} \left(\frac{\kappa}{2\pi}\right)^2 \frac{|g(\alpha)|^2}{\alpha^2} \tag{15}$$

To compute the expectation value of x we use the result (see Equation (9))

$$\langle \bar{k}, \bar{r} | x | \bar{k}, \bar{r} \rangle \phi_\nu(\bar{k}) = \frac{1}{e\epsilon} \left[E_\nu - E(\bar{k})\right] \phi_\nu(\bar{k})$$

so that

$$\langle x\rangle_{f_\nu} = -\frac{1}{e\varepsilon}\sum_\nu |f(\nu_0-\nu)|^2 E_\nu + \frac{1}{e\varepsilon}\sum_\alpha e^{i\alpha\left(\frac{2\pi e\varepsilon}{\hbar\kappa}\right)t} g(\alpha)F_\alpha(E(\bar{k}))$$

The term in E_ν can be simplified if we invoke the postulated symmetry $f(\nu_0-\nu) = f(\nu_0+\nu)$:

$$\sum_\nu |f(\nu_0-\nu)|^2 E_\nu = E_{\nu_0}|f(0)|^2 + \sum_{-\infty}^{\nu_0-1}|f(\nu_0-\nu)|^2 E_\nu + \sum_{\nu_0+1}^{\infty}|f(\nu_0-\nu)|^2 E_\nu$$

$$= E_{\nu_0}|f(0)|^2 + \sum_{\alpha=1}^{\infty}|f(\alpha)|^2 (E_{\nu_0+\alpha} + E_{\nu_0-\alpha})$$

but

$$E_{\nu_0+\alpha} + E_{\nu_0-\alpha} = 2E_{\nu_0}$$

and

$$2\sum_{\alpha=1}^{\infty}|f(\alpha)|^2 = 1 - |f(0)|^2$$

hence

$$\sum_\nu |f(\nu_0-\nu)|^2 E_\nu = E_{\nu_0}$$

and

$$\langle x\rangle_{f_\nu} = \frac{1}{e\varepsilon}\left(-E_{\nu_0} + \sum_\alpha e^{i\alpha\left(\frac{2\pi e\varepsilon}{\hbar\kappa}\right)t} g(\alpha)F_\alpha(E(\bar{k}))\right).$$

The time average over one period of $|\langle x\rangle_{f_\nu}|^2$ is

$$\frac{1}{T}\int_0^T dt\,|\langle x_{f_\nu}\rangle|^2 = \frac{1}{e^2\varepsilon^2}\left[E_{\nu_0} + \sum_\alpha |g(\alpha)|^2 |F_\alpha(E(\bar{k}))|^2 - 2E_{\nu_0}\langle E(\bar{k})\rangle_\kappa\right].$$

Finally the expectation value of x^2 is

$$\langle x^2\rangle_{f_\nu} = \frac{1}{e^2\varepsilon^2}\sum_\nu |f(\nu_0-\nu)|^2 E_\nu^2$$

$$+\sum_\infty e^{i\alpha\left(\frac{2\pi e\varepsilon}{h\kappa}\right)t}\left\{g(\alpha)F_\alpha\left(\frac{E(\bar{k})^2}{e^2\varepsilon^2} - X_{nn}^2(\bar{k}) + \Xi_{nn}(\bar{k})\right)\right.$$

$$\left. -\left[\sum_\nu 2(E_\nu+E_{\nu-\alpha})f^*(\nu_0-\nu+\alpha)f(\nu_0-\nu)\right]F_\alpha\left[\frac{E(\bar{k})}{e\varepsilon}\right]\right\}$$

The first term of this rather complicated expression can be simplified:

$$\sum_\nu E_\nu^2|f(\nu_0-\nu)|^2 = E_{\nu_0}^2|f(0)|^2 + \sum_{\alpha=1}^{\infty}|f(\alpha)|^2(E_{\nu_0+\alpha}^2 + E_{\nu_0-a}^2)$$

and

$$E_{\nu_0+\alpha}^2 + E_{\nu_0-\alpha}^2 = (E_{\nu_0+\alpha} + E_{\nu_0-\alpha})^2 - 2E_{\nu_0-a}E_{\nu_0+\alpha}$$

$$= (2E_{\nu_0})^2 - 2\left[(\nu_0^2-\alpha^2)\left(\frac{2\pi e\varepsilon}{\kappa}\right)^2 + 2\nu_0\frac{2\pi e\varepsilon}{\kappa}\langle E^{(1)}\rangle_\kappa + \langle E^{(1)}\rangle_\kappa^2\right]$$

$$= 2E_{\nu_0}^2 + 2\alpha^2\left(\frac{2\pi e\varepsilon}{\kappa}\right)^2$$

because $E_\nu = \frac{2\pi\nu}{\kappa}e\varepsilon + \langle E^{(1)}\rangle_\kappa$

and so, using also $2\sum_{\alpha=1}^{\infty}|f(\alpha)|^2 = 1 - |f(0)|^2$

$$\sum_\nu E_\nu^2|f(\nu_0-\nu)|^2 = E_{\nu_0}^2 + 2\sum_{\alpha=1}^{\infty}\left(\frac{2\pi e\varepsilon}{\kappa}\right)^2\alpha^2|f(\alpha)|^2.$$

The time average of $\langle x^2(t)\rangle_{f_\nu}$ is (see Equation (12))

$$\frac{1}{T}\int_0^T dt\langle x^2\rangle_{f_\nu} = \frac{1}{e^2\varepsilon^2}E_{\nu_0}^2 + 2\sum_{\alpha=1}^{\infty}\left(\frac{2\pi}{\kappa}\right)^2\alpha^2|f(\alpha)|^2$$

$$+\left\langle\frac{E^2(\bar{k})}{e^2\varepsilon^2} - X_{nn}^2(\bar{k}) + \Xi_{nn}(\bar{k}) - 2E_{\nu_0}\frac{E(\bar{k})}{e^2\varepsilon^2}\right\rangle_\kappa.$$

The squared uncertainty of position is

$$(\Delta x(t))^2 = \langle x^2 \rangle_{f_\nu} - |\langle x \rangle_{f_\nu}|^2$$

with time average

$$\frac{1}{T}\int_0^T dt(\Delta x(t))^2 = 2\sum_{\alpha=1}^{\infty}\left(\frac{2\pi}{\kappa}\right)^2\alpha^2|f(\alpha)|^2 - \frac{1}{e^2\varepsilon^2}\sum_{\alpha=-\infty}^{\infty}|g(\alpha)|^2 F_\alpha(E(\bar{k}))|^2$$

$$+ \frac{1}{e^2\varepsilon^2}\left[\langle E(\bar{k})^2\rangle_\kappa\right] - X_{nn}^2(\bar{k}) + \Xi_{nn}(\bar{k}) \qquad (16)$$

3.4.4 Uncertainty Product and Band Structure

We have now worked out the expectation values for wave packets of Stark states of k_x, k_x^2, x, and x^2. These quantities are periodic functions of time, with the Zener oscillation period. If the weighting function $f(\nu_0-\nu)$ goes to $\delta_{\nu\nu_0}$, the expectation values reduce to those of a Stark state.

If the uncertainty product $\Delta x(t)\Delta k_x(t) = I(t)$ takes the value $I(t_0)$, at time t_0, it will in general change with time, and will return to $I(t_0)$ at $t = t_0 + T$, where $T = \kappa h/e\varepsilon$. Thus if a weighting function $f(\nu_0-\nu)$ is chosen to minimize $I(t_0)$, it will not in general produce a minimum uncertainty product at other times. Some optimization criterion should be chosen. The criterion will presumably depend on the application to be made, but some general remarks can be made.

One may wish to minimize the time average of I:

$$\frac{1}{T}\int_0^T I(t)dt = \langle I \rangle_T$$

or some combination of $\langle I \rangle_T$ and the fluctuations of I(t) over a cycle

$$\frac{1}{T}\int_0^T (I^2(t) - \langle I \rangle_T^2)dt$$

or the maximum value sup I(t).

Alternatively one might wish to minimize the spread of k_x or x. In every instance, the quantity to be deduced is the weight function $f(\nu)$. The determination of this weight function is now a mathematical design problem related to the optimization criterion that has been chosen.

In connection with this problem it should be observed that the expectation values we have computed contain the Fourier expansions of the band structure and polarization matrix elements $E(\bar{k})$, $X^2_{nn}(\bar{k})$ and $\Xi(\bar{k})$. A band structure of interest, that of the conduction band of GaAs, can be quite adequately described by five Fourier coefficients (see Chapter 4 below). We also know, from the discussion in Chapters 2, 2.3 and 3, 3.3, that the polarization matrix elements are negligible compared with the contribution of the band structure.

We can rewrite the squared momentum and position uncertainties, time averaged over an oscillation periods, from Equations (15) and (16):

$$\frac{1}{T}\int_0^T (\Delta k_x(t))dt = \frac{\kappa^2}{12} - \frac{\kappa^2}{2\pi^2}\sum_{\alpha=1}^{\infty}\frac{|g(\alpha)|^2}{\alpha^2} \tag{17}$$

$$\frac{1}{T}\int_0^T (\Delta x(t))^2 dt = \frac{1}{e^2\varepsilon^2}\left[\langle E(\bar{k})^2\rangle_\kappa - |\langle E(\bar{k})\rangle_\kappa|^2\right] + \langle \Xi_{nn} - X^2_{nn}\rangle_\kappa$$

$$- \sum_{\substack{\alpha=-\infty \\ \alpha\neq 0}}^{\alpha=\infty} |g(\alpha)|^2 |F_\alpha(E(\bar{k}))|^2$$

$$+ \sum_{\alpha=1}^{\infty} \frac{(2\pi)^2}{\kappa}\alpha^2 |f(\alpha)|^2 \tag{18}$$

In these formulas, the function $g(\alpha)$, it will be recalled, is defined in terms of the weighting function $f(\nu_0-\nu)$ as

$$g(\alpha) = \sum_{\nu=-\infty}^{\infty} f^*(\nu_0-\nu+\alpha) f(\nu_0-\nu).$$

This can be viewed as the autoconvolution of $f(\nu_0-\nu)$, and therefore $g(\alpha)$ will be somewhat broader than $f(\nu_0-\nu)$.

The leading terms of Equations (17) and (18) are the squared uncertainties $(\Delta k_x)^2$ and $(\Delta x)^2$ of a Stark state

$$(\Delta k_x)^2_\nu = \frac{\kappa^2}{12}$$

$$(\Delta x)^2_\nu = \frac{1}{e^2\mathcal{E}^2}\left[\langle E(\bar{k})^2\rangle_\kappa - |\langle E(\bar{k})\rangle_\kappa|^2\right] + \langle \Xi_{nn} - X^2_{nn}\rangle_\kappa$$

As we have pointed out in Chapter 3, 3.3, the position uncertainty of a pure Stark level is effectively accounted for by the size of the Zener oscillation orbit. We now see from Equation (18), that forming a wave packet of Stark states has two consequences: It broadens the uncertainty slightly (last term in Equation (18)), because adjacent "Stark orbits" are displaced from each other by (roughly) a lattice parameter; and it can lead to a much larger reduction due to the correlation of the orbits, with each harmonic of the band structure contributing to the reduction.

For example, for a sinusoidal band, as would be exhibited by an extreme tight-binding model

$$E(k_x) = -A \cos\ k_x a$$

the band-structure dependent dominant part of $(\Delta x)^2$ (neglecting the small broadening due to the last term in Equation (18)) becomes

$$(\Delta x)^2 \approx \frac{1}{e^2\varepsilon^2}\left[\langle E^2\rangle_\kappa - \langle E\rangle_\kappa^2 - \sum |g(\alpha)|^2 |F_\alpha(E)|^2\right]$$

$$= \frac{A}{e^2\varepsilon^2}\left(\frac{1}{2} - \frac{1}{2}|g(1)|^2\right) .$$

Furthermore, we see from Equations (13), (14) and (17) that the band structure does not affect the spread of crystal momentum.

3.4.5 An Example in the Tight-Binding Approximation

The detailed analysis and design of a wavepacket representing an experimental situation depends on the band structure of the semiconductor, and will require numerical work. Still it should be possible to obtain insights and observe trends which might be independent of the particular material, using simple models and analytical methods. One such model, the sinusoidal tight-binding band structure, was introduced in the last paragraph. We now study an example of the behavior of wave packets in a model solid with this band structure, a Real Equal Weight Packet.

We assume a superposition of Stark states centered on ν_0 with weights.

$$f(\nu-\nu_0) = \begin{cases} \frac{1}{\sqrt{N}} & -(N-1)/2 < (\nu-\nu_0) < (N-1)/2 \\ 0 & \text{otherwise} \end{cases}$$

It is easily found that

$$g(\alpha) = \sum_{\nu} f^*(\nu_0-\nu+\alpha)f(\nu_0-\nu) = (N-\alpha)/N$$

$$F_{\pm 1}[E(k)] = A/2 \qquad \text{all other } F_j[E(k)] = 0$$

$$F_0[E^2(k)] = A^2/2, \quad F_{\pm 2}[E^2(k)] = A^2/4, \quad \text{all other } F_j[E^2(k)] = 0$$

In addition the following needed expression can be reduced to a simpler form

$$C_1 = 2 \sum_{\nu} (E_\nu + E_{\nu+1})f^*(\nu_0-\nu-1)f(\nu_0-\nu)$$

$$= 2 \sum_{\alpha} (E_{\nu_0-\alpha} - E_{\nu_0-\alpha-1})f^*(\alpha + 1)f(\alpha)$$

$$= 4E_{\nu 0} \sum_{\alpha} f^*(\alpha + 1)f(\alpha)$$

$$-2\Delta E \sum_{\alpha} (2\alpha + 1)f^*(\alpha + 1)f(\alpha)$$

$$= 4E_{\nu 0} \sum_{\alpha} f^*(\alpha + 1)f(\alpha) = 4E_{\nu_0} g(1)$$

where we have used $f^*(-\alpha) = f(\alpha)$, true for a real wavepacket .

Let us use these results in order to compute the expectation $\langle x \rangle_{f(\nu)}$ and uncertainty Δx for the rectangular wavepacket. We find for our tight binding band

$$\langle x \rangle = \frac{1}{e\varepsilon} \left[-E_{\nu_0} + Ag(1) \cos \left(\frac{ae\varepsilon t}{\hbar} \right) \right]$$

$$\Delta x^2 = \frac{1}{e^2\varepsilon^2} \left[\sum_{\nu} |f(\nu-\nu_0)|^2 E_\nu^2 - E_{\nu_0}^2 \right.$$

$$+ \left(\frac{A^2}{2} - \frac{1}{2} A^2 g(1)^2 \right)$$

$$+ \left(2AE_{\nu_0} g(1) - \frac{A}{2} C_1 \right) \cos \frac{ae\varepsilon t}{\hbar}$$

$$\left. + \left(\frac{A^2}{2} g(2) - \frac{A^2}{2} g(1)^2 \right) \cos \frac{2ae\varepsilon t}{\hbar} \right]$$

Applying these formulas to our real rectangular wavepacket we find

$$\langle x \rangle = \frac{1}{e\varepsilon} \left[-E_{\nu_0} + A \left(\frac{N-1}{N} \right) \cos \left(\frac{ae\varepsilon t}{\kappa} \right) \right]$$

$$\Delta x^2 = \frac{1}{e^2\varepsilon^2} \left[2(ae\varepsilon)^2 \frac{1}{N} \sum_{\alpha=1}^{(N-1)/2} \alpha^2 \right.$$

$$+ A^2 \left(\frac{1}{2} - \frac{1}{2} \left(\frac{N-1}{N} \right)^2 \right)$$

$$\left. + A^2 \left(\frac{1}{2} \frac{(N-2)}{N} - \frac{1}{2} \left(\frac{N-1}{N} \right)^2 \right) \cos \frac{2ae\varepsilon t}{\kappa} \right]$$

with the series $\frac{2}{N} \sum_{\alpha=1}^{(N-1)/2} \alpha^2 = \frac{2}{N} \left\{ \frac{(N-1)/2}{6} \left(2((N-1)/2)^2 + 3 \frac{(N-1)}{2} + 1 \right) \right\}$

$$\approx \frac{N^2}{12} + \frac{N}{4} + \frac{1}{6} \approx \frac{N^2}{12} \text{ for N large}$$

Note that the amplitude of the oscillation increases rapidly with the number N of states in the packet. The "centroid" of a single state is

fixed; as more states are superposed, it oscillates, reaching a maximum amplitude corresponding to the width of the "classical" Zener orbit.

The position uncertainty Δx^2 contains a band-structure dependent term

$$\frac{A^2}{e^2\varepsilon^2}\left[\left(\frac{1}{2}-\frac{1}{2}\left(\frac{N-1}{N}\right)^2\right)+\left(\frac{1}{2}\frac{N-2}{N}-\frac{1}{2}\left(\frac{N-1}{N}\right)^2\right)\cos\frac{2ae\varepsilon t}{\hbar}\right]$$

which narrows as the number of states is increased, and a second term which asymptotically increases as N^2 for N very large.

This is indeed what one might expect on the basis of plausible reasoning. A single Stark state represents an electron which has a time-independent probability of being found at each point of its orbit--it is "spread out" over the entire orbit. As other states are superposed to form something like a coherent state, they interfere constructively in the vicinity of some point along the orbit, the probability density becomes localized and time dependent, more or less describing a classical oscillating particle.

This localization can narrow and persist only if the wave functions of the Stark states forming the packet overlap in space; that is to say, if the range of Stark energies E_n is less than the energy width 2A of the band, or the number of states is less than $2A/e\varepsilon a$. Stark states which are separated in energy by more than 2A do not overlap and cannot interfere; they contribute to a probability density extending beyond the "classical" Zener orbit, and contribute to an increase in Δx, which asymptotically becomes proportional to the size of the classically permitted region. The narrowest localization occurs for $N \tilde{=} 1.14\left(\frac{2A}{e\varepsilon a}\right)^{2/3}$.

3.4.6 Minimum Uncertainty Product Wavepackets

The rectangular wavepacket used in the preceding section was chosen arbitrarily. We should like now to attempt to select a wavepacket to minimize the uncertainty product $\Delta x \Delta k_x$. To facilitate this attempt we will first investigate the somewhat simpler problem of minimum uncertainty wavepackets in the field-free crystal, in a basis of Bloch functions. Since a minimum uncertainty product packet of plane wave states is known to be strongly time-dependent, we will only undertake to construct the packet at a time t at which the phase $\exp\left[-(i/\hbar)(t'-t)E(\bar{k})\right]$ of the Bloch wave is unity and the wave packet has the form

$$\psi = \frac{1}{\kappa}\int_{-\kappa/2}^{\kappa/2} dk_x \phi(k_x)\psi(\bar{k},\bar{r})$$

We will try now to derive the required wavepacket shape for which the minimum uncertainty possible allowed by the Heisenberg relation, is reached at a time t.

In order to attain this purpose we will use a method similar to that used to construct the Glauber States and the minimum uncertainty wavepacket of plane waves.

We showed that in the Bloch representation $[\bar{r},\bar{k}] = i$, which implies that $D(r_i)D(k_i) \geq \frac{1}{2}$.

Let us call $\phi_G(k_x)$ the state which satisfies the equality in this relation.

Let us look at the origin of the uncertainty relation

$$\frac{1}{2} = \frac{1}{2} \left|\langle\phi|[x,k_x]|\phi\rangle\right|$$

$$= \frac{1}{2} \left|\langle\phi|[\Delta x,\Delta k_x]|\phi\rangle\right|$$

where $\Delta x = x - \langle\phi|x|\phi\rangle$

$$\Delta k_x = k_x - \langle\phi|k_x|\phi\rangle$$

Using the triangle inequality we find

$$\frac{1}{2} = \frac{1}{2} \left|\langle\phi|[\Delta x,\Delta k_x]|\phi\rangle\right| \leq \left|\langle\phi|\Delta x\Delta k_x|\phi\rangle\right|$$

Using the Schwartz inequality we can further write:

$$\frac{1}{2} \leq \left[\langle\phi|\Delta x^2|\phi\rangle\right]^{1/2}\left[\langle\phi|\Delta k_x^2|\phi\rangle\right]^{1/2}$$

$$\frac{1}{2} \leq D(x)D(k_x)$$

The state ϕ_G which achieves the Schwartz equality should satisfy

$$\Delta k_x|\phi_G(k_x)\rangle = ib\Delta x|\phi_G(k_x)\rangle \tag{19}$$

where ib is an arbitrary imaginary constant. We will have to determine which number b realizes the triangle equality.

We can rewrite equation (19) as follows:

$$(k_x - ibx)\phi_G(k_x) = (\langle\phi_G|k_x|\phi_G\rangle - ib\langle\phi_G|x|\phi_G\rangle)\phi_G \tag{20}$$

We know that if $\phi_G(k_x)$ is also a solution of the crystal Hamiltonian perturbed by the electric field, then $\langle k_x\rangle$ and $\langle x\rangle$ will be periodic functions of time. In the ideal case $\phi_G(k_x)$ will satisfy the equality at all times. In a more restrictive case $\phi_G(k_x)$ will only satisfy the

equality at a given time. In any case the function $\phi_G(k_x)$, at all times or at a given time, will be a solution of equation (20).

Let us first solve the simpler equation (20) where

$$\langle k_x \rangle = K(t) \text{ and } \langle x \rangle = R(t)$$

Using $x = i\frac{\partial}{\partial k_x} + X_{nn}(\bar{k})$ we can rewrite (20) as follows

$$\left(k_x + b\frac{\partial}{\partial k_x} - ibX_{nn}(\bar{k}) \right)\phi_G(k_x) = \Delta(t)\phi(k_x)$$

$$\text{with } \Delta(t) = K(t) - ibR(t) \tag{21}$$

The general solution is

$$\phi_G(k_x) = C(t)e^{-\frac{1}{2b}k_x^2 + \frac{\Delta(t)}{b}k_x + i\int_0^{k_x} X(\bar{k})dk_x} \tag{22}$$

We will now proceed to a study of the proposed solution (22) of equation (20).

To normalize the wave packet, write

$$\phi_G(k_x) = e^{-\frac{k_x^2}{2b} + \frac{Kk_x}{b} + ik_xR} e^{i\int_0^{k_x} X(\bar{k})dk_x}$$

using $\frac{\Delta(t)}{b} = \frac{K-ibR}{b} = \frac{K}{b} - iR$.

Since $X_{nn}(\bar{k})$ is real

$$\phi_G^*(k_x)\phi_G(k_x) = |C|^2 e^{\frac{K^2}{2b}} e^{-\frac{(k_x-K)^2}{b}}$$

and the normalization is determined by

$$1 = |C|^2 \, e^{\frac{k^2(t)}{2b}} \int_{K(t)-\kappa/2}^{K(t)+\kappa/2} e^{-\frac{(k_x - K(t))^2}{b}} \, dk_x \, .$$

We find immediately

$$\langle \phi_k | k_x | \phi_k \rangle = K(t)$$

$$D^2(k_x) = \frac{1}{2} b, \quad b \to 0$$

To determine other expectation values, we rewrite

$$\phi_G(k_x) = C(t) e^{-\frac{1}{2b} k_x^2 + Dk_x + i \int_0^{k_x} X(\bar{k}') dk'_x}$$

with $D = \frac{\Delta(t)}{b} = \frac{K(t)}{b} - iR$

Let us derive the average $\langle x \rangle_G$

$$\langle \phi_G | \kappa | \phi_G \rangle = \langle \phi_G | i \frac{\partial}{\partial k_x} + X(\bar{k}) | \phi_G \rangle$$

$$= \int_{K(t)-\kappa/2}^{K(t)+\kappa/2} \phi_G^* \phi_G \left[i \left(- \frac{k_x}{b} + D + iX(\bar{k}) \right) + X(\bar{k}) \right] dk_x$$

$$= - i \frac{K}{b} + i \left(\frac{K}{b} - iR \right)$$

$$= R(t)$$

We see that the proposed solution (22) is a solution of equation (20) since $\langle k_x \rangle_G = K(t)$ and $\langle x \rangle_G = R(t)$. We have tested $\phi_G(k_x)$ against equation (20). However, we need to check also the triangle inequality.

For this purpose let us derive the deviation D(x) of our coherent state (see Appendix 6.3).

$$\langle\phi_G|x^2|\phi_G\rangle = \langle\phi_G|-\frac{\partial^2}{\partial k_x^2} + 2iX(\bar{k})\frac{\partial}{\partial k_x} - \Xi(\bar{k})|\phi_G\rangle$$

Let us first deal with $\langle -\frac{\partial^2}{\partial k_x^2}\rangle_G$

$$\langle -\frac{\partial^2}{\partial k_x^2}\rangle_G = -\int_{K-\kappa/2}^{K+\kappa/2} \phi_G^*(k_x)\frac{\partial}{\partial k_x}\left[\left(-\frac{k_x}{b} + D + iX(\bar{k})\right)\phi_G(k_x)\right]dk_x$$

$$\langle -\frac{\partial^2}{\partial k_x^2}\rangle_G = -\left\langle\left[-\frac{1}{b} + i\frac{\partial}{\partial k_x}X(\bar{k}) + \left(-\frac{k_x}{b} + D + iX(\bar{k})\right)^2\right]\right\rangle_G$$

Let us expand the square term

$$-\left(-\frac{k_x}{b} + D + iX\right)^2 = -\frac{k_x^2}{b^2} - D^2 + X^2(\bar{k}) + \frac{2D}{b}k_x - 2iX(\bar{k})\left(-\frac{k_x}{b} + D\right)$$

then we can write

$$\langle -\frac{\partial^2}{\partial k_x^2}\rangle_G = \int_{K-\kappa/2}^{K+\kappa/2}\left(\frac{1}{b} - \frac{k_x^2}{b^2} - D^2 + \frac{2D}{b}k_x\right)\phi_G^*\phi_G dk_x$$

$$+\int_{K-\kappa/2}^{K+\kappa/2} Y^2(\bar{k}) - 2iX(\bar{k})\left(-\frac{k_x}{b} + D\right) - i\frac{\partial}{\partial k_x}X(\bar{k})dk_x \quad (23)$$

We can evaluate the first term of the right hand side of (23)

$$\langle\frac{1}{b} - \frac{k_x^2}{b^2} - D^2 + \frac{2D}{b}k_x\rangle_G = \frac{1}{b} - D^2 + \frac{2D}{b}K - \frac{\langle k_x^2\rangle_G}{b^2}$$

$$= \frac{1}{b} - \left(\frac{K^2}{b^2} - R^2 - 2iR\frac{K}{b}\right) + \frac{2K}{b}\left(\frac{K}{b} - iR\right) - \frac{\langle k_x^2\rangle_G}{b^2}$$

$$= \frac{1}{b} - \frac{D(k_x)^2}{b^2} + R(t)^2$$

Then $\langle x^2 \rangle_G = \langle - \frac{\partial^2}{\partial k_x^2} + 2iX(\bar{k}) \frac{\partial}{\partial k_x} + \Xi(\bar{k}) \rangle_G$

$$= \frac{1}{b} - \frac{1}{b^2} D^2(k_x) + R^2(t) + \langle \Xi(\bar{k}) - X^2(\bar{k}) \rangle_G$$

Recall that $\langle \rangle_G$ means

$$\langle f \rangle_G = \int_{K-\kappa/2}^{K+\kappa/2} \phi_G^*(k_x) \phi_G(k_x) f(k_x) dk_x \ .$$

Since $\phi_G^* \phi_G$ and K are time-dependent, $\langle \rangle_G$ is also time dependent. Also note that $\langle \rangle_G \neq \langle \rangle_\kappa$.

The deviation $D^2(x)$ is

$$D^2(x) = \langle x^2 \rangle_G - \langle x \rangle_G^2 = \frac{1}{b} - \frac{1}{b^2} D^2(k_x) + \langle \Xi(\bar{k}) - X^2(\bar{k}) \rangle_G$$

and the uncertainty product is

$$D^2(k_x) D^2(x) = \frac{1}{b} D^2(k_x) - \frac{1}{b^2} D^4(k_x) + D^2(k_x) \langle \Xi(\bar{k}) - X^2(\bar{k}) \rangle_G$$

The sum of the first two terms, and the last term are each positive. $D(k_x)^2$ is a function of b

$$D(k_x)^2 = \frac{\int_{-\kappa/2}^{\kappa/2} k_x^2 \, e^{-k_x^2/b} \, dk_x}{\int_{-\kappa/2}^{\kappa/2} e^{-k_x^2/b} \, dk_x}$$

$$0 \leq \frac{b}{2} = \lim_{b \to 0} D^2(k_x) \leq D^2(k_x) \leq \lim_{b \to \infty} D(k_x)^2 = \frac{\kappa^2}{12}$$

Some values of $\frac{D(k_x)^2}{b} - \frac{D(k_x)^2}{b^2} = B(b)$ are shown in this table

b	$.02\kappa^2$	$.08\kappa^2$	$.18\kappa^2$	$.32\kappa^2$	$.5\kappa^2$
B(b)	.2496	.2474	.2162	.1666	.1250

Since the uncertainty I^2 is greater than 1/4 we deduce that the positive term

$$D(k_x)^2 \langle \Xi(\bar{k}) - X^2(\bar{k}) \rangle_b \geq a^2 D(k_x)^2$$

is greater than $\frac{1}{4} - B(b)$.

Since the term $\langle \Xi - X^2 \rangle_b$ depends on the form of the Bloch functions it remains crystal dependent and is not likely to yield $I^2 = \frac{1}{4}$ for $b>0$. The Bloch state appears then as the only minimum uncertainty state since $I^2(b=0) = \frac{b/2}{b} - \frac{(b/2)^2}{b^2} = \frac{1}{4}$ for $b \to 0$.

Mathematically the reason arises from the fact that only the Schwartz equality is always satisfied whereas the triangle inequality is only satisfied exactly for b=0. For small b these states are, however, very close to achieving $I^2 = \frac{1}{4}$. Let us call them quasicoherent and let us denote them $|\gamma\rangle_b$.

Does the family $|\gamma\rangle$ constitute a family of states which minimize I^2? In the procedure chosen we know that they are uniquely determined. However, there do exist other procedures to minimize I^2. For example we could have tried to satisfy the triangle inequality first. We have shown only that the only exact minimum uncertainty states of this type are the Bloch functions (b=0). The family $|\gamma\rangle_b$ are not necessarily

those states which minimize I^2. The family $|\gamma>_b$ is derived from a special criterion. This criterion is: we will try to minimize I^2 by satisfying the Schwartz equality. It is difficult to analyze the usefulness of this criterion. However, it is possible to analyze the result which is:

$$I^2 = \frac{D(k_x)^2}{b} - \frac{D(k_x)^4}{b^2} + D(k_x)^2 <\Xi^2(\bar{k}) - X^2(\bar{k})>_G$$

We have already pointed out that the family $|\gamma>_b$ comes close to satisfying $I^2 = \frac{1}{4}$ for b small relative to $\kappa (b < \frac{\kappa}{10})$, since $D(k_x)^2 \approx \frac{b}{2}$ and the polarization terms are weighted by $D(k_x)$.

Since the ultimate purpose of this discussion is to explore methods of localizing crystal electrons in the presence of a field in regions of reciprocal and direct space small compared with the Brillouin zone and with the size of a Zener orbit respectively, the $|\gamma>_b$ states evidently provide a fruitful basis for the discussion.

3.4.7 Gaussian Wavepackets

We now attempt to apply the calculation of the last section to the complete crystal-plus-field Hamiltonian. Since the Stark states are a complete basis for the direction of a reciprocal lattice vector, it should be possible to construct a wavepacket with the properties of a $|\gamma>_b$ state from Stark states, and we shall attempt to approach this criterion as closely as possible.

We begin with

$$\psi_G(t,\bar{r}) = \sum_{\nu=-\infty}^{\infty} f_G(\nu)\psi_\nu(t,\bar{r})$$

$$= \sum_{\nu=-\infty}^{\infty} f_G(\nu)\,\frac{1}{\sqrt{\kappa}}\int_{K-\kappa/2}^{\kappa/2+K} \psi(\bar{k},\bar{r})e^{-i\frac{E_\nu t}{\hbar}}$$

$$e^{-i\frac{1}{e\varepsilon}\int_0^{k_x} E^{(1)}(\bar{k})dk_x}\, e^{i E_\nu \frac{k_x}{e\varepsilon}}\, dk_x$$

$$= \frac{1}{\sqrt{\kappa}}\int_{K-\kappa/2}^{K+\kappa/2} \psi(\bar{k},\bar{r})e^{-\frac{i}{e\varepsilon}\int_0^{k_x} E^{(1)}(\bar{k})}$$

$$\sum_{\nu=-\infty}^{\infty} f_G(\nu)\, e^{i E_\nu\left(\frac{k_x}{e\varepsilon} - \frac{t}{\hbar}\right)}$$

where $E_\nu = \frac{\nu 2\pi e\varepsilon}{\kappa} + \langle E^{(1)}(\bar{k})\rangle_\kappa$ We can write the waveform $\phi_G(k_x,t)$ in the Bloch representation as:

$$\phi_G(k_x t) = \frac{1}{\sqrt{\kappa}}\, e^{-\frac{i}{e\varepsilon}\int_0^{x} E^{(1)}(\bar{k})dk_x}\, e^{i\langle E^{(1)}(\bar{k})\rangle_\kappa\left(\frac{k_x}{e\varepsilon} - \frac{t}{\hbar}\right)}$$

$$\sum_{\nu=-\infty}^{\infty} f(\nu)_G e^{+\,i\nu\frac{2\pi}{\kappa}\left(-\frac{e\varepsilon t}{\hbar} + k_x\right)} \qquad (24)$$

Let us define $h_G(s) = \sum_{\nu=-\infty}^{\infty} e^{i\nu\frac{2\pi}{\kappa}s} f_G(\nu)$

with $s = k_x - \frac{e\varepsilon}{\hbar}t$

we have $f_G(\nu) = \frac{1}{\kappa}\int_{K-\kappa/2}^{\kappa/2+K} e^{-i\nu\frac{2\pi}{\kappa}s} h_G(s)ds$

As we clearly see that the term h(s) will never allow the destruction of the phase modulation $e^{-\frac{i}{e\varepsilon}\int_0^{k_x} E(\bar{k}')dk'_x}$ if f(ν) is time

independent and hence $\psi_G(k_x,t)$ will never have the form of the solution (22) of our quasicoherent state $|\gamma>_b$ at all times.

However, using a gaussian distribution $f_G(\nu-\nu_0) \propto e^{-\sigma^2(\nu-\nu_0)^2}$ we can generate a periodic gaussian function $h_G(s)$ centered at zero with a small deviation such that for $s \left[K - \frac{\kappa}{2}, \frac{\kappa}{2} + K\right]$

$$h(s) \propto \int_{-\infty}^{\infty} e^{i\nu \frac{2\pi}{x} s} f_G(\nu) d\nu$$

$$\propto \int_{-\infty}^{\infty} e^{i\nu \frac{2\pi}{\kappa} s} e^{-\sigma^2(\nu-\nu_0)^2} d\nu$$

$$= \int_{-\infty}^{\infty} e^{i \frac{2\pi}{\kappa} s(V+\nu_0)} e^{-\sigma^2 Vs} dV$$

$$= e^{i \frac{2\pi}{\kappa} s\nu_0} e^{-\frac{s^2}{2\sigma^2}} \quad \text{for } K - \frac{\kappa}{2} \leq s \leq \frac{\kappa}{2} + K$$

we see that h(s) is centered at zero. We also need σ to be small.

Let us substitute for h(s) in equation (24)

$$\phi_G(k_x t) \propto e^{-\frac{i}{e\varepsilon} \int_0^x E^{(1)}(\bar{k}) dk_x} e^{i<E^{(1)}(\bar{k})>_\kappa \left(\frac{k_x}{e\varepsilon} - \frac{t}{\hbar}\right)}$$

$$e^{i \frac{2\pi}{\kappa} \nu_0 \left(k_x - \frac{e\varepsilon t}{\hbar}\right)} e^{-\frac{k_x^2}{2\sigma^2}} e^{-\frac{e^2\varepsilon^2 t^2}{\hbar^2 2\sigma^2}} e^{+\frac{e\varepsilon t k_x}{\hbar\sigma^2}} \qquad (25)$$

except for the replacement of $X_{nn}(\bar{k})$ by $\frac{1}{e} E^{(1)}(\bar{k})$ equation (25) can be developed in the shape of equation (22)

$$\text{with } C(t) \propto e^{-i\langle E^{(1)}(\bar{k})\rangle \frac{t}{\hbar}} e^{-i\frac{2\pi}{\kappa}\nu_0 \frac{e\varepsilon t}{\hbar}} e^{-\frac{e^2\varepsilon^2 t^2}{\hbar^2 2\sigma^2}}$$

$$b = \sigma^2$$

$$\frac{\Delta(t)}{b} k_x = i\langle E^{(1)}(\bar{k})\rangle_\kappa \frac{k_x}{e\varepsilon} + i\frac{2\pi\nu_0}{\kappa} k_x + \frac{e\varepsilon t k_x}{\hbar\sigma^2}$$

$$\text{with } K(t) = + \frac{e\varepsilon t}{\hbar}$$

$$R(t) = -\frac{1}{e\varepsilon}\langle E^{(1)}(\bar{k})\rangle_\kappa - \frac{2\pi\nu_0}{\kappa}$$

we can write $\phi_G(k_x)$ as

$$\phi_G(k_x) = C(t) e^{-\frac{1}{2b}k_x^2 + \frac{\Delta(t)}{b}k_x - \frac{i}{e\varepsilon}\int_0^{k_x} E^{(1)}(\bar{k}')dk_x'}$$

What are the properties of this state? The expectation values have been calculated before. It is possible to replace $X_{nn}(\bar{k})$ by $E^{(1)}(\bar{k})$ in the average before any summation is done over $X_{nn}(\bar{k})$. We directly deduce, as before

$$\langle k_x\rangle_G = K(t)$$

$$D(k_x)^2 \simeq \frac{b}{2} = \frac{\sigma^2}{2} \qquad \text{if } \sigma^2 \text{ small}$$

$$\langle x\rangle_G = \frac{1}{e\varepsilon}\left[\langle E(\bar{k})\rangle_G - E_\nu\right]$$

$$\langle x^2 \rangle = \frac{1}{b} - \frac{D(k_x)^2}{b^2} + R(t)^2 + \langle \Xi(\bar{k}) - X^2(\bar{k}) \rangle_G$$

$$+ \frac{2R(t)}{e\varepsilon} \langle E(\bar{k}) \rangle_G + \left\langle \frac{E^2(\bar{k})}{e^2\varepsilon^2} \right\rangle_G$$

the deviation is finally

$$D(x)^2 = \frac{1}{b} - \frac{D(k_x)^2 b}{b^2} + \langle \Xi - X^2 \rangle_{G_b(t)}$$

$$+ \frac{1}{e^2\varepsilon^2} \left[\langle E^2(\bar{k}) \rangle_{G_b(t)} - \left(\langle E(\bar{k}) \rangle_{G_b(t)} \right)^2 \right]$$

We directly deduce that the Houston state is a minimum uncertainty state

since $\underset{b \to 0}{D(k_x)^2 D(x)^2} = \frac{1}{4} + \underset{b \to 0}{D(k_x)}(\ldots)$

$$= \frac{1}{4} \quad .$$

As we have done earlier with the rectangular wave packet of Stark states, we shall now study the behavior of a wave packet of Stark states with gaussian weighting, in a band with the tight-binding cosine form. Before we proceed to details, we should point out that our calculation so far has included an arbitrary restriction to wave packets with real weighting coefficients. As it turns out, this restriction is not altogether trivial. For example, we have seen in Equation (8) that in order to form a Houston state as a superposition of Stark states, it is necessary to use <u>essentially</u> complex expansion coefficients, that is to say, coefficients whose relative phase does not vanish at any time during the Zener cycle.

A consequence of the restriction in the present context is that the minimum "size of the electron" Δx to which a real-coefficient wave packet of Stark states can be localized is field-dependent, and as we shall see presently, may be relatively large; while a complex coefficient wavepacket is only band-structure limited, and can be of the size of a unit cell (e.g., a Wannier function).

As a practical matter, however, the restriction is not very serious. A strongly "compressed" electron, as one might expect, fluctuates dramatically in size over a Zener period, and is far from our notion of a coherent state. At the same time we shall see that states approaching this notion, whether formed with real or complex weights, have very similar properties.

We have determined that for a real gaussian weighting function with deviation $\sigma = \sqrt{\frac{b}{2}}$ in k-space, the uncertainty $\Delta x(t)$ oscillates. We shall now determine the deviation σ which minimizes both the minimum and maximum of $\Delta x(t)$; we already know that for narrow wave packets, $\sigma \leq \left(\frac{2\pi}{a}\right) \times 10^{-1}$, such gaussian wave packets come close to being coherent states with uncertainty product $\Delta x \Delta k_x \approx 0.5$.

From

$$\Delta x^2 \approx \frac{1}{2b} + \frac{1}{e^2 \varepsilon^2} \left\{ \langle E^2(\bar{k}) \rangle_{G(t)} - \left(\langle E(\bar{k}) \rangle_{G(t)} \right)^2 \right\} \quad \text{for small b}$$

with

$$E(\bar{k}) = -A \cos k_x a$$

$$G(t) = \frac{1}{\sqrt{2\pi}\sqrt{\frac{b}{2}}} e^{-\frac{1}{b}\left(k_x - \frac{e\varepsilon t}{\hbar}\right)^2} \quad \text{for small b}$$

its variance is $\Delta k_x = \sigma = \sqrt{\frac{b}{2}}$, let $K = \frac{e\varepsilon t}{h}$

$$\langle E(\bar{k}) \rangle_{G(t)} = \frac{-A}{\sqrt{2\pi}} \frac{1}{\sigma} \int_{-\infty}^{\infty} e^{-\frac{1}{2\sigma^2}(k_x - K)^2} \cos k_x a \; dk_x$$

let $y = k_x - K$

$$\langle E(\bar{k}) \rangle = \frac{-A}{\sqrt{2\pi}} \frac{1}{\sigma} \int_{\infty}^{\infty} e^{-\frac{1}{2\sigma^2} y^2} \cos(y+K)a \; dy$$

$$\cos (y+K)a = \cos ya \cdot \cos Ka - \sin ya \cdot \sin Ka$$

$$\langle E(\bar{k}) \rangle_{G(t)} = (-A) \left\{ \cos Ka \langle \cos ya \rangle_{N(0,\sigma)} - \sin Ka \langle \sin ya \rangle_{N(0,\sigma)} \right\}$$

$$= (-A) \cos Ka \; e^{-\frac{\sigma^2}{2} a^2}$$

where we use the expression of $\langle \cos ya \rangle_{N(0,\sigma)}$ and $\langle \sin ya \rangle_{N(0,\sigma)}$ tabulated in the appendix 6.5.

Similarly

$$\langle E^2(\bar{k}) \rangle_{G(t)} = A^2 \langle \frac{1}{2} \cos 2k_x a + \frac{1}{2} \rangle_{G(t)}$$

$$= \frac{A^2}{2} + \frac{A^2}{2} \cos 2Ka \; \langle \cos 2ya \rangle_{N(0,\sigma)}$$

$$= \frac{A^2}{2} + \frac{A^2}{2} \cos 2Ka \; e^{-2\sigma^2 a^2}$$

and finally

$$\Delta x^2 = \frac{1}{2b} + \frac{1}{e^2\varepsilon^2}\left\{\frac{A^2}{2} + \frac{A^2}{2}\cos\left(\frac{2e\varepsilon t}{\hbar}a\right)e^{-2\sigma^2 a}\right.$$

$$\left. - A^2\cos^2\left(\frac{e\varepsilon t}{\hbar}a\right)e^{-\sigma^2 a}\right\}$$

$$\Delta x^2 = \frac{1}{2b} + \frac{A^2}{2e^2\varepsilon^2}\left\{\left(1 - e^{-\frac{ba^2}{2}}\right)\right.$$

$$\left. + \cos\left(\frac{2e\varepsilon ta}{\hbar}\right)\left(e^{-ba^2} - e^{-\frac{ba^2}{2}}\right)\right\}$$

The position of this electron is given by

$$x = \frac{1}{e\varepsilon}\left[\langle E(\bar{k})\rangle_{G(t)} - E_\nu\right]$$

$$= \frac{1}{e\varepsilon}\left[-A\,e^{-\frac{b}{4}a^2}\cos\frac{e\varepsilon t}{\hbar}a - E_\nu\right]$$

The minimum value of Δx^2 is attained for $\cos\frac{2e\varepsilon ta}{\hbar} = 1$ which corresponds to the edge of the B.Z.:

$$\Delta x^2_{min} = \frac{1}{2b} + \frac{A^2}{2e^2\varepsilon^2}\left\{1 - 2\,e^{-\frac{ba^2}{2}} + e^{-ba^2}\right\}$$

For a given electric field ε the minimum size of the electron: Δx is given by

$$\frac{d\Delta x^2}{db} = 0$$

$$-\frac{1}{2b^2} + \frac{A^2}{2e^2\varepsilon^2}\left\{a^2 e^{-\frac{ba^2}{2}} - a^2 e^{-ba^2}\right\} = 0$$

$$a^4 b^2\left[e^{-a^2\frac{b}{2}} - e^{-a^2 b}\right] = \frac{4}{n^2} \quad \text{with } n = \frac{2A}{e\varepsilon a}$$

For a typical crystal $2A \simeq 2eV, a \simeq 5\mathring{A}$ and we have $n \simeq 0.4\,\frac{10^5}{\varepsilon}$ with ε expressed in kV/cm. We can now plot the results formed as a function of the electric field in Figure 1. We see that Δx is large at $t = T/4$, and the uncertainty product is large at that time.

Let us also derive the state where the maximum value of Δx is minimized

$$\Delta x^2 \text{ max} = \frac{1}{2b} + \frac{A^2}{2e^2\varepsilon^2}\left(1 - e^{-ba^2}\right)$$

$$\frac{d\Delta x^2}{db} = 0$$

$$-\frac{1}{2b^2} + \frac{n^2a^2}{8} a^2\, e^{-ba^2} = 0$$

$$e^{-ba^2}\, b^2 a^4 = \frac{4}{n^2}$$

$$n = \frac{2}{e^{-ba^2/2}\, ba^2}$$

Figure 2 shows a state with less fluctuations in spread Δx; its uncertainty product remains close to 0.5 at all times.

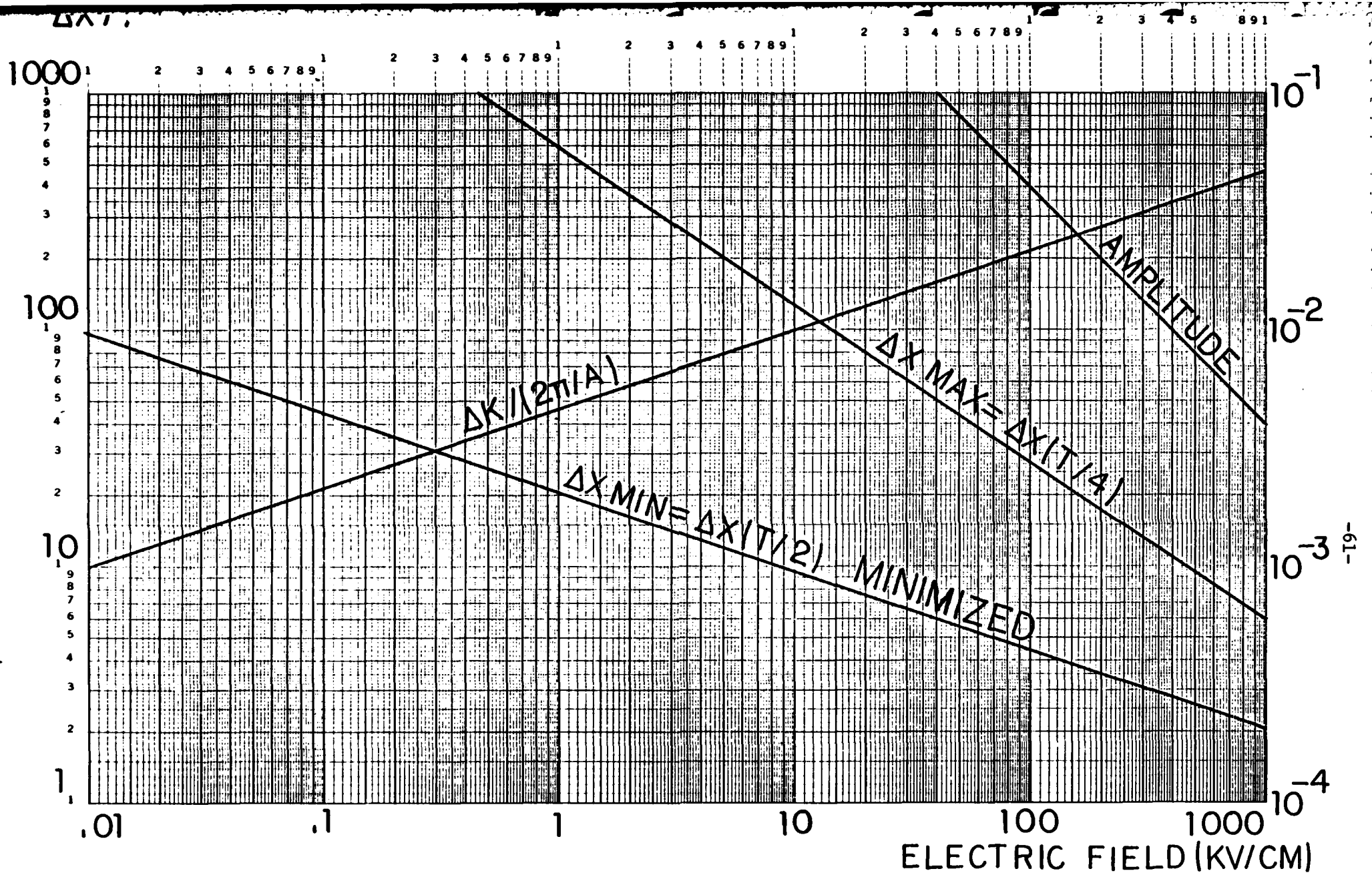

Figure 1. Localization of a real-coefficient wavepacket of Stark states with Δx_{min} minimized.

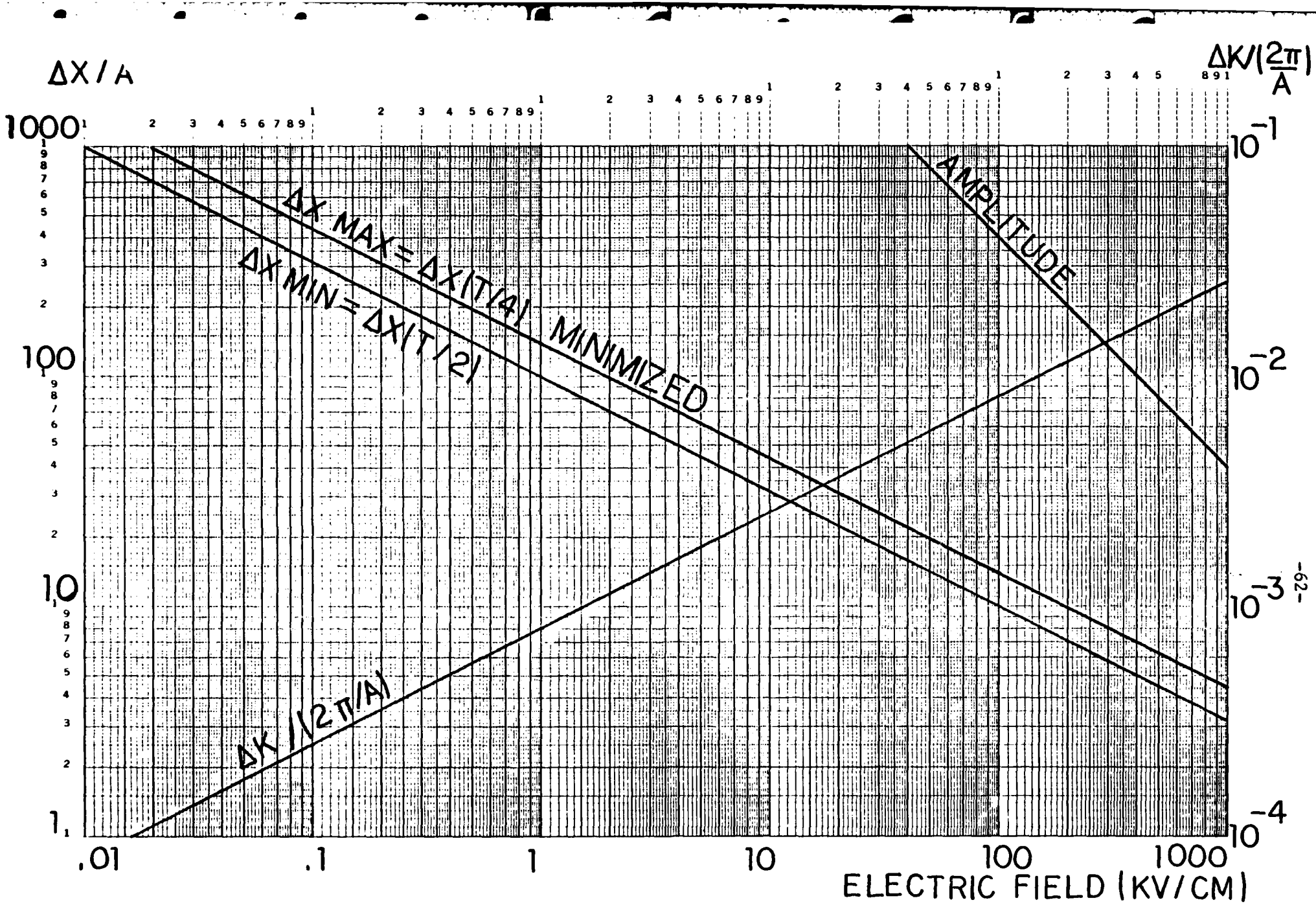

Figure 2. Localization of a quasicoherent state of the tight-binding band structure: Δx_{max} minimized.

We have earlier introduced the Houston functions (Equation (8) in Chapter 2, 2.2.3 and Chapter 3, 3.2) as superpositions of Stark states with complex weighting

$$f(\nu) = \int_{-\kappa/2}^{\kappa/2} dk_x(0) f(k_x(0)) e^{\frac{i}{e\varepsilon}\int_0^{k_x(0)} E^{(1)}(\bar{k}')dk'_x} e^{-\frac{i2\pi\nu}{\kappa} k_x(0)}$$

which is the Fourier coefficient of $f(k_x(0))$ weighted by $e^{\frac{i}{e\varepsilon}\int_0^{k_x(0)} E^{(1)}(\bar{k}')dk'_x}$. The weighting function $f(\nu)$ is real if and only if the waveform $f(k_x(0))$ contains a phase modulation $e^{-\frac{i}{e\varepsilon}\int_0^{k_x(0)} E^{(1)}(\bar{k}')dk'_x}$ which cancels that weighting $f(k_x(0))$. Real waveforms $f(\nu)$ generate the type of oscillations we have discussed up to now.

We will now consider a waveform $f(k_x(0))$ without this phase modulation. Such wavepackets generate a mode in which the size of the electron Δx is not bounded by a minimum value set by the electric field. Let us recall some previous results about wavepackets of Houston states. We will set $X(\bar{k}) = 0$ in this calculation. We have

$$\langle x \rangle = i\langle f^*(k_x(0)) f'(k_x(0)) \rangle_\kappa$$

$$+ \frac{1}{e\varepsilon} \left\langle \left\{ E\left(\frac{e\varepsilon t}{\hbar} + \bar{k}(0)\right) - E(\bar{k}(0)) \right\} | f(k_x(0)) |^2 \right\rangle_\kappa$$

$$\langle x^2 \rangle = -\langle f^*(k_x(0)) f''(k_x(0)) \rangle_\kappa$$

$$+ \frac{i}{e\varepsilon} \left\langle \left\{ E'\left(\bar{k}(0) + \frac{e\varepsilon t}{\hbar}\right) - E'(\bar{k}(0)) \right\} | f(k_x(0)) |^2 \right\rangle_\kappa$$

$$+ \frac{1}{e^2\epsilon^2} \left\langle \left\{ E\left(\bar{k}(0) + \frac{e\bar{\epsilon}t}{h}\right) - E(\bar{k}(0)) \right\}^2 |f(k_x(0))|^2 \right\rangle_\kappa$$

$$+ \frac{2i}{e\epsilon} \left\langle \left\{ E\left(\bar{k}(0) + \frac{e\bar{\epsilon}t}{\hbar}\right) - E(\bar{k}(0)) \right\} f^*(k_x(0)) f'(k_x(0)) \right\rangle_\kappa$$

$$+ \left\langle \Xi\left(\bar{k}(0) + \frac{e\bar{\epsilon}t}{h}\right) |f(k_x(0))|^2 \right\rangle_\kappa$$

with $\langle ( ) \rangle_\kappa = \frac{1}{\kappa} \int_{-\kappa/2}^{\kappa/2} dk_x(0) ( )$

Let us simplify these expressions by writing

$$E\left(\bar{k}(0) + \frac{e\bar{\epsilon}t}{h}\right) = E(t)$$

$$E(\bar{k}(0)) = E(0)$$

$$f(k_x(0)) = f(k) = f = |f| \, e^{j\phi}$$

We first wish to prove that it is possible to localize an electron in this mode. For this purpose let us simply build a Wannier state positioned at ℓ along the electric field. The corresponding wavepacket is

$$f(k_x(0)) = e^{-ik_x(0)\ell}$$

Using a cosine bandstructure

$$E(k) = -A \cos ak_x$$

we quickly find

$$\langle x \rangle = \ell$$

$$\Delta x^2 = \langle \Xi(\bar{k}(t)) \rangle_\kappa + \frac{A^2}{e^2\varepsilon^2} \left(1 - \cos \frac{ae\varepsilon t}{\hbar} \right)$$

At times $t = m \frac{\hbar}{ae\varepsilon} 2\pi$ our electron is localized to the extent allowed by $\Xi(k)$ which is of the order of one lattice parameter. Having done this the electron size will oscillate drastically to the size of the Zener oscillation. The point here is that the localization at a time t is not electric field limited but is bandstructure $\Xi(\bar{k})$ limited in this mode. However, its spread is electric field dependent. Let us generalize these results. We have:

$$\langle x^2 \rangle = -\langle f^* f'' \rangle_\kappa + \frac{1}{e^2\varepsilon^2} \langle \{E(t) - E(0)\}^2 |f|^2 \rangle_\kappa$$

$$+ \frac{i}{e\varepsilon} \langle \{E'(t) - E'(0)\} |f|^2 \rangle_\kappa$$

$$+ \frac{2i}{e\varepsilon} \langle \{E(t) - E(0)\} f^* f' \rangle_\kappa$$

We provisionally drop the $\Xi(\bar{k})$ term

$$\text{using } \langle \{ E'(t) - E'(0) \} |f|^2 \rangle = \frac{i}{e\varepsilon} \left[\{ E(t) - E(0) \} |f|^2 \right]_{-\kappa/2}^{\kappa/2}$$

$$- \frac{i}{e\varepsilon} \langle \{ E(t) - E(0) \} 2|f||f|' \rangle_\kappa$$

$$\text{and } f^* f' = f^* \left(|f|' e^{+j\phi} + j\phi' |f| e^{+j\phi} \right)$$

$$= 2|f||f|' + j\phi' |f|^2$$

we find $\langle \Delta x^2 \rangle = -\langle f^* f'' \rangle_\kappa$

$$+ \frac{1}{e^2\varepsilon^2} \langle \{E(t) - E(0)\}^2 |f|^2 \rangle_\kappa - \frac{2}{e\varepsilon} \langle \{E(t) - E(0)\}\phi' |f|^2 \rangle_\kappa$$

Since there is no phase modulation in f, the phase ϕ is only related to the initial position in the crystal: $\phi = -\ell k_x(0)$. In the desired term Δx all terms involving ℓ should cancel and we find (letting $\ell = 0$ for simplicity):

$$\Delta x^2 = -\langle f^* f'' \rangle_\kappa + \frac{1}{e^2\varepsilon^2} \langle \{E(t) - E(0)\}^2 |f|^2 \rangle_\kappa$$

$$- \frac{1}{e^2\varepsilon^2} \left(\langle \{E(t) - E(0)\} |f|^2 \rangle_\kappa \right)^2 + \langle \Xi(\bar{k}) |f|^2 \rangle_\kappa$$

$$\langle x \rangle = \frac{1}{e\varepsilon} \langle \{E(t) - E(0)\} |f|^2 \rangle_\kappa$$

For $t = 0$ the bandstructure terms cancel and Δx^2 reduces to $-\langle f^* f'' \rangle_\kappa$ which is the variance of the wavepacket related neither to the bandstructure nor to the field. These last equations can be compared with those of the superposition with real weights. In that mode no E(0) terms appears as a consequence of the phase modulation $e^{-\frac{i}{e\varepsilon}\int^{k_x} E(\bar{k})dk_x}$. If an electron is not too strongly localized at a time t its size will not oscillate so drastically. An interesting application will be to determine what is the minimum size of an electron traveling through the Brillouin zone. In ballistic transport the devices considered are usually at the order of a micron or smaller. It can be imagined that for such device dimensions the size of the electron may not be negligible on the scale of the device.

The wavepacket to be used is obviously the quasicoherent one

$$f(k_x(0)) = \frac{1}{(2\pi\sigma^2)^{1/4}} e^{-(k_x(0)-k_0)^2/4\sigma^2 - i\ell k_x(0)}$$

centered at k_0 with $\ell = 0$ (without any restrictions)

$$f'(k_x(0)) = f' = -\left(\frac{k_x(0)-k_0}{2\sigma^2}\right) f(k_x(0))$$

$$f''(k_x(0)) = f'' = \left(-\frac{1}{2\sigma^2} + \left(\frac{k_x(0)-k_0}{2\sigma^2}\right)^2\right) f(k_x(0))$$

and we find

$$\langle x \rangle = \frac{1}{e\epsilon} \langle \{E(t) - E(0)\} \rangle_{N(k_0,\sigma)}$$

$$\Delta x^2 = \frac{1}{2\sigma^2} - \left\langle \frac{(k_x(0)-k_0)^2}{4\sigma^4} \right\rangle_{N(k_0,\sigma)}$$

$$+ \frac{1}{e^2\epsilon^2} \left\{ \langle \{(E(t) - E(0)\}^2 \rangle_{N(k_0,\sigma)} - \left(\langle E(t) - E(0) \rangle_{N(k_0,\sigma)} \right)^2 \right\}$$

We look for a wavepacket of variance σ^2 which will minimize Δx^2. It will turn out again that such wavepackets are sufficiently narrow for the Gaussian wavepacket used to be nearly a coherent state $\Delta x \Delta k_x \simeq 0.5$. This will assure our result to be near optimum. In this calculation we set $k_0 = 0$ and we use the cosine bandstructure

$$E(k) = -A \cos a k_x(0) = E(0)$$

$$E(t) = -A \cos a\left(k_x(0) + \frac{e\epsilon}{\hbar} t\right)$$

For narrow wavepackets the two first terms of Δx^2 reduce to $\frac{1}{4\sigma^2}$. Let us compute the second term of Δx^2

$$\langle \{E(t) - E(0)\}^2 \rangle_{N(0,\sigma)}$$

$$= \langle A^2 \{\cos a(k+K) - \cos ak\}^2 \rangle_{N(0,\sigma)} \quad \text{with } K = \frac{e\varepsilon t}{\hbar}$$

$$= A^2 \langle 1 + \frac{1}{2}\cos 2a(k+K) + \frac{1}{2}\cos 2ak - \cos a(2k+K) \rangle - \cos aK \rangle_{N(0,\sigma)}$$

$$= A^2 \Big[1 + \frac{1}{2}\cos 2aK\, e^{-a^2 2\sigma^2} + \frac{1}{2} e^{-a^2 2\sigma^2} - \cos aK\, e^{-a^2 2\sigma^2} - \cos aK \Big]$$

where we have used the formula of appendix 6.5. The third term of Δx^2 is the square of

$$\langle E(t) - E(0) \rangle_{N(0,\sigma)} = -A \langle \cos a(k+K) - \cos ak \rangle_{N(0,\sigma)}$$

$$= -A\, e^{-a^2 \frac{\sigma^2}{2}} (\cos aK - 1)$$

and we can finally write

$$\Delta x^2 = \frac{1}{4\sigma^2} + \frac{A^2}{e^2 \varepsilon^2} \Big[1 - \cos aK - e^{-a^2\sigma^2} (1 - \cos aK)^2 + e^{-a^2 2\sigma^2} \cos aK\, (\cos aK - 1) \Big] \quad \text{with } K = \frac{e\varepsilon t}{h}.$$

At time $t = 0$: $\Delta x^2 = 1/4\sigma^2 = \Delta x^2$ min.

At the Brillouin zone edge $t = \frac{\hbar\pi}{e\varepsilon a} = \frac{T}{2}$:

$$\Delta x^2\left(t = \frac{\hbar}{e\varepsilon}\frac{\pi}{a}\right) = \Delta x^2\left(K = \frac{\pi}{a}\right)$$

$$= \frac{1}{4\sigma^2} + \frac{A^2}{e^2\varepsilon^2}\left\{2 - 4e^{-a^2\sigma^2} + 2e^{-2a^2\sigma^2}\right\}$$

$$= \frac{1}{2b} + \frac{2A^2}{e^2\varepsilon^2}\left\{1 - e^{-a^2b/2}\right\}^2$$

where we introduce $b = 2\sigma^2$ or $\sigma = \sqrt{\frac{b}{2}}$. Δx^2 is an interesting oscillating function of time. Its maximum occurs at $t = \frac{1}{2}\frac{\hbar}{e\varepsilon}\frac{\pi}{a} = \frac{T}{4}$ or $K = \frac{\pi}{2a}$ which is 1/4 of the Zener period T. This maximum is

$$\Delta x^2 = \frac{1}{2b} + \frac{A^2}{e^2\varepsilon^2}\left\{1 - e^{-a^2b/2}\right\}$$

To find the wavepacket which minimizes this quantity we find the solution of

$$\frac{d\Delta x^2}{db} = 0$$

$$\text{or } -\frac{1}{2b^2} + \frac{n^2a^2}{4}\cdot\frac{a^2}{2}e^{-a^2b/2} = 0$$

$$e^{-a^2b/2}\, b^2a^4 = \frac{4}{n^2}$$

$$n = \frac{2}{ba^2\, e^{-a^2b/4}}$$

The results found using these formulas are the same as for the Zener mode when $\Delta x(T/4)Max$ is minimized, although the expressions are not exactly the same (the differences are extremely small). We compare these results in the table.

Real Coefficients	Complex Coefficients
Δx Max minimized by $n = \dfrac{2}{ba^2 e^{-a^2 b/2}}$	Δx Max minimized by $n = \dfrac{2}{ba^2 e^{-a^2 b/4}}$
Δx Max occurs at $\dfrac{T}{4}$ $\Delta x^2_{max} = \dfrac{1}{2b} + \dfrac{n^2 a^2}{8}\left\{1-e^{-a^2 b/2}\right\}$	Δx Max occurs at $\dfrac{T}{4}$ $\Delta x^2_{max} = \dfrac{1}{2b} + \dfrac{n^2 a^2}{4}\left\{1-e^{-a^2 b}\right\}$
Δx Min occurs at $\dfrac{T}{2}$ $\Delta x^2_{min} = \dfrac{1}{2b} + \dfrac{n^2}{8}\left\{1 - e^{-\frac{a^2 b}{2}}\right\}^2$	Δx Min occurs at $t = 0$ $\Delta x^2_{min} = \dfrac{1}{2b}$
Remark $T = \dfrac{\hbar}{e\mathcal{E}}\dfrac{2\pi}{a}$ = Zener period	for $n = \dfrac{2}{ba^2 e^{-a^2 b/4}}$ which minimizes Δx Max $\Delta x^2(T/2)$ $= \dfrac{1}{2b} + \dfrac{n^2}{2}\left\{1-e^{-\frac{a^2 b}{2}}\right\}^2$ $\simeq \dfrac{1}{2b}$

therefore

Δx Max $\simeq$ Δx Max

real complex

Δx Min $\simeq$ Δx Min

This is only true for the Δx max minimized wavepackets!

The graph for the dependence of Δx max minimized in the complex coefficient mode is then the same as graph 2 of the real case. The uncertainty product is nearly 0.5 at all times.

In order to show that the Δx max minimized state is a special case we have also studied a different case where the electron is localized initially at t=0 over 10 lattice parameters ($\Delta x = 10a$). We have plotted on Graph 3 Δx for different times:

$\Delta x(0) = 10a = \Delta x_{min}$

$\Delta x(10^{-12}$ sec), 10^{-12} sec $\simeq$ scattering time

$\Delta x(T/4) = \Delta x_{max}$

$\Delta x(T/2) = \Delta x$ on the Brillouin zone edges

On graph 4 we show the time dependence of Δx for $\Delta x(0) = 10a$ for $\varepsilon = 0.1$, $\varepsilon = 1$, $\varepsilon = 10$, $\varepsilon = 100$ kV/cm.

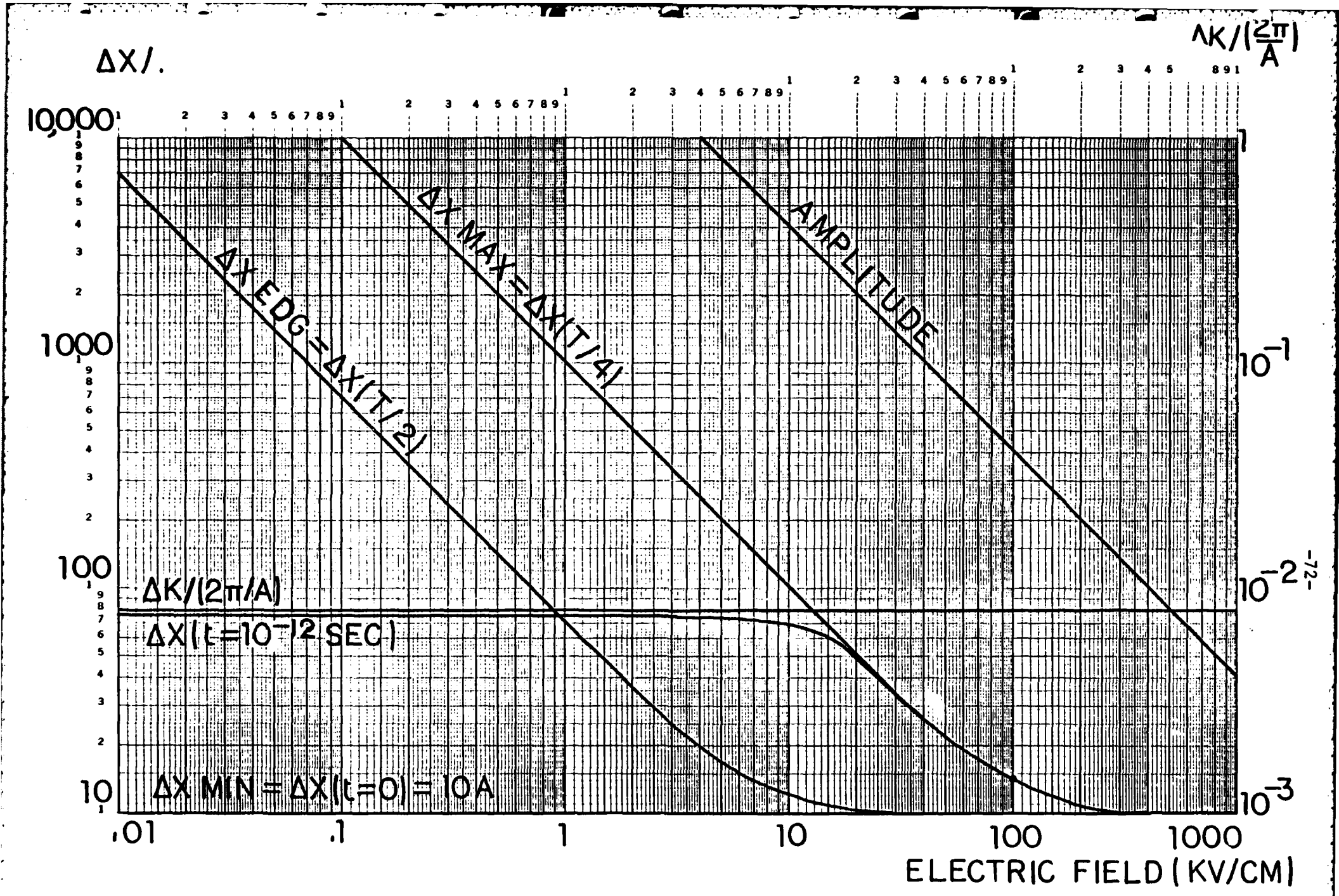

Figure 3. Localization of a real-coefficient wavepacket of Houston states with Δx_{min} equal 10 lattice parameters.

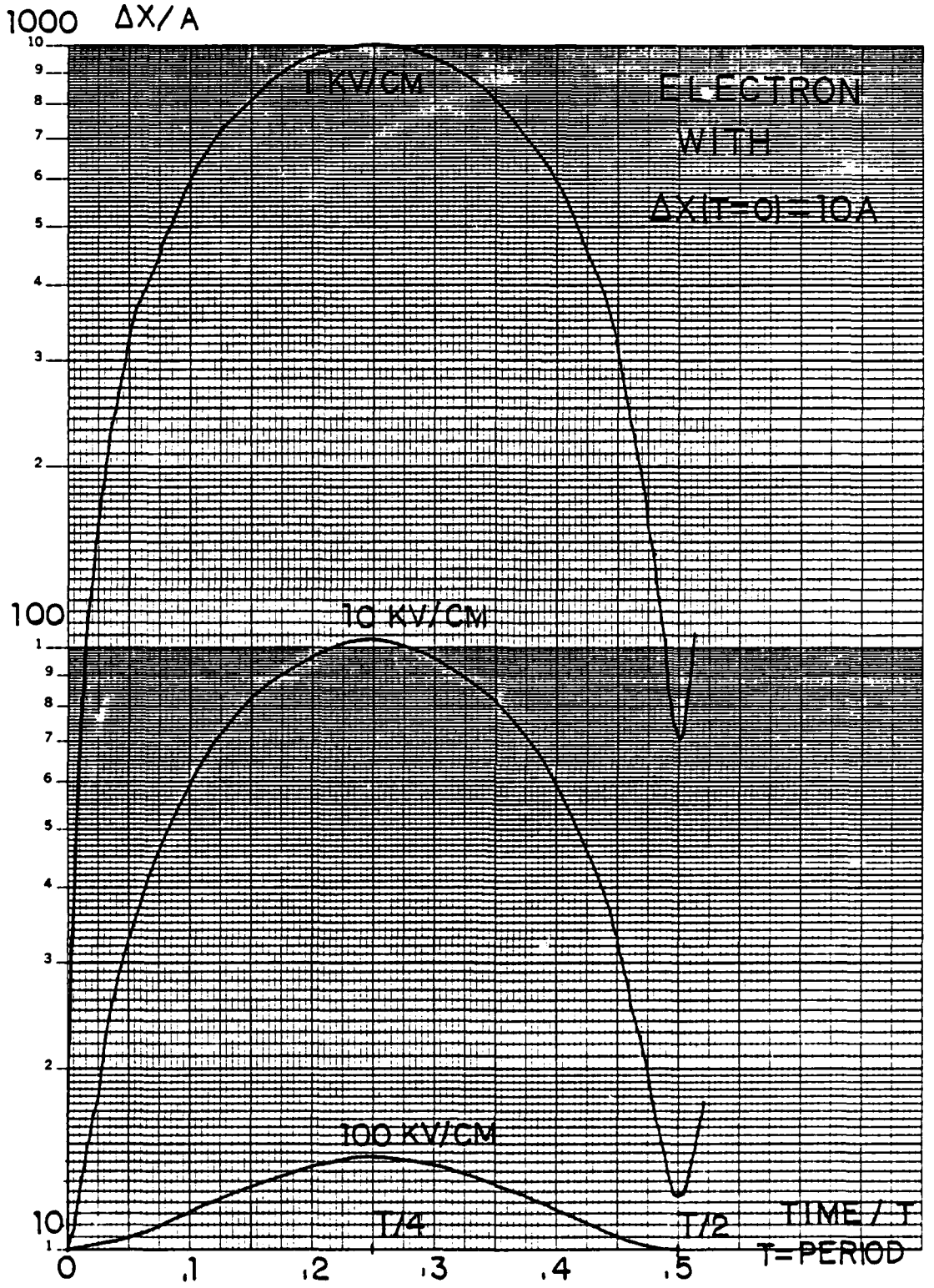

Figure 4. Size fluctuation of the wavepacket of Figure 3 during a half-cycle of the Zener oscillation.

4. FOURIER SPECTRUM OF THE GaAs CONDUCTION BAND

4.1 MOTIVATION

We have seen that the coefficients of the Fourier series expansion (FSC) of the band structure in the k_x direction appear as parameters in the general formula for wave packets of Stark states. Since conduction electrons in GaAs are possible candidates for the observation of Zener oscillations, the FSC of the GaAs conduction band will play a role in the design of wave packets.

More importantly, these FSC are also used for calculating the radiative transition probabilities between Stark levels. We shall demonstrate this by working out the probability $p_{\nu\mu}$ of a transition from an initial state $|\nu\rangle$ to a final state $|\mu\rangle$.

We assume the Stark states to be exact eigenstates of the crystal plus electric field Hamiltonian H_0

$$H_0|\nu\rangle = E_\nu|\nu\rangle$$

the total Hamiltonian is then

$$H_{total} = H_0 + \bar{p}\cdot\bar{A}$$

where $\bar{A}$ is the vector potential of the electromagnetic field and $\bar{p}$ the electron momentum. If we assume the interaction potential to be sufficiently small (compared to the inverse of the observation time) for first order perturbation theory to be valid, then in the dipole approximation the transition probability $p_{\nu\mu}$ is proportional to the square of the matrix element $\langle\mu|p_x|\nu\rangle$. Let us evaluate this matrix element:

$$\langle\mu|p_x|\nu\rangle = \langle\mu|xH_{total} - H_{total}x|\nu\rangle = (E_\nu - E_\mu)\langle\mu|x|\nu\rangle$$

$$= (E_\nu - E_\mu)\frac{1}{\kappa}\int_{-\kappa/2}^{\kappa/2} \phi_\mu^*(k_x')\phi_\nu(k_x)\left[\frac{1}{e\varepsilon}(E^{(1)}(\bar{k}) - E_\nu) + X_{nn}(\bar{k})\right] dk_x$$

$$= (E_\nu - E_\mu)\left[-\frac{E_\nu}{e\varepsilon}\delta_{\nu\mu} + \frac{1}{\kappa}\int_{-\kappa/2}^{\kappa/2} \frac{E(\bar{k})}{e\varepsilon} e^{\frac{i}{e\varepsilon}(E_\nu - E_\mu)k_x} dk_x\right]$$

$$= (E_\nu - E_\mu)\frac{1}{e\varepsilon}\frac{1}{\kappa}\int_{-\kappa/2}^{\kappa/2} e^{i2\pi(\nu-\mu)\frac{k_x}{\kappa}} E(\bar{k})\ dk_x$$

We conclude that this transition probability is proportional to the square of the amplitude of the FSC: $F_{\nu-\mu}$ of the bandstructure $E(\bar{k})$. The transition probability is the basis of the phenomenological interpretation of radiation where the ideally unscattered Zener electron initially prepared in state $|\nu\rangle$ moves to Stark states of lower energy in the field direction and releases its potential energy as radiation.

The process that we have just described is the usual picture of the incoherent emission of radiation. For the device application of Zener oscillations as a coherent radiation source we are more interested in a classical description, in which the conduction electrons oscillate in phase. In this classical picture the radiation originates from an oscillating dipole which is formed from a superposition of eigenstates. We have studied such superpositions or wavepackets at length. The additional feature is that as it radiates the wavepacket will move and spread. We know that for a wavepacket not too wide in $\Delta k_x \leq \frac{\kappa}{10}$ the expected position of the electron is given by

$$x(t) = x(0) + \frac{1}{e\varepsilon}\left[E\left(\bar{k}(0) + \frac{e\bar{\varepsilon}}{h}t\right) - E(\bar{k}(0))\right].$$

We also found that this electron was localized in a size $2\Delta x$ which is also oscillating. Most of our studies emphasized the various kinds of behavior of Δx for different wavepackets. For the optimal wavepacket where Δx_{MAX} is minimized it was seen that Δx does not fluctuate much the product $\Delta x \Delta k_x$ being nearly optimal at all times. For such a wavepacket the oscillating electron is a simple classical dipole, Δx being small compared to the amplitude of oscillation. The frequency of oscillation of this dipole is then given by the Fourier analysis of $x(t)$ which is simply the Fourier analysis of the bandstructure. The Fourier analysis then yields the radiation spectrum of an unscattered Zener electron. Our studies of wavepackets have enabled us to establish the conditions under which the unscattered Zener electron exhibits classical behavior.

4.1.1 Fourier Series Computation

The bandstructure of the GaAs conduction band was kindly furnished by Prof. Karl Hess of the University of Illinois. It is given at 156 sampled points in (1/48)th of the GaAs Brillouin zone (see Figure 5 and program DATABAND). For convenience we use the bravais cell of the reciprocal space which has simple boundaries. Using the 48 fold symmetry of the Brillouin zone we fill $\frac{1}{8}$ of this Bravais cell (see Figure 6 and program FILLBZ2) and store in the file CUBEBAND. The Fourier computation is carried out by the program called ZENER2 (see Figure 7). This calculation is carried out for each desired direction of periodicity $\bar{\kappa}$ in reciprocal space starting from any point $\overline{\kappa 0}$ of the Brillouin Zone. An accuracy of one percent was required. This accuracy is determined by the number M of points used for the interpolation of the bandstructure along the path $[\overline{\kappa 0}, \overline{\kappa 0} + \bar{\kappa}]$. This interpolation uses a

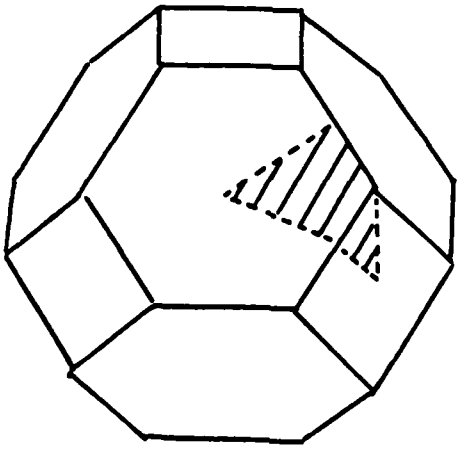

Figure 5. Sampled area of the Brillouin zone.

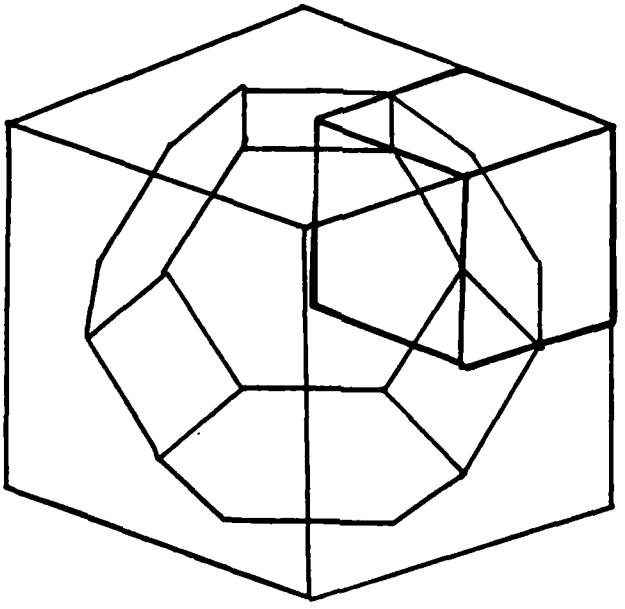

Figure 6. Cubic region used by the computer.

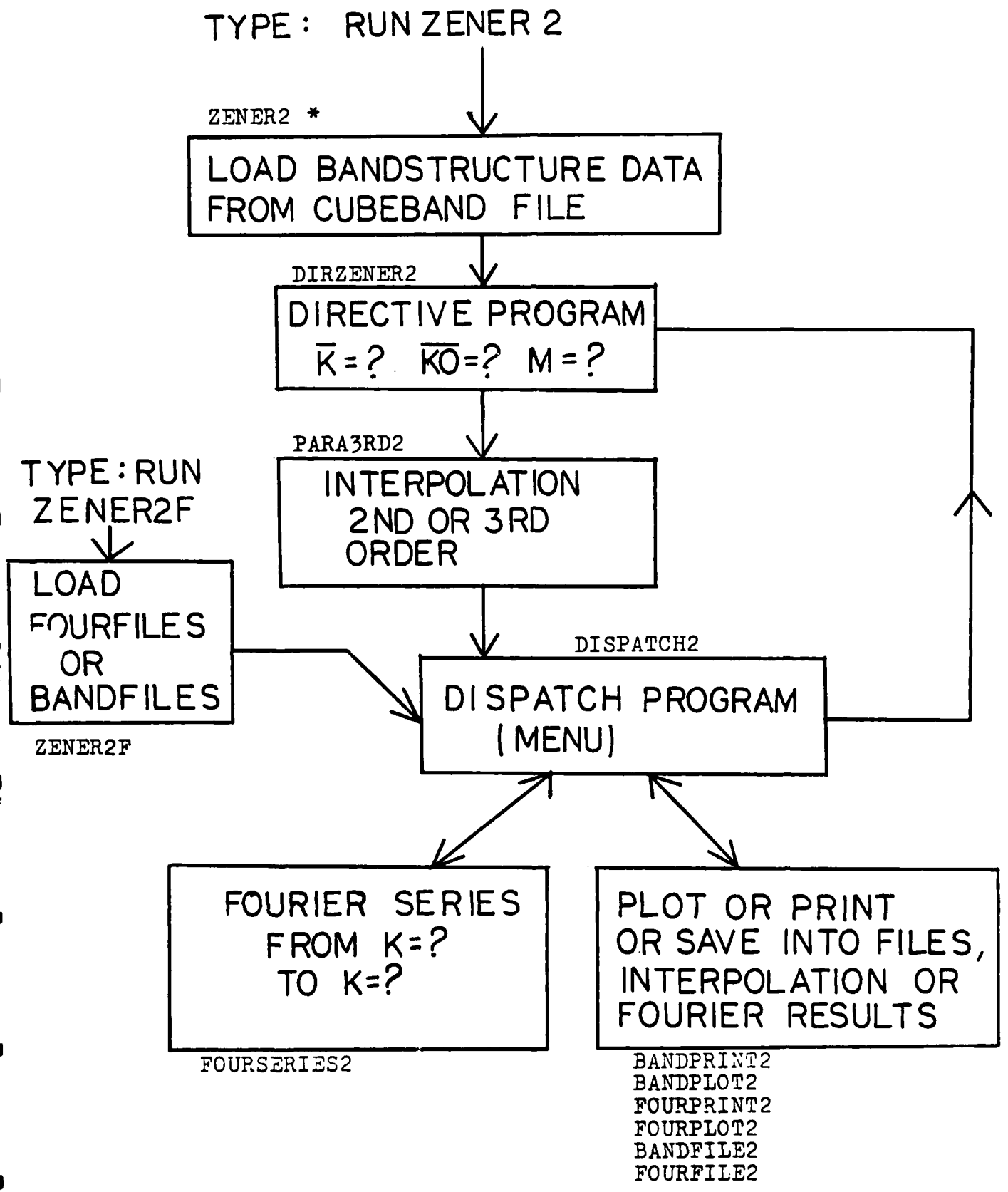

* Actual name of the programs

Figure 7. Block diagram of the computer programs used to Fourier analyze the band structure in an arbitrary direction.

polynomial expansion of 3rd order using 19 coefficients fitted to the local sampled data. The formula for the point located at (x,y,z) of the closest sampled point (W1,W2,W3) is:

$$E(x+W1,\ y+W2,\ z+W3) = E(W1,\ W2,\ W3)$$
$$+A(0)x + A(1)y + A(2)z$$
$$+B(0)x^2 + B(1)y^2 + B(2)z^2$$
$$+G(0)x^3 + G(1)y^3 + G(2)z^3$$
$$+F(0)yz + F(1)xz + F(2)xy$$
$$+H(1)x^2y + H(2)xy^2$$
$$+H(3)yz^2 + H(4)y^2z$$
$$+H(5)x^2z + H(6)xz^2$$
$$+H(7)xyz$$

The Fourier computation is made using the trapeze method. The results are saved in files labelled $\bar{\kappa}$, $\overline{\kappa 0}$ and M. $\bar{\kappa}$ and $\overline{\kappa 0}$ are given in Miller notation and correspond to a body centered cubic reciprocal lattice. In Figure 7 the block diagram for these programs is shown. Those programs are given in appendix 6.6).

4.1.2 Results

The Fourier calculations are given for $\bar{\kappa}$ = (100), (110), (111) on pages 82-84 . Five harmonics (10 for (111)) are sufficient for an accurate description of the GaAs bandstructure. In practice it might

be interesting to use for example the fourth harmonic in the (111) direction in order to maximize the number of oscillations of an electron before it is scattered.

The same calculations were done with k_x at a slight angle with respect to a principal direction in order to evaluate the effect of misalignment of the field. As expected the radiation spectrum is largely conserved except for a broadening and a curious splitting. It is possible to account for this behavior analytically, but a plausibility argument is a good deal more instructive.

If the field is along a principal lattice direction, the trajectory in the extended Brillouin zone that describes the motion of the electron, beginning for example at Γ, traverses an identical path in each repetition of the central zone, that is to say, it is periodic with period κ, and the Fourier coefficients are determined by the band structure along this segment of "length" κ.

If the field deviates from a principal lattice direction, the trajectory, starting at Γ, may traverse many repetitions of the central zone before it again reaches the point Γ. Thus the fundamental period of the periodic motion may be long, to be exact, the length of the reciprocal lattice vector of the trajectory. Furthermore, the trajectory will sample different regions of the central zone as it crosses successive repetitions. However, if the deviation from a principal direction is small, then because of the continuity of the band structure, successive segments of the trajectory will be quite similar, changing only slowly in the course of the transit from Γ to Γ. Thus the long-period periodic motion can be viewed equivalently as a short (κ) period modulated motion, with a "low-frequency" modulation

corresponding to the gradual change of the band structure segment that is being traversed. From this viewpoint, the broadening of the spectrum arises from a low frequency frequency modulation of a high-frequency carrier.

Furthermore, although the change is gradual, corresponding to a low modulation frequency, it can be quite substantial for a band structure as complicated as that of the GaAs conduction band: adjacent segments of the trajectory are rather alike, but segments remote from each other can be quite different. In the language of frequency modulation, this means that the modulation index may be large. It is a familiar result that such a "deeply modulated" signal may have sidebands that are larger than the carrier, or even a missing carrier. This is the phenomenon of spectral line splitting seen in Figures 8,9 and 10.

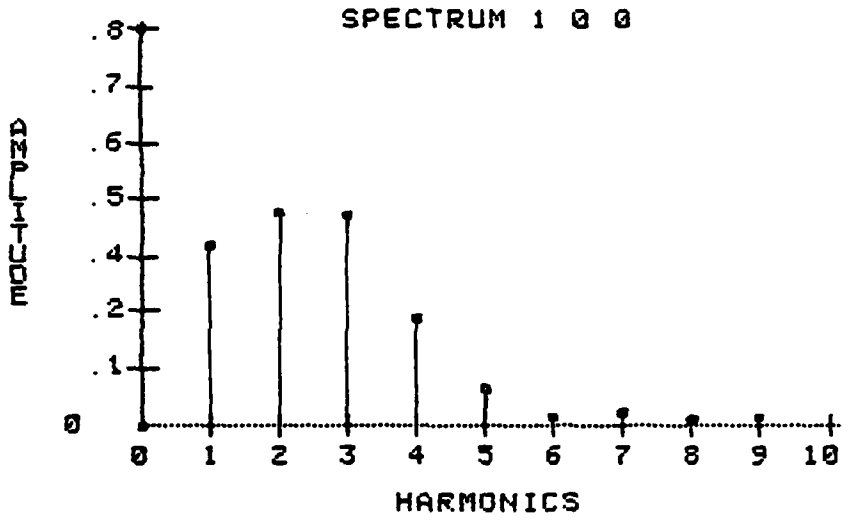

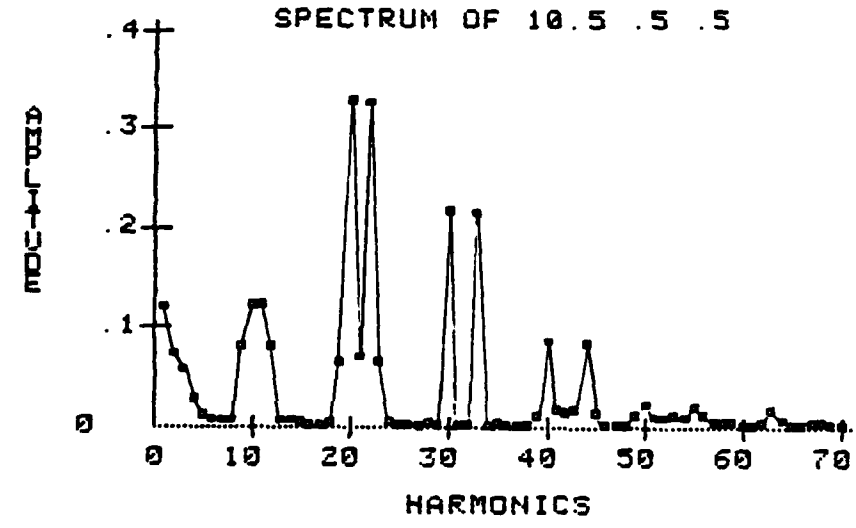

Figure 8. Spectrum 1 0 0 and 10.5 .5 .5.

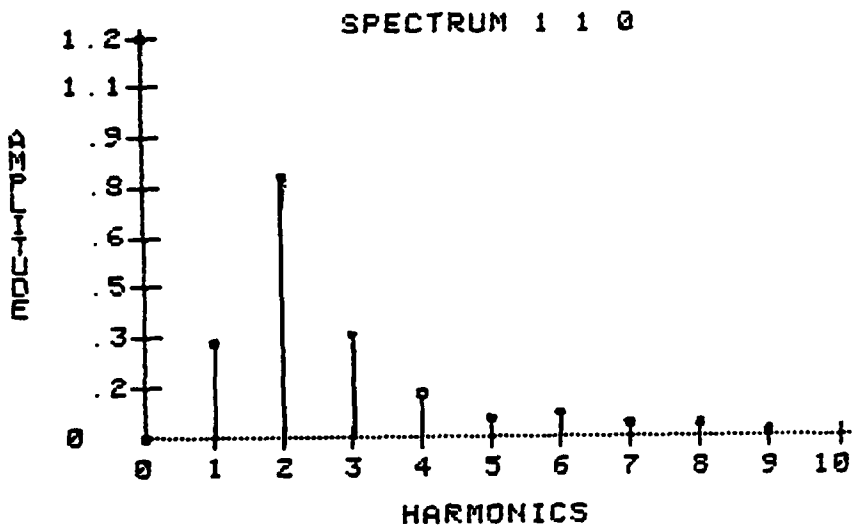

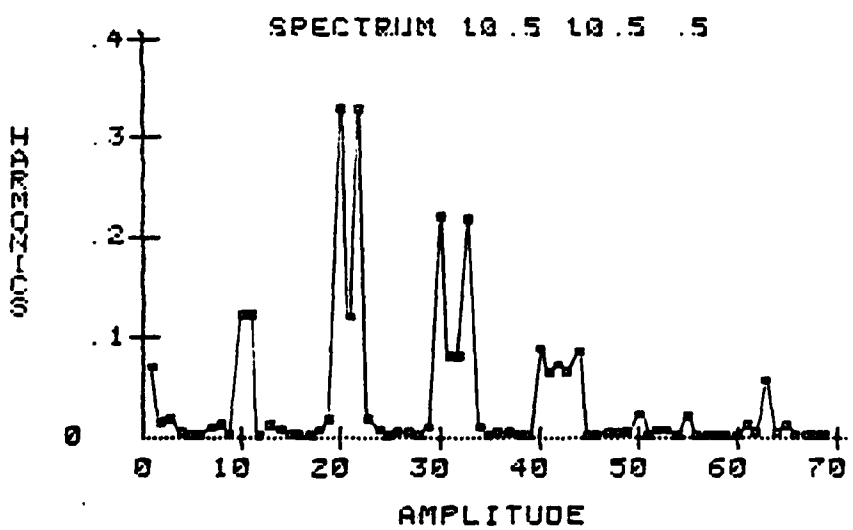

Figure 9. Spectrum 1 1 0 and 10.5 10.5 .5.

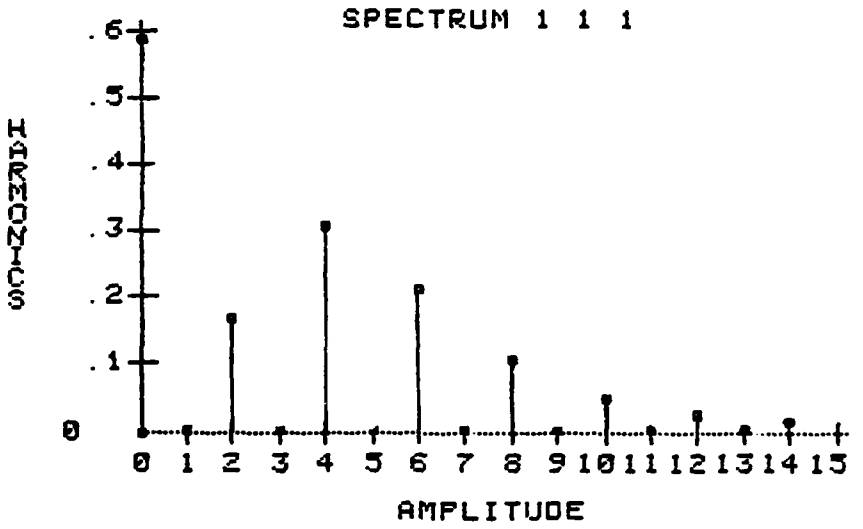

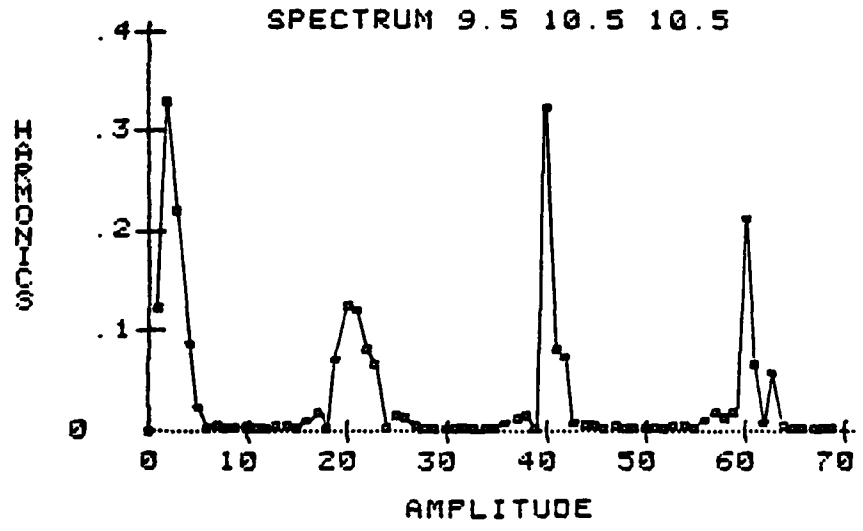

Figure 10. Spectrum 1 1 1 and 9.5 10.5 10.5.

5. SUMMARY

This work is devoted to a general study of the one-band oscillation of an electron under a high applied electric field, the so-called Zener oscillation.

First we review the acceleration theorem and the introduction of the one-band approximation. The existence of the Stark state and Stark ladder seems to be definitely theoretically established in the literature.

We study general Zener oscillation states which correspond to wavepackets of Stark states or Houston states. The analysis is carried out in terms of the expectation values and uncertainties of both the position and quasimomentum operators.

The position expectation and the size Δx of the Zener electron oscillate in time with an amplitude that depends on the wavepacket. We discuss in detail two different types of modes: the real wavepacket of Stark states with electric-field-dependent minimum size; the real wavepacket of Houston states with arbitrary minimum size and a resulting more or less large fluctuation of the size Δx.

We determine that the Houston state is the only state to satisfy exactly the equality in the Heisenberg relation: $\Delta x \Delta k_x \geq \frac{1}{2}$. However, for narrow wavepackets with Δk_x small the Heisenberg equality is nearly realized.

We determine a classical state corresponding to a quasicoherent state $\Delta x \Delta k_x \simeq \frac{1}{2}$, with maximal oscillation amplitude and minimal size fluctuation of the Zener electrons. This classical state, for a model

tight binding band structure, corresponds to a Gaussian wavepacket with a variance which is a function of the electric field.

Finally we give the spectrum of such a classical Zener oscillation in the GaAs conduction band for different electric field directions. This spectrum is broadened but not destroyed for small misalignment of the electric field.

6. APPENDICES

APPENDIX 6.1

Orthogonality of Stark States

$$\langle\psi_\mu(\bar{r},t)|\psi_\nu(\bar{r},t)\rangle$$

$$= \iint_{-\kappa/2}^{\kappa/2} dk_x dk'_x \phi_\nu(\bar{k})\phi^*_\mu(\bar{k}') \int d\bar{r}\psi^*_n(\bar{k}',\bar{r})\psi_n(\bar{k},\bar{r}) e^{-i\frac{(E_\nu-E_\mu)}{h}t}$$

$$= e^{-i\frac{(E_\nu-E_\mu)}{h}t} \int_{-\kappa/2}^{\kappa/2} dk_x \phi^*(\bar{k}')\phi_\nu(\bar{k})$$

$$= e^{-i\frac{(E_\nu-E_\mu)}{h}t} \frac{1}{\kappa}\int_{-\kappa/2}^{\kappa/2} e^{i\frac{k_x}{e\varepsilon}(E_\nu-E_\mu)} dk_x$$

since $E_\nu - E_\mu = \frac{2\pi e\varepsilon}{\kappa}(\nu-\mu)$ we have:

$$\frac{1}{\kappa}\int_{-\kappa/2}^{\kappa/2} e^{i\frac{k_x}{e\varepsilon}(E_\nu-E_\mu)}dk_x = \frac{1}{\kappa}\int_{-\kappa/2}^{\kappa/2} e^{i\frac{2\pi}{\kappa}(\nu-\mu)k_x} dk_x$$

$$= \delta_{\nu\mu}$$

therefore:

$$\langle\psi_\mu(\bar{r},t)|\psi_\nu(\bar{r},t)\rangle = e^{-i\frac{(E_\nu-E_\mu)}{h}t}\delta_{\nu\mu} = \delta_{\nu\mu}$$

APPENDIX 6.2

Computation of $\langle\psi_\nu(\bar{r},t)|H_{total}|\psi_\nu(\bar{r},t)\rangle$

$$H_{total} = H_0 - e\epsilon x$$

$$\langle\nu|H_{total}|\nu\rangle = \int\int_{-\kappa/2}^{\kappa/2} dk'_x dk_x \phi^*(\bar{k}')\langle\psi(\bar{r},\bar{k}')|H_{total}|\psi(\bar{r},\bar{k})\rangle\phi(\bar{k})$$

$$\langle\psi(\bar{r},\bar{k}')|H_0 - e\epsilon x|\psi(\bar{r},\bar{k}')\rangle = E(\bar{k}) - e\epsilon\left(\frac{i\partial}{\partial k_x} + X_{nn}(\bar{k})\right)\delta(k_x - k'_x)$$

Using the result (7)

$$\langle\nu|H_{total}|\nu\rangle = \frac{1}{\kappa}\int_{-\kappa/2}^{\kappa/2}\left\{E(\bar{k}) - e\epsilon\left[\frac{(-1)}{e\epsilon}\left[E_\nu - E^{(1)}(\bar{k})\right] + X_{nn}(\bar{k})\right]\right\}dk_x$$

$$= E_\nu$$

APPENDIX 6.3

Bloch Function Matrix Elements

$\langle \bar{k}', n | x | \bar{k}, n \rangle$ and $\langle \bar{k}', n' | x^2 | \bar{k}, n \rangle$

Differentiate the expression

$$\int \psi^*_{n'}(\bar{k}', \bar{r}) \psi_n(\bar{k}, \bar{r}) d\bar{r} = \delta_{n'n} \delta(\bar{k} - \bar{k}')$$

with respect to k_x:

$$\frac{\partial}{\partial k_x} \delta_{n'n} (\bar{k} - \bar{k}') = \frac{\partial}{\partial k_x} \int e^{i(\bar{k} - \bar{k}') \cdot \bar{r}} u^*_{n'}(\bar{k}') u_n(\bar{k}) d\bar{r}$$

$$= i \int e^{i(\bar{k} - \bar{k}') \cdot \bar{r}} u^*_{n'}(\bar{k}') x u_n(\bar{k}) d\bar{r}$$

$$+ \int e^{i(\bar{k} - \bar{k}') \cdot \bar{r}} u^*_{n'}(\bar{k}') \frac{\partial}{\partial k_x} u_n(\bar{k}) d\bar{r} \qquad \text{(C2)}$$

$$= i \langle k', n' | x | k, n \rangle - i X_{n'n} \delta(\bar{k} - \bar{k}') \qquad \text{(C3)},$$

defining $$X_{n'n} = \frac{i(2\pi)^3}{\Omega} \int_{\text{u.c.}} u^*_{n'}(\bar{k}', \bar{r}) \frac{\partial}{\partial k_x} u_n(\bar{k}, \bar{r}) d\bar{r} \ .$$

The step leading to (C3) can be taken because $u^*_{n'} \frac{\partial}{\partial k_x}$ has the crystal periodicity and hence the last integral in (C2) is proportional to $\delta(\bar{k} - \bar{k}')$.

So we have the result

$$\langle \bar{k}', n' | x | \bar{k}, n \rangle = -i \delta_{n'n} \frac{\partial}{\partial k_x} \delta(\bar{k} - \bar{k}') + X_{n'n}(\bar{k}') \delta(\bar{k} - \bar{k}')$$

Now differentiate both (C2) and (C3) with respect to k_x:

AD-A121 500 ZENER OSCILLATIONS(U) WASHINGTON UNIV ST LOUIS MO DEPT 2/2
OF ELECTRICAL ENGINEERING P ROBIN ET AL. SEP 82
TR-ONR-82-6 N00014-79-C-0840

UNCLASSIFIED F/G 9/1 NL

END

FILMED

DTIC

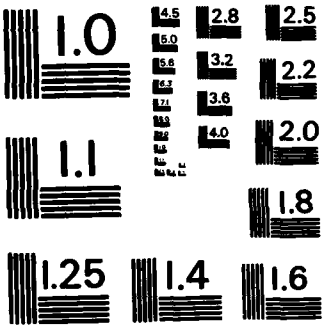

MICROCOPY RESOLUTION TEST CHART
NATIONAL BUREAU OF STANDARDS-1963-A

$$\frac{\partial^2}{\partial k_x^2}\delta_{n',n}\delta(\bar{k}-\bar{k}') = -\int e^{i(\bar{k}-\bar{k}')\cdot\bar{r}}\, u^*_{n',}(\bar{k}')x^2 u_n(\bar{k})d\bar{r}$$

$$+ i2\int e^{i(\bar{k}-\bar{k}')\cdot\bar{r}}\, u^*_{n',}(\bar{k}')x\frac{\partial}{\partial k_x}u_n(\bar{k})d\bar{r}$$

$$+\int e^{i(\bar{k}-\bar{k}')\cdot\bar{r}}\, u^*_{n',}(\bar{k}')\frac{\partial^2}{\partial k_x^2}u_n(\bar{k})d\bar{r} \qquad (C4)$$

$$\frac{\partial^2}{\partial k_x^2}\delta_{n',n}\delta(\bar{k}-\bar{k}') = -\int e^{i(\bar{k}-\bar{k}')\cdot\bar{r}}\, u^*_{n',}(\bar{k}')x^2 u_n(\bar{k})d\bar{r}$$

$$+ i\int e^{i(\bar{k}-\bar{k}')\cdot\bar{r}}\, u^*_{n',}(k')x\frac{\partial}{\partial k_x}u_n(\bar{k})d\bar{r}$$

$$- i\, X_{n',n}(\bar{k}')\frac{\partial}{\partial k_x}\delta(\bar{k}-\bar{k}') \qquad (C5)$$

We can use (C4) and (C5) to evaluate the troublesome middle integral on the rhs of both:

$$i\int e^{i(\bar{k}-\bar{k}')\cdot\bar{r}}\, u^*_{n',}x\frac{\partial}{\partial k_x}u_n d\bar{r} = -\int e^{i(\bar{k}-\bar{k}')\cdot\bar{r}}\, u^*_{n',}(\bar{k}')\frac{\partial^2}{\partial k_x^2}u_n(\bar{k})d\bar{r}$$

$$- iX_{n',n}(\bar{k}')\frac{\partial}{\partial k_x}\delta(\bar{k}-\bar{k}')$$

and we find

$$\langle k',n'|x^2|\bar{k},n\rangle = -\frac{\partial^2}{\partial k_x^2}\delta_{n',n}\delta(\bar{k}-\bar{k}') - 2iX_{n',n}(\bar{k}')\frac{\partial}{\partial k_x}\delta(\bar{k}-\bar{k}')$$

$$-\int e^{i(\bar{k}-\bar{k}')\cdot\bar{r}}\, u^*_{n',}(\bar{k}')\frac{\partial^2}{\partial k_x^2}u_n(\bar{k})d\bar{r} \qquad (C6)$$

For the states of a single band, $n=n'$, we can take advantage of the Hermitean property of the coordinate operator to simplify this expression. Starting with the normalization integral

$$\frac{1}{\Omega}\int u^*_{n'}(\bar{k})u_n(\bar{k})d\bar{r} = \delta_{n'n}$$

and differentiating with respect to k_x we find

$$\int\left(\frac{\partial u^*_{n'}}{\partial k_x}u_n + u^*_{n'}\frac{\partial u_n}{\partial k_x}\right)d\bar{r} = 0$$

or

$$X^*_{nn'} - X_{n'n} = 0, \quad X_{nn} \text{ real}$$

and

$$-iX_{nn} = \frac{(2\pi)^3}{\Omega}\int \frac{\partial u^*_n}{\partial k_x}\, u_n d\bar{r}$$

as well as its derivative

$$-i\,\frac{\partial X_{nn}(\bar{k})}{\partial k_x} = \frac{(2\pi)^3}{\Omega}\int\left[\frac{\partial^2 u^*_n}{\partial k_x^2}u_n + \frac{\partial u^*_n}{\partial k_x}\frac{\partial u_n}{\partial k_x}\right]d\bar{r}$$

are pure imaginary. But since $|\partial u_n/\partial x|^2$ is real we can define a real quantity

$$\Xi_{nn} = \frac{(2\pi)^3}{\Omega}\int\left|\frac{\partial u_n}{\partial k_x}\right|^2 d\bar{r}$$

and then

$$\frac{(2\pi)^3}{\Omega}\int\frac{\partial^2 u^*_n}{\partial k_x^2}u_n d\bar{r} = -i\,\frac{\partial X_{nn}}{\partial k_x} - \Xi_{nn}$$

and

$$\langle\bar{k}',n|x^2|\bar{k},n\rangle = \delta(\bar{k}-\bar{k}') - \left[\frac{\partial^2}{\partial k_x^2} + \Xi_{nn} + 2iX_{nn}\frac{\partial}{\partial k_x} + i\,\frac{\partial X_{nn}}{\partial k_x}\right] \qquad (C7)$$

In this expression the last term is imaginary, and it cancels the imaginary part of the third term in the bracket.

APPENDIX 6.4

a) $$\frac{1}{\kappa}\int_{-\kappa/2}^{\kappa/2} ke^{i2\pi\alpha\frac{k}{\kappa}}\,dk = \frac{1}{\kappa}\left[\frac{\kappa}{i2\pi\alpha}\,ke^{i2\pi\alpha\frac{k}{\kappa}}\Big|_{-\kappa/2}^{\kappa/2} - \frac{\kappa}{i2\pi\alpha}\int_{-\kappa/2}^{\kappa/2} e^{i2\pi\alpha\frac{k}{\kappa}}\,dk\right]$$

$$= \frac{\kappa}{i4\pi\alpha}\left(e^{i\pi\alpha} + e^{-\pi\alpha i}\right) + \frac{\kappa}{4\pi^2\kappa^2}\left(e^{i\pi\alpha} - e^{-i\pi\alpha}\right)$$

$$= \frac{\kappa}{i2\pi\alpha}\cos\pi\alpha + \frac{i\kappa}{2\pi^2\alpha^2}\sin\pi\alpha = (-1)^{\alpha}\frac{\kappa}{i2\pi\alpha} \quad \alpha \neq 0$$

$$\frac{1}{\kappa}\int_{-\kappa/2}^{\kappa/2} kdk = 0 \quad \alpha = 0$$

b) $$\frac{1}{\kappa}\int_{-\kappa/2}^{\kappa/2} k^2dk = \frac{\kappa^2}{12} \quad (\alpha = 0)$$

$$\frac{1}{\kappa}\int_{-\kappa/2}^{\kappa/2} k^2e^{i2\pi\alpha\frac{k}{\kappa}}\,dk = \frac{1}{\kappa}\left[\frac{\kappa}{i2\pi\alpha}\,k^2e^{i2\pi\alpha\frac{k}{\kappa}}\Big|_{-\kappa/2}^{\kappa/2} - \frac{2\kappa}{i2\pi\alpha}\int_{-\kappa/2}^{\kappa/2} ke^{i2\pi\alpha\frac{k}{\kappa}}\,dk\right]$$

$$= -\frac{2\kappa}{i2\pi\alpha}(-1)^{\alpha}\frac{\kappa}{i2\pi\alpha} = (-1)^{\alpha}\frac{\kappa^2}{2\pi^2\alpha^2}$$

APPENDIX 6.5

For a narrow wavepacket

$$\langle \cos ay \rangle_{N(0,\sigma)} \simeq \frac{1}{\sqrt{2\pi}\sigma} \int_{-\infty}^{\infty} e^{-\frac{y^2}{2\sigma^2}} \cos ay \, dy$$

$$= e^{-\frac{\sigma^2 a^2}{2}} \quad \text{(see Dwight table)}$$

$$\langle \sin ay \rangle_{N(0,\sigma)} \simeq \frac{1}{\sqrt{2\pi}\sigma} \int_{-\infty}^{\infty} e^{-\frac{y^2}{2\sigma^2}} \sin ay \, dy = 0$$

since for small variance $\sigma < 10^{-2}\kappa$ it is possible to replace the integration over $\left[-\frac{\kappa}{2}\frac{\kappa}{2}\right]$ by $]-\infty,\infty[$

$$\int_{-\kappa/2}^{\kappa/2} (\ )dk = \int_{-\infty}^{\infty} (\ )dk$$

Let us evaluate the error e:

$$e = \int_{-\infty}^{-\kappa/2} + \int_{\kappa/2}^{\infty} \frac{1}{\sqrt{2\pi}\sigma} e^{-y^2/2\sigma^2} \cos ay \, dy$$

$$\leq \frac{1}{\sqrt{2\pi}\sigma} \int_{-\infty}^{-\kappa/2} + \int_{\kappa/2}^{\infty} e^{-y^2/2\sigma^2} \, dy$$

let $x = y/\sigma$

$$\leq \frac{1}{\sqrt{2\pi}} \int_{-\infty}^{\kappa/2\sigma} + \int_{\kappa/2\sigma}^{\infty} e^{-x^2/2} \, dx \leq e^{-\left(\frac{\kappa}{2\sigma}\right)^2/2}$$

$\leq e^{-\kappa^2/8\sigma^2}$ using the Chernoff bound on the error function. In our calculation $\frac{\sigma}{\kappa} \leq \cdot 1$ the error is $e \leq 3.8\ 10^{-6}$.

APPENDIX 6.6

Computer Programs

DATABAND

```
90  DIM EB(10,10,10)
100  REM  DATA BAND
110  FOR Y = 3 TO 7
120  READ EB(4,Y,5)
130  DATA  0.9517 ,0.5256 ,0.4920 ,0.8602 ,1.3776
140  NEXT Y
150  FOR Y = 4 TO 6
160  READ EB(5,Y,5)
170  DATA  0.4920,0.2352 ,0.4920
180  NEXT Y
190 EB(6,5,5) = 0.4920
200  FOR Y = 2 TO 9
210  READ EB(3,Y,4)
220  DATA  1.2081,0.7419,0.6448,0.9517,1.3836,1.6178,1.5956,1.5174
230  NEXT Y
240  FOR Y = 3 TO 8
250  READ EB(4,Y,4)
260  DATA  0.6448,0.3333,0.5256,1.0043,1.4160,1.5591
270  NEXT Y
280  FOR Y = 4 TO 7
290  READ EB(5,Y,4)
300  DATA  0.5256,0.4920,0.8602,1.3787
302  NEXT Y
305 EB(6,5,4) = 0.8602
310 EB(6,6,4) = 1.0043
320  FOR Y = 1 TO 10
330  READ EB(2,Y,3)
340  DATA  1.5422,1.0875,0.9567,1.2081,1.5525,1.6272,1.4612,1.2645,1.1264,1.0796
350  NEXT Y
360  FOR Y = 2 TO 10
370  READ EB(3,Y,3)
380  DATA  0.9567,0.6097,0.7419,1.1476,1.4292,1.4058,1.2594,1.1368,1.0937
390  NEXT Y
400  FOR Y = 3 TO 9
410  READ EB(4,Y,3)
420  DATA  0.7419,0.6448,0.9517,1.3836,1.6178,1.5956,1.5174
430  NEXT Y
440  FOR Y = 4 TO 8
450  READ EB(5,Y,3)
460  DATA  0.9517,1.0393,1.3776,1.8322,2.1598
470  NEXT Y
480  FOR Y = 5 TO 7
490  READ EB(6,Y,3)
500  DATA  1.3776,1.4160,1.6178
510  NEXT Y
520 EB(7,6,3) = 1.6178
530  FOR Y = 0 TO 10
540  READ EB(1,Y,2)
550  DATA  1.3548,1.2464,1.2442,1.5422,1.8326,1.7128,1.4302,1.1628,0.9516,0.8188,0.7726
560  NEXT Y
570  FOR Y = 1 TO 10
580  READ EB(2,Y,2)
590  DATA  1.2442,0.9695,1.0875,1.4402,1.5865,1.4180,1.1596,0.9330,0.7841,0.7316
600  NEXT Y
610  FOR Y = 2 TO 10
620  READ EB(3,Y,2)
630  DATA  1.0875,0.9567,1.2081,1.5525,1.6272,1.4612,1.2645,1.1264,1.0796
640  NEXT Y
650  FOR Y = 3 TO 10
660  READ EB(4,Y,2)
670  DATA  1.2081,1.2455,1.5404,1.8999,2.0175,1.9071,1.7938,1.7530
680  NEXT Y
690  FOR Y = 4 TO 9
700  READ EB(5,Y,2)
710  DATA  1.5404,1.5737,1.7734,2.1599,2.6307,2.6858
720  NEXT Y
730  FOR Y = 5 TO 8
740  READ EB(6,Y,2)
750  DATA  1.7734,1.5591,1.5956,1.9071
760  NEXT Y
770 EB(7,6,2) = 1.5954
780 EB(7,7,2) = 1.2594
790  FOR Y = 0 TO 10
800  READ EB(0,Y,1)
810  DATA  0.5005,0.7479,1.3548,2.0045,1.6654,1.2703,0.9486,0.7105,0.5632,0.5015,0.4972
```

```
820  NEXT Y
830  FOR Y = 0 TO 10
840  READ EB(1,Y,1)
850  DATA  0.7479,0.8537,1.2464,1.7591,1.7343,1.3392,1.0677,0.8107,0.6295,0.5228,0.4874
860  NEXT Y
870  FOR Y = 1 TO 10
880  READ EB(2,Y,1)
890  DATA  1.2464,1.2442,1.5422,1.8326,1.7137,1.4302,1.1623,0.9516,0.8188,0.7726
900  NEXT Y
910  FOR Y = 2 TO 10
920  READ EB(3,Y,1)
930  DATA  1.5422,1.5609,1.8326,2.0857,2.0010,1.7745,1.5723,1.4402,1.3919
940  NEXT Y
950  FOR Y = 3 TO 10
960  READ EB(4,Y,1)
970  DATA  1.8325,1.8616,2.0667,2.4171,2.5681,2.4162,2.2929,2.2508
980  NEXT Y
990  FOR Y = 4 TO 10
1000  READ EB(5,Y,1)
1010  DATA  2.0667,1.8806,1.9162,2.2077,2.6867,3.1456,3.1939
1020  NEXT Y
1030  FOR Y = 5 TO 9
1040  READ EB(6,Y,1)
1050  DATA  1.9162,1.5513,1.5174,1.7938,2.2929
1060  NEXT Y
1070  FOR Y = 6 TO 8
1080  READ EB(7,Y,1)
1090  DATA  1.5174,1.1368,1.1264
1100  NEXT Y
1110 EB(8,7,1) = 1.1264
1120  FOR Y = 0 TO 10
1130  READ EB(0,Y,0)
1150  DATA  0,0.5005,1.3455,1.8974            ,1.4650,1.0616,0.7353,0.4956            ,0.3547,0.3018,0.3053
1155  NEXT Y
1160  FOR Y = 0 TO 10
1170  READ EB(1,Y,0)
1180  DATA  0.5005,0.7479,1.3548,2.0045,1.6664,1.2708,0.9486,0.7105,0.5632,0.5015,4972
1190  NEXT Y
1200  FOR Y = 1 TO 10
1210  READ EB(2,Y,0)
1220  DATA  1.3548,1.5133,1.9341,2.1836,1.8290,1.5170,1.2303,1.1227,1.0465,1.0255
1230  NEXT Y
1240  FOR Y = 2 TO 10
1250  READ EB(3,Y,0)
1260  DATA  1.9340,1.9745,2.2685,2.6056,2.3196,2.0368,1.9264,1.8307,1.7992
1270  NEXT Y
1280  FOR Y = 3 TO 10
1290  READ EB(4,Y,0)
1300  DATA  2.2685,2.1562,2.2767,2.6204,2.9899,2.8644,2.7664,2.7289
1310  NEXT Y
1320  FOR Y = 4 TO 10
1330  READ EB(5,Y,0)
1340  DATA  2.2767,1.9586,1.9352,2.1955,2.6533,3.1939,3.4634
1350  NEXT Y
1360  FOR Y = 5 TO 10
1370  READ EB(6,Y,0)
1380  DATA  1.9352,1.5341,1.4850,1.7530,2.2597,2.7289
1390  NEXT Y
1400  FOR Y = 6 TO 9
1410  READ EB(7,Y,0)
1420  DATA  1.4850,1.0936,1.0796,1.3930
1430  NEXT Y
1440 EB(8,7,0) = 1.0796
1450 EB(8,8,0) = 0.7315
1600  PRINT  CHR$ (4);"BLOAD CHAIN,A520"
1610  CALL 520"FILLBZ3"
```

FILLBZ2

```
90  REM  FILLBZ3
100  PRINT "FILL BRILLOUIN ZONE"
110  FOR X = 0 TO 10
120  FOR Y = 0 TO 10
130  FOR Z = 0 TO 10
150  IF EB(X,Y,Z) < > 0 THEN 190
160 EB(X,Y,Z) = EB(X,Z,Y)
170  IF EB(X,Y,Z) < > 0 THEN 190
180 EB(X,Y,Z) = EB(Z,Y,X)
190  NEXT Z
195  NEXT Y
200  NEXT X
210  PRINT "END OF 3/48 BZ"
220  FOR X = 0 TO 10
230  FOR Y = 0 TO 10
240  FOR Z = 0 TO 10
250  IF EB(X,Y,Z) < > 0 THEN 280
260 EB(X,Y,Z) = EB(10 - Y,10 - X,10 - Z)
280  NEXT Z
290  NEXT Y
300  NEXT X
310  PRINT "END OF 6/48 BZ"
320  FOR X = 0 TO 10
330  FOR Y = 0 TO 10
340  FOR Z = 0 TO 10
350  IF EB(X,Y,Z) < > 0 THEN 380
360 EB(X,Y,Z) = EB(Y,X,Z)
380  NEXT Z
385  NEXT Y
390  NEXT X
400  PRINT "END OF 12/48=1/4 BZ OR 1/8 CUBE
410  FOR X = 0 TO 10
412  FOR Y = 0 TO 10
414  FOR Z = 0 TO 10
416  IF EB(X,Y,Z) < > 0 THEN 420
418  PRINT "EB(";X;",";Y;",";Z;")"
420  NEXT Z
422  NEXT Y
424  NEXT X
500 D$ =  CHR$ (4); REM  CTRL-D
510  PRINT D$;"OPEN CUBEBAND"
520  PRINT D$;"DELETE CUBEBAND"
530  PRINT D$;"OPEN CUBEBAND"
540  PRINT D$;"WRITE CUBEBAND"
550  FOR X = 0 TO 10
560  FOR Y = 0 TO 10
570  FOR Z = 0 TO 10
580  PRINT EB(X,Y,Z)
590  NEXT Z
600  NEXT Y
610  NEXT X
620  PRINT D$;"CLOSE CUBEBAND"
```

ZENER2

```
100  REM  ZENER 2
110  REM  DIMENSION
112  DIM K(2)
114  DIM KK(2)
116  DIM Y(2)
118  DIM W(2)
120  DIM A(2)
122  DIM B(2)
124  DIM F(2)
126  DIM D(2)
128  DIM C(100)
130  DIM S(100)
132  DIM R(100)
134  DIM X(1000)
136  DIM E(1000)
210  PRINT "RETREIVE ENERGY BAND"
215  PRINT " IN A CUBE (2 TIMES B,Z,)"
220  REM  RETREIVE CUBEBAND FILE
225  DIM EB(10,10,10)
230 D$ =  CHR$ (4): REM  CTRL-D
240  PRINT D$;"OPEN CUBEBAND"
250  PRINT D$;"READ CUBEBAND"
260  FOR X = 0 TO 10
270  FOR Y = 0 TO 10
280  FOR Z = 0 TO 10
290  INPUT EB(X,Y,Z)
300  NEXT Z
310  NEXT Y
320  NEXT X
330  PRINT D$;"CLOSE CUBEBAND"
610  PRINT "IS THE DISK IN THE DRIVE1?"
615  INPUT A$
620  PRINT  CHR$ (4);"BLOAD CHAIN,A520"
630  CALL 520"DIRZENER2"
```

DIRZENER2

```
100  REM  DIRECTORY PROGRAM
105  PRINT "DIRZENER2 CHAINED"
400  REM  PARAMETER SECTION
405 PI = 3.141592653
410  REM  LATTICE PARAM.
415 LP = 5.64
420 LI = PI / LP
500  PRINT "INPUT PERIODIC VECTOR K(HKL)"
505  INPUT "H=";K(0)
506 K(0) = K(0) * 2
510  INPUT "K=";K(1)
512 K(1) = K(1) * 2
515  INPUT "L=";K(2)
517 K(2) = K(2) * 2
520  PRINT "INPUT INITIAL VECTOR KO(HKL)"
525  INPUT "H=";KO(0)
527 KO(0) = KO(0) * 2
530  INPUT "K=";KO(1)
532 KO(1) = KO(1) * 2
535  INPUT "L=";KO(2)
537 KO(2) = KO(2) * 2
538  PRINT "GIVE ORDER OF INTERPOLATION"
539  INPUT "ORDER";O
540  PRINT "GIVE NUMBER OF POINTS"
542  PRINT "TO BE INTERPOLATED FOR"
544  PRINT "FOURIER SERIES CALCULATION"
545 KL = ((K(0) / 2) ↑ 2 + (K(1) / 2) ↑ 2 + (K(2) / 2) ↑ 2) ↑ (1 / 2)
546  PRINT "WITH N>=" INT (21 * KL)
550  INPUT "N=";N
570  HOME
572  PRINT "DATA GIVEN:"
575  PRINT "K=("K(0) / 2","K(1) / 2","K(2) / 2")"
580  PRINT "KO=("KO(0) / 2","KO(1) / 2","KO(2) / 2")"
582  PRINT O"ORDER"
585  PRINT "N="N
595  PRINT "OK?"
597  INPUT B$
600  IF B$ = "OK" THEN 610
605  GOTO 500
610  REM  CHAIN WITH INTERP.
612  PRINT "IS THE DISK IN THE DRIVE1?"
614  INPUT A$
615  IF O = 2 THEN 640
616  IF O = 3 THEN 620
619  GOTO 539
620  PRINT  CHR$ (4);"BLOAD CHAIN,A520"
630  CALL 520"PARA3RD2"
640  PRINT  CHR$ (4);"BLOAD CHAIN           ,A520"
650  CALL 520"PARA2ND2"
```

PARA3RD2

```
100  REM   PARABOLIQUE INTERP.3RD
110  PRINT "PARA3RD CHAINED"
200  DEF  FN B(X) =  ABS (X - 5 + 5 * ( - 1 ↑  INT (X / 10)) - 10 *  INT (X / 10))
210  FOR I = 0 TO M - 1
212 E(I) = 0
220 X(I) = I * KL / (M - 1) * LI
230  FOR J = 0 TO 2
235  REM  Y(J) IS A POINT OF INTERPOLATION
240 Y(J) = 10 * (K(J) * I / (M - 1) + KO(J))
245  REM   W(J) CLOSEST POINT
250 W(J) =  INT (Y(J)) +  INT (1 / 2 + Y(J) -  INT (Y(J)))
255 D(J) = Y(J) - W(J)
260  NEXT J
262 W1 =  FN B(W(0))
264 W2 =  FN B(W(1))
266 W3 =  FN B(W(2))
268 E = EB(W1,W2,W3)
270  IF D(0) > 0 THEN 276
272 A1 =  - 1
274  GOTO 278
276 A1 = 1
278  IF D(1) > 0 THEN 284
280 A2 =  - 1
282  GOTO 286
284 A2 = 1
286  IF D(2) > 0 THEN 292
288 A3 =  - 1
290  GOTO 310
292 A3 = 1
310 W4 =  FN B(W(0) + 1)
311 W5 =  FN B(W(1) + 1)
312 W6 =  FN B(W(2) + 1)
313 W7 =  FN B(W(0) - 1)
314 W8 =  FN B(W(1) - 1)
315 W9 =  FN B(W(2) - 1)
316 V1 =  FN B(W(0) + A1)
317 V2 =  FN B(W(1) + A2)
318 V3 =  FN B(W(2) + A3)
319 V4 =  FN B(W(0) + 2 * A1)
320 V5 =  FN B(W(1) + 2 * A2)
321 V6 =  FN B(W(2) + 2 * A3)
330 A(0) = ((4 * A1 + 2) * (EB(W4,W2,W3) - E) + (2 - 4 * A1) * (EB(W7,W2,W3) - E) + E - EB(V4,W2,W3)) / 6 / A1
332 B(0) = (EB(W4,W2,W3) + EB(W7,W2,W3)) / 2 - E
334 G(0) = ( - (2 + A1) * (EB(W4,W2,W3) - E) + (A1 - 2) * (EB(W7,W2,W3) - E) - E + EB(V4,W2,W3)) / 6 / A1
340 A(1) = ((4 * A2 + 2) * (EB(W1,W5,W3) - E) + (2 - 4 * A2) * (EB(W1,W8,W3) - E) + E - EB(W1,V5,W3)) / 6 / A2
342 B(1) = (EB(W1,W5,W3) + EB(W1,W8,W3)) / 2 - E
344 G(1) = ( - (2 + A2) * (EB(W1,W5,W3) - E) + (A2 - 2) * (EB(W1,W3,W3) - E) - E + EB(W1,V5,W3)) / 6 / A2
350 A(2) = ((4 * A3 + 2) * (EB(W1,W2,W6) - E) + (2 - 4 * A3) * (EB(W1,W2,W9) - E) + E - EB(W1,W2,V6)) / 6 / A3
352 B(2) = (EB(W1,W2,W6) + EB(W1,W2,W9)) / 2 - E
354 G(2) = ( - (2 + A3) * (EB(W1,W2,W6) - E) + (A3 - 2) * (EB(W1,W2,W9) - E) - E + EB(W1,W2,V6)) / 6 / A3
360 H = EB(V1,V2,W3) - EB(V1,W2,W3) - EB(W1,V2,W3) + E
362 L = EB(V4,V2,W3) - EB(V4,W2,W3) - EB(W1,V2,W3) + E
364 N = EB(V1,V5,W3) - EB(V1,W2,W3) - EB(W1,V5,W3) + E
370 F(2) = A1 * A2 * (3 * H - (L + N) / 2)
372 W(1) = A2 * (L / 2 - H)
374 W(2) = A1 * (N / 2 - H)
390 H = EB(V1,W2,V3) - EB(V1,W2,W3) - EB(W1,W2,V3) + E
392 L = EB(V4,W2,V3) - EB(V4,W2,W3) - EB(W1,W2,V3) + E
394 N = EB(V1,W2,V6) - EB(V1,W2,W3) - EB(W1,W2,V6) + E
390 F(1) = A1 * A3 * (3 * H - (L + N) / 2)
392 W(5) = A3 * (L / 2 - H)
394 W(6) = A1 * (N / 2 - H)
400 H = EB(W1,V2,V3) - EB(W1,V2,W3) - EB(W1,W2,V3) + E
402 L = EB(W1,V2,V6) - EB(W1,V2,W3) - EB(W1,W2,V6) + E
404 N = EB(W1,V5,V3) - EB(W1,W2,V3) - EB(W1,V5,W3) + E
410 F(0) = A3 * A2 * (3 * H - (L + N) / 2)
412 W(3) = A2 * (L / 2 - H)
414 W(4) = A3 * (N / 2 - H)
430 W(7) = EB(V1,V2,V3) - EB(V1,W2,W3) - EB(W1,V2,W3) - EB(W1,W2,V3) + 2 * E - F(0) * A2 * A3 - F(1) * A1 * A3 - F(2) * A1 *
    A2
432 W(7) = (W(7) - A1 * (W(2) + W(6)) - A2 * (W(1) + W(3)) - A3 * (W(4) + W(5))) / A1 / A2 / A3
498 E(I) = EB(W1,W2,W3)
500  FOR J = 0 TO 2
502 E(I) = E(I) + A(J) * D(J) + B(J) * D(J) ↑ 2 + G(J) * D(J) ↑ 3
503  NEXT J
```

```
504 E(I) = E(I) + H(1) * D(0) ↑ 2 * D(1) + H(2) * D(0) * D(1) ↑ 2 + F(2) * D(0) * D(1)
508 E(I) = E(I) + H(5) * D(0) ↑ 2 * D(2) + H(6) * D(0) * D(2) ↑ 2 + F(1) * D(0) * D(2)
512 E(I) = E(I) + F(0) * D(1) * D(2) + H(3) * D(1) * D(2) ↑ 2 + H(4) * D(1) ↑ 2 * D(2)
516 E(I) = E(I) + H(7) * D(0) * D(1) * D(2)
540  PRINT "E("I")="E(I)
550  NEXT I
590  PRINT "IS THE DISK IN THE DRIVE1?"
595  INPUT A$
600  PRINT  CHR$ (4);"BLOAD CHAIN,A$20"
610  CALL 520"DISPATCH2"
```

FOURSERIES2

```
100  REM  FOURIER CALCULATION
110  PRINT "FOURSERIES CHAINED"
150 RX = 20
155 PI = 3.141592653
157 A = KL * PI / LP
160  PRINT "COMPUTE R(I) FROM "
164  INPUT "I=";EZ
166  PRINT "TO"
168  INPUT "I=";FZ
169  IF EZ > 0 THEN 200
170  IF FZ > 100 THEN 160
172 R(0) = 0
173  FOR N = 0 TO N - 2
175 R(0) = R(0) + (X(N + 1) - X(N)) * (E(N) + E(N + 1)) / 2
178  NEXT N
179 R(0) = R(0) / A
180 EZ = 1
182  PRINT "R(0)="R(0)
200  FOR K = EZ TO FZ
205 H = K * PI * 2 / A
210 S(K) = 0
212 C(K) = 0
214 R(K) = 0
215  FOR N = 0 TO N - 2
220 L = N + 1
225 D = (E(L) - E(N)) / (X(L) - X(N))
230 CD = (E(N) * X(L) - E(L) * X(N)) / (X(L) - X(N))
235 C = CD + X(L) * D
240 F = CD + X(N) * D
245 C(K) = C(K) + C *  SIN (H * X(L))
250 C(K) = C(K) - F *  SIN (H * X(N))
255 C(K) = C(K) + D / H * ( COS (H * X(L)) -  COS (H * X(N)))
280 S(K) = S(K) - C *  COS (H * X(L))
285 S(K) = S(K) + F *  COS (H * X(N))
290 S(K) = S(K) + D / H * ( SIN (H * X(L)) -  SIN (H * X(N)))
300  NEXT N
310 S(K) = S(K) / K / PI
315 C(K) = C(K) / K / PI
320 R(K) = (S(K) ↑ 2 + C(K) ↑ 2) ↑ (1 / 2)
325  PRINT "S("K")="S(K)
326  PRINT "C("K")="C(K)
327  PRINT "R("K")="R(K)
330  NEXT K
350  PRINT "IS THE DISK IN THE DRIVE 1?"
360  INPUT A$
400  PRINT  CHR$ (4);"BLOAD CHAIN,A520"
410  CALL 520"DISPATCH2"
```

DISPATCH2

```
100  REM  DISPATCH PROGRAM
102  HOME
104  PRINT "DISPATCH CHAINED"
105  PRINT "FOURIER COMPONENT COMPUTED"
106  FOR I = 0 TO 100
108  IF R(I) = 0 THEN 112
110  PRINT " R("I")"
111 CZ = I
112  NEXT I
140  PRINT "CHOOSE THE NEXT PROCESS"
150  PRINT "<1> IS BANDPRINT"
160  PRINT "<2> IS BANDPLOT"
170  PRINT "<3> IS FOURIER SERIES COMPUTATION"
180  PRINT "<4> IS FOURPRINT"
190  PRINT "<5> IS FOURPLOT"
200  PRINT "<6> IS INPUT NEW K AND KO"
210  PRINT "<7>SAVES FOUR IN FOURFILE"
215  PRINT "<8>SAVES BAND IN BANDFILE"
250  INPUT "CHOICE:";CH
255  PRINT "IS THE DISK IN THE DRIVE1?"
256  INPUT A$
260  IF CH = 1 THEN 350
270  IF CH = 2 THEN 360
280  IF CH = 3 THEN 370
290  IF CH = 4 THEN 380
300  IF CH = 5 THEN 390
310  IF CH = 6 THEN 400
320  IF CH = 7 THEN 410
330  IF CH = 8 THEN 420
350  PRINT  CHR$ (4);"BLOAD CHAIN,A520"
355  CALL 520"BANDPRINT2"
360  PRINT  CHR$ (4);"BLOAD CHAIN           ,A520"
365  CALL 520"BANDPLOT2"
370  PRINT  CHR$ (4);"BLOAD CHAIN           ,A520"
375  CALL 520"FOURSERIES2"
380  PRINT  CHR$ (4);"BLOAD CHAIN           ,A520"
385  CALL 520"FOURPRINT2"
390  PRINT  CHR$ (4);"BLOAD CHAIN           ,A520"
395  CALL 520"FOURPLOT2"
400  PRINT  CHR$ (4);"BLOAD CHAIN           ,A520"
405  CALL 520"DIRZEHER2"
410  PRINT  CHR$ (4);"BLOAD CHAIN,A520"
415  CALL 520"FOURFILE2"
420  PRINT  CHR$ (4);"BLOAD CHAIN,A520"
425  CALL 520"BANDFILE2"
```

ZENER2F

```
52  DIM E(1000)
54  DIM R(100)
56  DIM S(100)
58  DIM C(100)
60  DIM X(1000)
64 LP = 5.64
66  DIM K(2)
68  DIM KO(2)
100  PRINT "RETRIEVE BAND# H K L HO KO LO"
102  INPUT "H";H
103  INPUT "K";K
104  INPUT "L";L
105 KL = (H ↑ 2 + K ↑ 2 + L ↑ 2) ↑ (1 / 2)
106  INPUT "HO";HO
107  INPUT "KO";KO
108  INPUT "LO";LO
109 K(1) = 2 * K
110  PRINT "GIVE M"
112  INPUT "M=";M
114 A$ = "BAND" +  STR$ (H) + " "
116 A$ = A$ +  STR$ (H) + " " +  STR$ (K) + " " +  STR$ (L) + "  "
118 A$ = A$ +  STR$ (HO) + " " +  STR$ (KO) + " " +  STR$ (LO)
120  PRINT "FILE: "A$
125  PRINT "THIS FILE IS"
130  PRINT "ON WHICH DRIVE ?"
140  INPUT "DRIVE #";DR
141 B$ =  STR$ (2)
142  IF DR = 1 GOTO 150
143 B$ =  STR$ (1)
150 D$ =  CHR$ (4): REM  CTRL-D
155 C$ = A$ + ",S6,D" +  STR$ (DR)
160  PRINT D$;"OPEN"C$
170  PRINT D$;"READ"A$
180  INPUT M
185  INPUT I
190  FOR I = 0 TO M - 1
200  INPUT K
210  INPUT E(I)
220  NEXT I
230  PRINT D$;"CLOSE"A$
240 PI = 3.141592653
242 LI = PI / LP
244  FOR I = 0 TO M - 1
246 X(I) = I * KL / (M - 1) * LI
248  NEXT I
250 K(0) = H * 2
254 K(2) = L * 2
256 KO(0) = HO * 2
258 KO(1) = KO * 2
260 KO(2) = LO * 2
500  PRINT "IS THE DISK IN DRIVE1"
510  INPUT A$
520  PRINT  CHR$ (4);"BLOAD  CHAIN,A520,S6,D"B$
530  CALL 520"DISPATCH2"
```

7. BIBLIOGRAPHY

1. R. W. Koss and L. M. Lambert, Physical Review B5, 1479 (1972).

2. Semiconductor Millimeter Wavelength Electronics, Annual Report ONR 80-1, Department of Electrical Engineering, Washington University.

3. R. Glauber, Physical Review 131, 2766 (1963).

4. J. Zak, "The kq-Representation in the Dynamics of Electronics in Solids", Solid State Physics 27 (1972), Academic Press, New York and London.

5. J. M. Ziman, Principles of the Theory of Solids, Cambridge University Press (1964).

6. Joseph Callaway, Quantum Theory of the Solid State B, p. 465, Academic Press, New York and London (1974).

7. C. L. Roy and P. K. Mahapatra Journal of Physics C: Solid State Physics 13, 5365-81 (1980).

8. J. Callaway Physical Review 130, 549 (1963), Physical Review 134 A, 998 (1964).

9. G. H. Wannier and D. R. Fredkin, Decoupling of Bloch Bands in Presence of Homogeneous Fields, Physical Review 125, 1910 (1962).

DISTRIBUTION LIST
CONTRACT N00014-79-C-0840

Code 414 — 4
Office of Naval Research
Arlington, VA 22217

Naval Research Laboratory
4555 Overlook Avenue, S.W.
Washington, D.C. 20375
Code 6811 — 1
6850 — 1
6820 — 1
6851 — 1

Defense Documentation Center — 12
Building 5, Cameron Station
Alexandria, VA 22314

Dr. Y. S. Park — 1
AFWAL/DHR
Building 450
Wright-Patterson AFB
Ohio 45433

Texas Instruments — 1
Central Research Lab
M.S. 134
13500 North Central Expressway
Dallas, TX 75265
ATTN: Dr. W. Wisseman

Dr. R. M. Malbon/M.S. 1C — 1
Avantek, Inc.
3175 Bowers Avenue
Santa Clara, CA 94304

Dr. R. Bierig — 1
Raytheon Company
28 Seyon Street
Waltham, MA 02154

Dr. Mike Driver — 1
Westinghouse Research and
Development Center
Beulah Road
Pittsburgh, PA 15235

Dr. F. Eisen — 1
Rockwell International
Science Center
P.O. Box 1085
Thousand Oaks, CA 91360

Dr. C. Krumn — 1
Hughes Research Laboratory
3011 Malibu Canyon Raod
Malibu, CA 90265

Mr. Lothar Wandinger — 1
ECOM/AMSEL/TL/IJ
Fort Monmouth, NJ 07003

Dr. William Lindley — 1
MIT
Lincoln Laboratory
F124 A, P.O. Box 73
Lexington, MA 02173

Commander — 1
U.S. Army/ERADCOM
ATTN: V. Gelnovatch, DELET-M
Fort Monmouth, NJ 07703

RCA — 1
Microwave Technology Center
Dr. F. Sterzer
Princeton, NJ 08540

Commander — 1
Naval Electronics Systems Command
ATTN: J. P. Letellier, Code 6142
Washington, D.C. 20360

Commander — 1
Naval Air Systems Command
ATTN: A. Glista, Jr., AIR 34
Washington, D.C. 20361

Dr. R. Bell, K-101 — 1
Varian Associates, Inc.
611 Hansen Way
Palo Alto, CA 94304

Hewlett-Packard Corporation 1
Dr. Robert Archer
1501 Page Road
Palo Alto, CA 94306

Watkins-Johnson Company 1
E. J. Crescenzi, Jr./
K. Niclas
3333 Hillview Avenue
Stanford Industrial Park
Palo Alto, CA 94304

Commandant 1
Marine Corps
Scientific Advisor (Code AX)
Washington, D.C 20380

Communications Transistor Corp. 1
Dr. W. Weisenberger
301 Industrial Way
San Carlos, CA 94070

Microwave Associates 1
Northwest Industrial Park
Drs. F. A. Brand/J. Saloom
Burlington, MA 01803

Commander, AFAL 1
AFWAL/AADM
Dr. Don Rees
Wright-Patterson AFB, OH 45433

Professor Walter Ku 1
Phillips Hall
Cornell University
Ithaca, NY 14853

Commander 1
Harry Diamond Laboratories
Mr. Horst W. A. Gerlach
800 Powder Mill Road
Adelphia, MD 20783

A.G.E.D. 1
201 Varick Street
9th Floor
New York, NY 10014

Dr. Ken Weller 1
MS/1414
TRW Systems
One Space Park
Redondo Beach, CA 90278

Professor L. Eastman 1
Phillips Hall
Cornell University
Ithaca, NY 14853

Professor Hauser and 1
Littlejohn
Department of Electrical Engr.
North Carolina State University
Raleigh, NC 27607

Professor J. Beyer 1
Department of Electrical and
Computer Engineering
University of Wisconsin
Madison, WI 53706

W. H. Perkins 1
Electronics Lab 3-115/B4
General Electric Company
P.O. Box 4840
Syracuse, NY 13221

Bryan Hill 1
AFWAL/AADE
Wright-Patterson AFB, OH 45433

H. Willing/Radar Directorate 1
BMD - Advanced Technical Center
P.O. Box 1500
Huntsville, AL 35807